LOCALIZATION AND DISTRIBUTION OF BINDING SITES FOR ATRIAL NATRIURETIC FACTOR IN THE RAT. A LIGHT AND ELECTRON MICROSCOPE RADIOAUTOGRAPHIC STUDY

by

CESARIO BIANCHI FILHO

M.D. (Faculdade de Ciencias Medicas da Santa Casa de Sao Paulo, Sao Paulo, Brazil)

M.Sc. (Université de Montréal)

A thesis submitted to
the Faculty of Graduate Studies and Research
in partial fulfillment of the
requirements for the degree of
Doctor of Philosophy

Department of Medicine
Division of Experimental Medicine
McGill University

Supervisor: Dr. Marc Cantin
Laboratory of Pathobiology
Institut de Recherches Cliniques de Montréal

ISBN 0-315-52395-6

ABSTRACT

Studies were undertaken to localize *in vivo* binding sites for atrial natriuretic factor (ANF) in rats by light and electron microscope radioautography. ANF binding sites were identified in the brain, kidney, eye and small intestine. In the brain, they were present in the circumventricular organs, blood vessels and choroid plexus. In the renal cortex, they were mainly localized in epithelial visceral cells. In addition , ANF inhibited the decrease in the size of isolated glomeruli induced by Angiotensin II. ANF binding sites in the renal medulla corresponded mainly to the descending vasa recta, and to papillary collecting tubules in the renal papilla. In the eye, ANF binding sites were present at the base of "pigmented" cells of the ciliary processes. In the small intestine, they were localized in fibroblast-like cells of the lamina propria, at the base of mature enterocytes and to a lesser extent in the capillaries. Such detailed map of ANF binding sites may be very helpful in our understanding of the mechanisms and implications of circulating ANF in physiological and pathophysiological states where this hormone seems to play a major role in the homeostasis of body fluid volume and blood pressure.

RESUMÉ

Nous avons entrepris des études radioautographiques en microscopie photonique et électronique dans le but de révéler les sites de liaison in vivo du facteur natriurétique auriculaire (FNA) chez le rat. Nous avons pu démontrer la présence de ces sites de liaison dans le cerveau, les reins, les yeux ainsi que l'intestin grêle. Dans le cerveau, les sites de liaison sont situés au niveau des organes circumventriculaires, des vaisseaux sanguin et du plexus choroide. Dans le cortex rénal, ils se retrouvent principalement localisés sur les cellules épithéliales viscérales. En outre, nous avons pu démontrer que le FNA inhibe la contraction des glomérules isolés en réponse à l'angiotensine II. Dans la médullaire rénale; les sites de liaison du FNA sont localisés sur les vasa recta descendants et les tubules collecteurs. Dans l'oeil, ils se trouvent à la base des cellules "pigmentées" du procès ciliaire. Les sites de liaison de l'intestin grêle se partagent entre les fibroblastes de la lamina propria et la base des entérocytes. Cette carte détaillée des sites de liaison du FNA devrait s'avérer d'une grande utilité pour la compréhension du rôle physiologique du FNA circulant et de ses implications physiopathologiques. phy-
siopathologiques.

ACKNOWLEDGEMENTS

I wish to thank Dr. Marc Cantin, director of the Hypertension Group of the IRCM, for the encouragement that I was given through his personal example as a great scientist and human being. I am greatly indebted for his generosity of time, spirit and untiring supervision throughout the period of my work in his laboratory.

I am deeply grateful to Dr. Jacques Genest, former director of IRCM, for his helpful advice and constructive criticism.

My most sincere thanks are extended to both, Dr. Jolanda Gutkowska, from IRCM for her contributions and Dr. Harry Goldsmith, director of the Division of Experimental Medicine, McGill University.

I would like to express my appreciation to the technical staff of Dr. Cantin's laboratory.

I also wish to thank the Canadian Heart Foundation and the Medical Research Council of Canada for granting me with financial support by a Fellowship award.

Many thanks to my friends and collegues for many years of fruitful discussions on basic sciences.

TABLE OF CONTENTS

LIST OF FIGURES

CHAPTER 2.

CHAPTER 3
Section A

LIST OF TABLES

PROLOGUE

This thesis describes the localization of atrial natriuretic factor (ANF) binding sites in the brain, kidneys, eyes and small intestine of rats. I have chosen the option provided in Section 7 of the Guidelines Concerning Thesis Preparation, of the Faculty of Graduate Studies and Research of McGill University, which reads as follows: "The candidate has the option, subject to the approval of the Department of including as part of the thesis the text of an original paper, or papers, suitable for submission to learned journals for publication. In this case, the thesis must still conform to all other requirements explained in the Guidelines Concerning Thesis Preparation. Additional material (experimental and design data as well as description of equipment) must be provided in sufficient detail to allow a clear and precise judgment to be made of the importance and originality of the research reported. Abstract, full introduction and conclusion must be included, and where more than one manuscript appears, connecting texts and common abstracts, introduction and conclusion are required. A mere collection of manuscripts is not acceptable; nor can reprints of published papers be accepted". This provision allows me to include the texts of five manuscripts (Chapters 2, 3, 4, and 5) submitted for publication concerning the

thesis research project. These texts appear in their original form with some minor modifications. Co-authorship of these manuscripts includes: Dr. Jolanta Gutkowska, who provided the iodinated peptide; Dr. André de Léan, who helped me with the analysis of binding data using a computerized program (SCATFITT, ALLFIT); Dr. Gaetan Thibault, who undertook the purification and biochemical analysis (high performance liquid chromatography) of the iodinated peptide; Mme Marie Ballak who assisted with the radioautographs; Dr. Raul Garcia, who showed me the animal perfusion techniques; Dr. Daniel Forthomme, who showed me the isolation of ciliary process of the eyes; Dr. Madhu Anand-Srivastava who performed the adenylate cyclase activity studies and Dr. Jacques Genest former Director of the Multidisciplinary Research Group on Hypertension.

Chapter 1 is a review of the literature on ANF and its role in blood pressure and extracellular fluid homeostasis. It is followed by the "research goals" of the thesis and Chapter 6 summarizes the conclusions and claims to originality. Appendix I includes a list of my publications.

CHAPTER 1

In 1981, De Bold and his colleagues discovered atrial natriuretic factor (ANF), a hormone produced and secreted by the heart. Their discovery opened a new era in our understanding of the regulation of blood pressure and body fluid volume. This important finding has identified the heart not only as a pump to propel blood but also as an endocrine organ secreting peptide hormones.

REVIEW OF LITERATURE

ATRIAL NATRIURETIC FACTOR

This review will familiarize the reader with the ANF system via a description of its biochemistry, physiology, pharmacology, and molecular biology and its implications in the control of blood pressure and body fluid volume.

HISTORICAL BACKGROUND

Morphological studies by Kisch (76) and Bompiani et al. (20) were the first to reveal the existence of particulate inclusions (called "corps denses") in atrial cardiomyocytes. Palade (109) reported a decrease of these secretory granules following reserpine treatment, suggesting the presence of catecholamines. Specific atrial cardiomyocytes have been extensively found by electron microscopy in a number of different mammalian species, and their endocrine function has been postulated (70).

Other investigations have demonstrated that the atrial appendages of lower vertebrates contain endocrine-like specific granules (18, 97) , also seen in ventricular cells of certain lower species (18). Structural experiments by Huet and Cantin (67) have shown that specific secretory granules in atrial cardiomyocytes contain substances of a proteinic nature. These results have been confirmed by De Bold (38). Marie et al. (95) have established that the atrial granule population varies with water and salt intake: water restriction increases the number of right atrial granules while

sodium loading plus deoxycorticosterone acetate decreases them. These results suggested, for the first time, a possible relationship between specific atrial granules and water and salt balance. They too were later confirmed by De Bold (35). In 1981, De Bold et al. (37) made the crucial observation that intravenous administration of rat atrial homogenates to rats culminated in rapid, massive, and short-lived diuresis and natriuresis accompanied by a fall in blood pressure (37). The diuretic and natriuretic properties of the atrial homogenates were rapidly backtracked to the specific endocrine granules (36, 46).

Early physiological studies indicated that cardiac atria played a role in the regulation of renal function, as evidenced by a dramatic increase in urinary excretion when the left atrium was dilated (52, 63). Initially, this effect was linked solely to atrial nerve receptors, but, since animals with denervated hearts or kidneys responded to atrial pressure increases, a hormonal pathway for this "cardio-renal axis" was also suspected (88), provoking a search for an atrial hormone.

BIOCHEMISTRY

The isolation of cardiac hormones was achieved in 1983 and 1984 by several independent laboratories. The ready availability of tissue sources (37) and the natriuretic activity associated with atrial granules (36, 46) strongly

suggested that they represented the storage site. Early studies revealed that ANF is comprised of heat-stable, protease-degradable polypeptides existing in both high- and low-molecular weight forms (36, 137, 140).

Structure of ANF and its precursor

Subsequently, a series of smaller structurally-related peptides, ranging between 21 and 35 amino acid residues, was isolated and sequenced in several laboratories (15, 33, 45, 72, 100, 120). The discrepancy in molecular size and in amino acid composition between these and the larger peptides was due to enzymatic degradation during isolation. Nevertheless all the peptides were biologically active. A number of generic terms other than ANF were proposed for these atrial peptides, including cardionatrin (45), atriopeptin (33) and auriculin (15). Recently, an international committee has suggested the designation ANF (41). A core sequence, including a 17-member ring formed by an intra-chain cystein disulfide bridge, is common to all these related peptides. However they vary in the length of their N- and C- terminal extensions. The human and rat sequences in this region of the precursor are identical, except for a single amino acid: Met is substituted for Ile in position 110 of the rat precursor. Although other forms of biologically active ANF may circulate, the results suggest that the principal low-molecular weight species of immunoreactive ANF (IR-ANF) pre-

sent in blood correspond to the 28-residue peptide, termed ANF (99-126) (119, 138).

MOLECULAR BIOLOGY

The availability of amino acid sequence data enabled several groups to identify and sequence complementary DNA (cDNA) corresponding to the ANF precursor,established from rat or human atrial poly A + (messenger) RNA (mRNA) (93, 122, 151). It was thus predicted early on that rat atrial peptides are derived from a 152-amino acid precursor (pre-pro-ANF) containing a hydrophobic signal peptide (24 residues in the rat), typical of secretory proteins, and the precursor proper (126 amino acids). A C-terminal basic dipeptide (Arg-Arg) has been predicted from rat cDNA but has never been isolated, suggesting that it is subjected to hydrolysis during processing. The remainder of this predicted sequence has, in fact, been validated since the intact 126-residue precursor (pro-ANF) has been purified from rat and human atria and sequenced (73). The human precursor has a similar general structure to that of the rat, although it contains 141 residues, has a longer (25-residue) signal peptide and lacks the C-terminal basic dipeptide (108). The latter finding is accounted for by a single base substitution, resulting in replacement of the first Arg codon in the rat by a termination signal in humans. Thus, both rat and human pro-ANFs contain 126 residues. There is

also nearly complete amino acid homology between the rat and human precursors in the C-terminal portion from which the biologically-active peptides (ANFs) are derived. Considerable differences occur in other portions of the precursor sequence, particularly, the signal peptide.

The nucleotide sequence of the human and mouse gene in cloned genomic DNA was determined by using labeled cloned cDNA as a probe (57, 121). It was thus established that the ANF precursor was derived from three coding sequences (exons) with two intervening sequences (introns) that were spliced during the processing of mRNA. A large intron separates the second coding sequence (which contains nearly the entire coding sequence for the biologically-active ANF peptides) from a third sequence, which codes only for the C-terminal tyrosinyl residue (tyr-Arg-Arg in the rat and mouse). It is noteworthy that a putative glucocorticoid recognition sequence has been identified in the second intron, and there are indications that glucocorticoids may regulate ANF gene expression in certain tissues (51). The ANF gene is localized on the distal half of the short arm of human chromosome 1 and mouse chromosome 4 (148).

SECRETION AND METABOLISM

The current understanding of ANF biosynthesis and storage is based on rather fragmented and, in some cases, contradictory observations, so that only tentative conclusions

can be offered. Using highly-stringent extraction conditions, Flynn and his co-workers found that the intact 126-residue precursor is by far the major form present in atrial tissue, with only small amounts of low-molecular weight peptide (Ser99-Tyr126) being isolated (44). Recently, Thibault et al. (138) isolated atrial granules on a sucrose gradient and clearly demonstrated that the intragranular form is composed solely of pro-ANF (Asn1-Tyr126). Interestingly, the peptide lacks the peptide signal and the two arginines which are present in the mRNA and gene of rats (as mentioned above). Based on findings in plasma, where ANF (Ser99-Tyr126) is the major constituent, it is assumed that the low-molecular weight form is mainly released, so that if the precursor is actually the major storage form, rapid proteolytic cleavage must in some way be linked to the process of secretion. Alternatively, it is possible that the precursor is released and rapidly processed in the extracellular space. Two membrane enzymes have been claimed to be putative processors of pro-ANF (17, 31). Human plasma kallikrein and thrombin also seem to cleave the ANF precursor, generating ANF (Ser99-Tyr126) (99) . The ANFs secreted by atrial cardiocytes appear to be of the high-molecular weight form (55) while in isolated hearts (Langensdorff preparation) they are of low-molecular weight (33). Because only the low-molecular weight form of ANF is detected in the coronary sinus (146),

it is likely that extracellular processing of pro-ANF occurs in cardiocytes plasmalemma or endothelial cells.

IR-ANF concentrations have been found to be markedly elevated in the coronary sinus, compared to peripheral blood, indicating that ANF secreted by either the left or right atrium may be released into the right atrial chamber (147). Other routes of release are likely to exist because (as will be discussed in the section on ANF localization) many other tissues contain IR-ANF . Various manoeuvres have been shown to acutely increase peripheral plasma ANF levels in intact animals and humans. The stimuli used included acute blood volume expansion in rats (81), mechanical distension of the left atrium in dogs (83), infusion of pressor agents, such as vasopressin (94) and angiotensin II (94), leading to elevations of right and left atrial pressure (94), and head -out-of-water immersion of humans (43), a manoeuvre known to augment cardiopulmonary blood volume (42). A common denominator of all these manoeuvres is an increase in atrial wall tension, a mechanism for release that has been demonstrated in the isolated heart (81, 40). Chronic changes in water and sodium homeostasis are more complex to interpret. Water deprivation decreases plasma levels of IR-ANF (69) which can be restored in minutes by rehydration (69). Rats kept for weeks on high, low or normal sodium diets modify their sodium balance accordingly, but

plasma ANF levels remain constant (90). Similarly, chronic changes in sodium balance in dogs are not accompanied by alterations in plasma ANF (114). As described in the section on molecular biology, glucocorticoids indeed stimulate not only mRNA content (51) but also circulating levels of ANF as well as its synthesis (80).

Because of the well known phenomenon of mineralocorticoid escape, observed in patients treated with these steroids, it has been hypothesized that ANF could be involved. These results are, however, inconsistent. Plasma ANF levels can be normal (16) or high in mineralocorticoid-treated rats. The effects of anesthesia have also been investigated. Horky et al. (66) have demonstrated that morphine, diethyl ether, chloral hydrate and ketamine chlorhydrate induce a substantial increase in plasma ANF whereas sodium pentobarbital and urethane decrease it. The effect of morphine is blocked by specific antagonists (59). The underlying mechanisms are yet unknown, but it appears that the central nervous system plays a role in ANF secretion. In this regard, it has been demonstrated that hypophysectomy blocks ANF release induced by volume expansion, which is fully restored if the anterior pituitary is reimplanted (149). Bilateral adrenalectomy has no effect (149) suggesting, that pituitary hormones mediate in part, the release of ANF.

The intracellular pathway responsible for the secretion

of ANF by atrial cardiocytes seems to be related to phosphoinositides and cyclic adenosine monophosphate (cAMP) systems. In two consecutive reports, Ruskoaho et al., have demonstrated that phorbol ester, calcium ionophore, the voltage-sensitive calcium channel agonist, BAIK-8644, and forskolin stimulate ANF secretion from isolated perfused hearts (111, 112). The latter stimulates adenylate cyclase via a non-receptor mediated mechanism and the former mobilizes calcium and activates protein kinase c.

ANF release from atrial minces was studied to avoid hemodynamic changes and to identify the possible involvement of a neuronal mechanism. Because α adrenergic and cholinergic drugs and vasopressin were able to stimulate ANF secretion from isolated atria (130), a receptor-mediated phenomenon was suggested. However, these results, could not be reproduced by others (80). Sodium stimulates the release of atrial ANF (13).

ANF levels in plasma are now well-established to range from 10 to 40 pmol/l in rats (66) and from 17 to 27 pmol/l in dogs (98). In humans, on a normal sodium diet, plasma ANF concentrations are between 2 to 13 pmol/l (146). However, in early studies, there was a marked discrepancy in plasma ANF levels which ranged from 1 pmol/l (125) to 2 nmol/l (58). Higher values have generally been obtained by direct radioimmunoassay of unextracted plasma, most likely due to

nonspecific cross-reacting substances. The most common extraction procedure has involved the use of octadecylsilane (C18) cartridges (44). As described earlier, anesthetics also play a significant role (66).

ANF metabolism has been studied in vivo and in vitro. It is not surprising that the disappearance of ANF from blood is rapid, in the order of 1-5 min in humans (147) and between 16 to 27 sec in conscious (89) and anesthetized rats (102), because 125I-ANF (101-126) binding sites are present in many organs and tissues (19). The roles of degradation and metabolites generated are not yet fully established. Whole blood is not, however, a major degrading system because 125I-ANF (99-126) is transformed very slowly into ANF (103-126), which is also biologically active (101).

The disappearance of ANF from blood is enhanced (89) or not modified (102) in anephric rats. The peptide is rapidly hydrolysed in kidney homogenates (61) and renal sections incubated in vitro for radioautography (Bianchi et al., unpublished results). Recently, it has been demonstrated that a neutral endopeptidase (EC 3.4.24.11) from the brush borders of proximal tubules in pigs hydrolyzes ANF, generating a biologically-inactive fragment (132). This degradative pathway does not seem to be receptor-mediated because proximal tubules are devoid of ANF binding sites (19). Degradation occurs when 125I-ANF (99-126) is injected

into isolated mesenteric arteries, mimicking, to some extent, its metabolism *in vivo* (101).

PHYSIOLOGY AND PHARMACOLOGY

Kidney

Because atrial extracts exert potent diuretic and natriuretic activities and decrease blood pressure (37) it is clear that the kidney and cardiovascular system are major target organs. These effects were used as tools to evaluate the biological activities of isolated and synthetic peptides until the development of specific radioimmunoassays.

The renal actions of ANF are multifactorial and as such are not yet fully understood. In animals and humans, administration of synthetic ANF produces natriuresis and diuresis similarly to atrial extracts. In early studies, huge increases in the excretion of sodium, potassium, phosphorus, magnesium and calcium were noted, suggesting that the transport functions of proximal tubules (75) as well as papillary sodium transport were inhibited by ANF (129). When isolated kidneys were perfused with ANF in the presence of vasoconstrictors, a significant reduction in renal vascular resistance was observed (24). It was also proposed that ANF had a weak vasoconstrictor action and that the mechanism was Ca^{+}-dependent (92). The glomerular filtration rate (GFR) increased mainly due to selective vasodilation of afferent arterioles and vasoconstriction of efferent arterioles (23).

Using labeled microspheres, it was found that atrial extracts significantly increased inner cortical blood flow and decrease outer cortex blood flow (21). The uptake of labeled albumin by the inner medulla was augmented , suggesting an increase in blood flow in this part of the nephron (21). Up to now, the influence of the GFR, cortical versus medullary blood flow, and the papillary transport of sodium has been considered together or independently, as major mechanisms by which ANF exerts its diuretic and natriuretic effects. To quote T. Maack and H.D. Kleinert (91), "the localization of specific receptors for ANF in the kidney and the elucidation of the kinetics of receptor-ANF interactions in particular structures of the kidney may be decisive pieces of information to fully understand the physiological role of ANF and the mechanisms of the renal effects of ANF". As seen in Chapter 3 Sections A and B, and in the general discussion, we have contributed to the elucidation of possible mechanisms involved in the renal actions of ANF.

Cardiovascular system

The vasorelaxant activity of ANF was clearly demonstrated when synthetic peptides became available (49). Although crude atrial extracts (32) and partially purified ANF (47) exert vasorelaxant effects on precontracted vascular strips, the presence of a contaminant which had spasmolytic activity could not be ruled out.

Heterogenous responses of different vascular segments have been reported (49). The presence of high-affinity ANF vascular receptors in membranes (103) and the specific binding of ^{125}I-ANF under *in vivo* radioautography (19) confirmed the hypothesis of a receptor-mediated phenomenon. Although vasorelaxation was not dependent on the integrity of the endothelium (118), binding sites for ^{125}I-ANF were detected in both endothelial and smooth muscle cells in several organs (19).

The spasmolytic effect of ANF is less pronounced in resistance vessels of the brain and mesenteric territories compared to renal arteries (1). *In vivo* studies have demonstrated that ANF decreases peripheral vascular resistance, suggesting an action in the resistance vessels (65) of dogs which had their autonomic compensatory reflex attenuated. Venous tone is also affected by ANF but to a lesser extent than arteries (144). ANF counteracts the effects of vasoconstrictors, and is a particularly powerful antagonist of angiotensin II-induced contraction of rabbit aorta strips (77). Structure-activity studies have indicated the relative importance of the C- and N-terminal of the ANF molecule for vasorelaxation of isolated strips of rabbit aorta (145). Tyr126 is of little importance, whereas deletion of Phe124-Arg125 significantly reduces the vasoactive and natriuretic effects of ANF (26, 32, 134). Deletion of the

N-terminal up to Ser^{103} does not change the relative biological activity of ANF (26). The order of apparent vasorelaxant activity of ANF in the rabbit aorta may be summarized as follows: ANF (99-126) = ANF (100-126) = ANF (101-126) > ANF (102-126) = ANF (102-125) > ANF (103-126) = ANF (103-125) >>> ANF (103-123). The disulfide bridge between Cys^{105} and Cys^{121} is essential for vasorelaxant and for all the known biological activities of ANF (28).

In normotensive animals, ANF consistently decreases blood pressure but to a relatively low extent (26, 37, 92). The hemodynamic mechanisms of ANF responsible for reducing blood pressure have not been fully elucidated. The pioneering work of Ackermann et al. (3) has shown that the blood pressure decrease by atrial extracts in anesthetized rats is mainly due to a fall in cardiac output. In vagotomized rats, the hypotensive effect is less pronunced, suggesting a reduction in total peripheral resistance. In addition, denervation of the carotid sinus potentiates the hypotensive effect of atrial extracts, indicating a direct vasodilatory action of ANF on peripheral vascular resistance which is not compensated by an increase in cardiac performance. In conscious rats, electromagnetic flow probes have revealed that ANF decreases cardiac output and enhances vascular peripheral resistance (82). The same is true in conscious sheep (22). In sympathectomized rats, ANF slightly reduces total

peripheral resistance but this effect is not evident in intact rats (116). The decrease in blood pressure do not, however, seem to be a consequence of the diuretic effect of ANF because it occurs before any significant urinary losses (92), and their replacement does not restore blood pressure to normal levels (92). Using radiolabeled microspheres, it has been observed that ANF administration to normotensive rats elicits no significant changes in cardiac output but increases renal blood flow and diminishes total peripheral resistance (48). Thus, the effects of ANF on the cardiovascular system are due to a decrease in cardiac output, although it has no direct negative inotropic impact on cardiac muscles (104). The reduction in total peripheral vascular resistance may explain the small, albeit significant hypotensive action of ANF. The discrepancies between the powerful effects of ANF in the relaxation of precontracted arteries *in vitro* and the small decrease in blood pressure *in vivo* are due to counteraction of the baroreceptor-mediated increase in sympathetic activity.

INTERACTION WITH OTHER HORMONAL SYSTEMS

Adrenal cortex

Atrial extracts (14) and synthetic ANF (29) are powerful inhibitors of rat aldosterone secretion stimulated by angiotensin II *in vivo* (29) as well as *in vitro* (28) and suppress cortisol secretion in bovine (39) adrenal zona

glomerulosa stimulated by angiotensin II, potassium, prostaglandins and adrenocorticotropic hormone. Although the depressive effect of ANF on aldosterone secretion has been demonstrated, its influence on basal levels *in vitro* is controversial since some investigators have reported an inhibition (14) whereas others have recorded little or no change (28). The presence of specific, high affinity receptors in membranes from the adrenal zona glomerulosa of cows (39) and rats (117), and the inhibitory potency of ANF, suggest that its effects are receptor-mediated. These results have also been confirmed *in vivo* in rats, in which ^{125}I-ANF binding sites were localized on adrenal zona glomerulosa cells (19). Basal aldosterone secretion is not inhibited by ANF infusions *in vivo*, but the peptide suppresses aldosterone release stimulated by angiotensin II (14), potassium (135) and in sodium depletion in rats (30). The inhibition of aldosterone secretion by ANF *in vitro* suggests that this hormone blocks either the early pathway (110), or both the early and late pathways (25).

Pituitary

There is, unfortunately, no evidence of an effect of ANF on hormones of the anterior and intermediate lobes of the pituitary. The reported action of ANF on the release of adrenocorticotropic hormone, endorphin and corticotropin-releasing factor (126) appears to be due to contamination of

ANF by a potent gonadotropin-releasing hormone agonist (2). ANF stimulates cyclic GMP production in anterior pituitary cells (2) and inhibits adenylate cyclase activity (5).

In the isolated rat posterior pituitary, ANF inhibits basal and potassium- and angiotensin II-stimulated vasopressin release (106). In the cultured hypothalamo-neurohypophysial complex, the peptide suppresses vasopressin release stimulated by an increase in osmolarity at the hypothalamic site (68). Intravascular ANF injections significantly inhibit the elevation of plasma vasopressin induced by water deprivation and hemorrhage (53). The concentrations used (higher than 5 µg) are far above the normal values of IR-ANF in plasma. Intracerebroventricular injections of ANF suppress vasopressin release without affecting arterial pressure, plasma osmolarity and sodium levels (124).

Renin

The actions of ANF on renin release are still controversial. Studies on kidney slices are contradictory, since either an increase (107) or a decrease (24) in renin secretion is evoked . Antonipillai et al. (11) were unable to observe any inhibitory effect of ANF on basal renin release, but the peptide potentiated the suppressive action of angiotensin II. In cultured rat juxtaglomerular cells, ANF inhibits renin secretion at picomolar concentrations (79).

<u>In vivo</u> investigations have demonstrated that ANF inhi-

bits renin release in dogs with denervated, non-filtering kidneys (141), suggesting that its effects are not mediated by the macula densa which seems to be devoid of ANF binding sites (19).

LOCALIZATION OF ANF

The synthesis of ANF made it possible to raise specific antibodies against its molecules, and the labeling of these peptides facilitated the development of specific radioimmunoassays. Cloned cDNA has become available, and specific mRNA for ANF has been assesed in several tissues. As would be expected, IR-ANF has been detected in high concentrations in atrial tissues (58). However, other tissues, are now known to possess IR-ANF and ANF mRNA. They include the cardiac ventricle, anterior pituitary, lung, aortic arch, brain, eye, kidneys, adrenal medulla and sympathetic nervous system.

IR-ANF is detected by immunocytochemistry in the whole heart (53). Ventricle homogenates do not display diuretic and natriuretic activity probably because ventricular ANF is much lower than atrial ANF and bioassays have a low sensitivity. These reasons may explain why De Bold (37) was able to use ventricular extracts as negative controls. Recently, <u>in situ</u> hybridization with specific 32p-labeled ANF cDNA probes revealed that atrial cardiocytes account for about 100-fold more mRNA than ventricular tissues (105). The

molecular weight of ventricular ANF, as assessed by high performance liquid chromatography, is similar to that of atrial ANF, eluting at a position similar to the pro-hormone (ANF 1-126) (105).

The first report on extracardiac ANF peptides originated from specific radioimmunoassays of the rat hypothalamus (136). Rats fed a high salt diet had lower IR-ANF in the brain and higher plasma ANF, suggesting depletion of ANF. Immunocytochemical studies from brain sections revealed an extensive network of cell bodies and nerve fibers in several brain regions. Skofitch et al. (128), Saper et al. (115) and Standaert et al. (131) mapped the distribution of the IR-ANF. All these investigators agreed that the largest collection of IR-ANF neurons was indeed localized in the hypothalamus, as demonstrated earlier by Tanaka et al. (136). In these brain regions, neurons and fibers containing IR-ANF were observed adjacent to the anteroventral tip of the third ventricle, in the wall and in the paraventricular and caudate nuclei. The densest IR-ANF fibers were seen in the paraventricular nucleus of the hypothalamus, the bed nucleus of the stria terminalis, the median eminence, and the interpeduncular nucleus. IR-ANF neurons were also found in the lateral hypothalamic area, in the mammilary nuclei and central nucleus of the amygdala. Neurons of the pons and brain stem were immunoreactive to ANF antibodies. The molecular

forms of brain ANF are not yet well characterized, but brain ANF appears to be shorter than plasma ANF, as deduced from the high performance liquid chromatographic elution profile (127). Two major forms are present with high and low molecular weights. The former is comprised of pro-ANF (56) and the latter of a 24- and 25 amino-acid C-terminal (127). The anatomical distribution of IR-ANF in the antero ventral third ventricle region suggests that the peptide may well be implicated in the central regulation of the cardiovascular system.

IR-ANF has also been detected in the eye. There is about 31 and 8 ng/g of ANF wet tissue in the anterior uvea and retina, respectively. The reverse phase high performance liquid chromatographic elution profile suggests that 28-amino acid C-terminal ANF is the major form (133). Since no immunohistochemical studies have been performed on the eye, the localization of this ANF-like material is not yet known, making it difficult to ascertain its role. Because the major ANF-like peptide has a hydrophobicity similar to that of ANF (99-126), which circulates in rats, it is possible that this immunoreactive material may originate, in part, from circulating ANF bound to cells in the eyes (19).

IR-ANF has been detected in the kidney cortex by radioimmunoassay (113), in brush border proximal tubules of the cortex and collecting ducts of the renal medulla by

immunocytochemistry (96). Here again, as in the eye, but not in the brain, the ANF-like material is of low molecular weight indicating its possible origin from plasma. There is no correlation, however, with the localization of ANF binding sites in the kidney. IR-ANF in proximal tubules correlates with a high non specific uptake of ^{125}I-ANF (101-126) in brush border membranes, whereas in distal and collecting tubules it corresponds to the presence of ANF binding sites. Surprisingly ANF-like material is not evident in renal glomeruli (96), suggesting either the degradation of bound ANF by glomerular target cells, its dissociation, or both. Thus, the presence of low -molecular weight ANF-like material in the kidney may reflect an accumulation of filtered hormone (proximal tubules) or bound peptide in putative target cells (collecting tubules) (129).

IR-ANF has also been detected in the lung (113), anterior pituitary (96) and aortic arch (50). Since high-molecular weight ANF has been found in the lung (113), it is likely that this organ is a site of ANF synthesis, while in the pituitary, the origin of the ANF-like material is not yet known. ANF mRNA has been noted in the aortic arch (50), suggesting its local production in the adventitia of the aorta. Because the baroreceptors are believed to be localized in the latter, it is possible that ANF may play a role in modulating the baroreceptor reflex. Immunoreactive

ANF-like material has also been found in the adrenal medulla (96) and sympathetic ganglia (34), implicating the peptide in modulation of the sympathetic nervous system.

PUTATIVE SECOND MESSENGERS

There is some evidence of the involvement of two second messengers in ANFs actions on several tissues and organs. They are represented by the guanylate cyclase and adenylate cyclase systems.

Guanylate cyclase

Guanylate cyclases are composed of two isoenzymes. Although both enzymes are responsible for the conversion of GTP to cGMP, which activates a cGMP-dependent protein kinase resulting in the phosphorylation of specific intracellular proteins, they are different entities. The isoenzyme present in cytosol is soluble guanylate cyclase, while its counterpart in cell membranes is particulate guanylate cyclase. The soluble enzyme is activated by nitrovasodilators and endothelium dependent-vasodilators, whereas the particulate form is known to be activated by a heat-stable ST enterotoxin from Escherichia coli. ANF is the second peptide and the first hormone known to activate particulate guanylate cyclase.

The first indication that ANF increases cGMP came from the laboratory of Hamet and his team (60). In 1984, they

demonstrated that ANF elevates cGMP in kidney slices and in primary cultures of renal cortical cells. They also showed that ANF enhances urinary cGMP excretion in intact rats. Waldman et al. (143) reported that ANF increased cGMP by activating of particulate guanylate cyclase in a number of rat tissues, such as the kidney, lung, liver, small intestine and testes. Similar results were obtanined in the rat adrenal cortex (142) and aorta (145).

Between 2 and 10 nM of ANF were necessary to increase 50% of the maximum response in a concentration-dependent manner (145). In different kidney fractions from dogs, it was also demonstrated that the rise in cGMP correlated with the distribution of particulate guanylate cyclase, which was much higher in isolated glomeruli followed by the collecting tubules and loop of Henle (139). Other studies attempting to purify the ANF receptor from rat lung demonstrated that a solubilized ANF binding protein with a molecular weight of 130 kda retained binding to 125I-ANF. Because particulate guanylate cyclase and the 130 Kda ANF binding protein had similar biochemical properties, it was suggested that the ANF receptor and the enzyme resided in the same transmembrane glycoprotein complex (78). In rat lung fibroblasts, it was shown that ANF elevated cGMP levels by 100-fold, which corresponded to a 10-fold increase in particulate guanylate cyclase, without any effect on the soluble form (84).

Furthermore, sodium nitroprusside increased cGMP by 500-fold and activated soluble guanylate cyclase. Conjointly ANF and sodium nitroprusside exerted additive effects. It was concluded that these two vasodilators increased cGMP levels by activating different isoenzymes of guanylate cyclase.

The presence of an heterogenous population of ANF receptors was first proposed by Leitman et al. (85). These investigators reported that, in endothelial cells from bovine aorta in culture, ANF (103-123) competed for the majority of ANF receptors but did not antagonize the effect of ANF (101-126) on cGMP accumulation. This finding was later confirmed by affinity cross-linking techniques which demonstrated the presence of two ^{125}I-ANF binding proteins with molecular weights of 130 kda and 60 Kda respectively under non-reducing conditions (85). Under reducing conditions, three distinct forms of ANF binding protein were revealed. They comprised an unreduced minor component of 130 kda, two major components of reduceable 130 kda (in two 60 kda), and a non-reduceable 66 kda. Because ANF (103-123) was able to compete for the majority of ANF binding sites in cultured cells but was a very weak activator of particulate guanylate cyclase (85), additional cross-linking studies were performed using as displacing substances ANF (101-126) and ANF (103-123). It was clearly demonstrated that ANF (103-123) competed with very high affinity for the ANF

binding protein of 60-66 kda at nanomolar concentration, but was a very weak activator of particulate guanylate cyclase (85). In contrast, ANF (101-126) competed for the non-reduceable 130 Kda binding protein and activated particulate guanylate cyclase over 400-fold. Because ANF (103-123) was very weak in competing for the 130 kda protein while ANF (101-126) competed for both the 130 kda and 66 kda protein with similar affinities, these results strongly suggest that the nonreduceable 130 kda binding protein is the ANF receptor coupled to guanylate cyclase.

Since the activation of particulate guanylate cyclase requires a GTP binding site, parallel studies were conducted to investigate if there was a relationship between the three binding proteins revealed in the cross-linking experiments and their ability to bind to GTP-affinity chromatographic columns. Indeed, it was demonstrated that the unreduceable 130 kda binding protein was retained in the GTP-affinity columns while the reduceable 130 kda and the unreduceable 66 kda did not possess GTP-binding sites. In addition, when the 130 kda binding protein was eluted by GTP, the specific activity of particulate guanylate cyclase were increased by more than 40-fold (86).

The role of cGMP in mediating the physiologic effects of ANF is not yet clearly understood. The spasmolytic activity of ANF seems to be related to an increase in cGMP because

such as vasodilators as sodium nitroprusside, elevate cGMP through activation of guanylate cyclase (soluble form). The molecular mechanism whereby cGMP promotes vascular relaxation is not yet known, but it is assumed that calcium flux could be involved (87). The effects of ANF, bradykinin and vasopressin on calcium in cultured endothelial cells suggest that ANF has no influence on either resting calcium concentrations or on the rise in cytosolic calcium in response to vasopressin or bradykinin (87). In rat smooth muscle cells, ANF is unable to affect basal calcium levels or angiotensin II-or vasopressin-stimulated cytosolic calcium (27). Although it is likely that cGMP is the second messenger for ANF's spasmolytic activity, the molecular events are unknown.

ANF increases cGMP in the kidney, which correlates with diuresis and natriuresis, suggesting a relationship between cGMP and the renal effects of the peptide. When ANF is injected intra renaly in only one dog kidney, both kidneys react to a rise in urinary cGMP while only the injected kidney responds with natriuresis (123). These results indicate that the cGMP elevation observed in the non-injected kidney is originally from an extra-renal source and does not mediate the renal effects of ANF. It has recently, been demonstrated that 8-bromo-cGMP (a cGMP analog that penetrates the cell) is a potent inhibitor of angiotensin II-induced con-

traction of rat mesangial cells (12) and an inhibitor of sodium entry in rabbit papillary collecting ducts (150). Thus, it appears that the discrepancies in the results on cGMP may be due to the fact that 8-bromo-cGMP, but not cGMP, penetrates the cell interior.

Adenylate cyclase

The adenylate cyclase system is composed of three distinct and separate components: a hormone receptor, a GTP-binding protein, and adenylate cyclase which catalyzes the conversion of ATP to cAMP. The GTP-binding protein is composed of stimulatory guanine nucleotide regulatory protein (Gs) that mediates the activation of adenylate cyclase by stimulatory agents, and an inhibitory guanine nucleotide regulatory protein (Gi) that suppresses adenylate cyclase activation in response to inhibitory agents (54).

The first report that ANF inhibits basal and stimulated adenylate cyclase activity was derived from studies on vascular tissue (4). Conversely, ANF had no influence on adenylate cyclase activity in the spleen, skeletal muscle, adrenal medulla and testes. This effect was later extended to the heart sarcolemma (8), adrenal cortical membranes (6) and pituitary gland (5).

In the dog kidney, ANF inhibits the activity of adenylate cyclase in isolated glomeruli, collecting tubules and loop of Henle without any action on proximal tubules or

whole kidney membranes (9). As we will see in Chapter 4, the peptide decreases adenylate cyclase activity in the ciliary process of the rabbit. These effects are observed whether at basal levels or after stimulation by several agonists, such as forskolin, epinephrine, norepinephrine, isoproterenol and dopamine. The apparent inhibition constant ranges between 100 pM and 10 nM and maximum inhibition is between 20 and 60%. Recent studies indicate that the effect of ANF on adenylate cyclase activity is due to ANF receptor coupling to Gi. Ninhibin, a factor isolated from bovine sperm (74), and pertussin toxin (71), which inactivates Gi, attenuate the ANF-mediated inhibition of adenylate cyclase in aorta membranes (7, 10). These results on ANF inhibition of adenylate cyclase activity have been confirmed in adrenal cortical membranes (142) and the posterior pituitary (107), but not in the anterior pituitary (62). In the latter, the inability of ANF to suppress adenylate cyclase activity is due to the high concentrations of GTP (300 μM) used (53).

Although there is clear evidence of the negative coupling of ANF receptors on adenylate cyclase through Gi, its significance in the physiological effects of ANF remains to be elucidated.

LOCALIZATION OF ANF-BINDING SITES: OUR OWN WORK

In 1984, the synthetic, biologically-active ANF fragment (Ser^{101}-Tyr^{126}) became available. This peptide was iodinated

Table 1. Localization of ANF binding sites in rats

ORGAN	TARGET CELL
Heart	Endocardium of four heart chambers.
Lung	Endothelial and smooth muscle cells of arteries, arterioles, veins, venules, and endothelium of alveolar capillaries.
Adrenal	Zona glomerulosa cells; adrenal medulla; smooth muscle cells and endothelial cells of arteries, arterioles, veins, venules and endothelium of capillaries.
Kidney	Glomerular capillaries; endothelial and smooth muscle cells of arteries, arterioles, veins, venules and endothelium of capillaries. Vasa recta in the outer and inner medulla.
Liver	Endothelium and smooth muscle cells of arteries, arterioles, veins, venules and endothelium of capillaries; hepatocytes.
Small intestine	Mature columnar epithelium of villi.
Colon	Smooth muscle cells of the muscularis layer.
Eye	Epithelium of the ciliary body.

at Tyr^{126} and used as a radioligand in binding studies on membranes and in in vivo radioautography of intact rats (19). The latter technique demonstrated that ^{125}I-ANF binding sites were localized in many peripheral tissues and cells. These results are summarized in Table I.

Since the conditions for in vivo radioautography of ^{125}I-ANF were established in rats, we started a long series of investigations which constitute this thesis. Once the target cells were identified, we set up quantitative in vitro radioautographic equipment coupled to a computerized microdensitometer in an attempt to, pharmacologically, characterize the ANF-binding sites present in the small intestine. These results appear in Chapter 5.

RESEARCH GOALS

The mechanism of action of hormones and the target cells involved has been readily identified with the development of radioligand binding techniques for the study of hormone receptors. One of the important questions is the localization of these receptors at the anatomical and cellular levels. Although biochemical procedures together with microdissection provide excellent information on the organ and region distribution of receptors, they are limited in their anatomical resolution in highly-organized organs which are built up of distinct cell types. Radioautographic techniques both *in vivo* and *in vitro* have addressed some of these problems.

Since ANF is a circulating hormone and because the electron microscope has a greater resolution than light microscopy, we felt that *in vivo* radioautography at the light and electron microscopic level would be the technique of choice for the localization of ANF binding sites in rats. It was thus decided that the distribution of ANF binding sites would be studied in the brain, kidneys, eye and small intestine. In the brain, the technical approach was modified to allow the use of paraffin sections (5 μm), and this organ could only be investigated at the light microscopic level, with a better resolution than *in vitro* radioautography but an inability to visualize binding sites located inside the blood-brain barrier. In the remaining organs,

both light and electron microscope radioautography were employed. In the small intestine,the results of light and electron microscopy were corroborated by *in vitro* radioautography which allows the pharmacological characterization of binding sites.

REFERENCES

1. Aalkjaer, C., Mulvany, M.J., Nyborg, N.C.B. Atrial natriuretic factor causes specific relaxation of rat renal arcuate arteries. Br. J. Pharmacol. 86:447-453,1985.

2. Abou-Samra, A.B., Catt, K.J., Aguilera, G. Synthetic atrial natriuretic factors (ANFs) stimulate guanine 3', 5'- monophosphate production but not hormone release in rat pituitary cells: Peptide contamination with a gonadotropin- releasing hormone agonist explains luteinizing hormone-releasing activity of certain ANFs. Endocrinology. 120:18-24, 1987.

3. Ackermann, U., Irizama, T.G., Milojevic, S., Sonnenberg, H. Cardiovascular effects of atrial extracts in anaesthetized rats. Can. J. Physiol. Pharmacol. 62:819-826, 1984.

4. Anand-Srivastava, M.B., Franks, D.J., Cantin, M., Genest, J. Atrial natriuretic factor inhibits adenylate cyclase activity. Biochem. Biophys. Res. Commun. 121:855-862, 1984.

5. Anand-Srivastava, M.B., Cantin, M., Genest, J. Inhibition of pituitary adenylate cyclase by atrial natriuretic factor. Life Sci. 36:1873-1879, 1985.

6. Anand-Srivastava, M.B., Genest, J., Cantin, M. Inhi-

bitory effect of atrial natriuretic factor on adenylate cyclase activity in adrenal cortical membranes. FEBS Lett. 181:199-202, 1985.

7. Anand-Srivastava, M.B., Johnson, R.A., Picard, S., Cantin, M. Ninhibin: a sperm factor attenuates the atrial natriuretic factor mediated inhibition of adenylate cyclase: possible involvement of inhibitory guanine nucleotide regulatory protein. Biochem. Biophys. Res. Commun. 129:171-178, 1985.

8. Anand-Srivastava, M.B., Cantin, M. Atrial natriuretic factor receptors are negatively coupled to adenylate cyclase in cultured atrial and ventricular cardiocytes. Biochem. Biophys. Res. Commun. 138:427-436, 1986.

9. Anand-Srivastava, M.B., Vinay, P., Genest, J., Cantin, M. Effect of atrial natriuretic factor on adenylate cyclase in various nephron segments. Am. J. Physiol. 251:F417-F423, 1986.

10. Anand-Srivastava, M.B., Srivastava, A.K., Cantin, M. Pertussis toxin attenuates atrial natriuretic factor-mediated inhibition of adenylate cyclase: involvement of inhibitory guanine nucleotide regulatory protein. J. Biol. Chem. 262:4931-4934, 1987.

11. Antonipillai, I., Vogelsang, J., Horton, R. Role of atrial natriuretic factor in renin release. Endocri-

nology. 119:318-322, 1986.

12. Appel, R.G., Wang, J., Simonson, M.S., Dunn, M.J. A mechanism by which atrial natriuretic factor mediates its glomerular actions. Am. J. Physiol. 251:F1036-F1042, 1986.

13. Arjamaa, O., Vuoteenaho, O. Sodium ion stimulates the release of atrial natriuretic polypeptides (ANP) from rat atria. Biochem. Biophys. Res. Commun. 132:375-381, 1985.

14. Atarashi, K., Mulrow, P.J., Franco-Saenz, R. Effect of atrial peptides on aldosterone production. J. Clin. Invest. 76:1807-1811, 1985.

15. Atlas, S.A., Kleinert, H.D., Camargo, M.J., Januszewicz, A., Sealey, J.E., Laragh, J.H., Schilling, J.W., Lewiki, J.A., Johnson, L.K., Maack, T. Purification, sequencing and synthesis of natriuretic and vasoactive rat atrial peptide. Nature. 309:717-719, 1984.

16. Ballermann, B.J., Bloch, K.D., Leidman, J.G., Brenner, B.M. Atrial natriuretic transcription, secretion and glomerular receptor activity during mineralocorticoid scape in the rat. J. Clin. Invest. 78:840-843, 1986.

17. Baxter, J.H., Wilson, I.B., Harris, R.B. Identification of an endogenous protease that processes atrial

natriuretic factor at its aminoterminus. Peptides. 7:407-411, 1986.

18. Bencosme, S.A., Berger, J.M. Specific granules in mammalian and non-mammalian vertebrate cardiocytes. In Meth. Achievm. Exp. Path. Edited by Bajusz, E. and Jasmin, G. Basel: Karger. 5:173-213, 1971.

19. Bianchi, C., Gutkowska, J., Garcia, R., Thibault, G., Genest, J., Cantin, M. Radioautographic localization of ^{125}I-atrial natriuretic factor (ANF) in rat tissues. Histochemistry. 82:441-452, 1985.

20. Bompiani, G.D., Roviller, C.H., Hatt, P.Y. Le tissue de conduction du coeur chez le rat. Étude au microscope électronique. I. Le tronc commun du faisceau de Hiss et les celllules claires de l'oreillette droite. Arch. Mal. Coeur. 52:1257-1274, 1959.

21. Borenstein, H.B., Cupples, W.A., Sonnenberg, H., Veress, A.T. The effect of a natriuretic atrial extract on renal haemodynamics and urinary excretion in anaesthetized rats. J. Physiol. 334:133-140, 1983.

22. Breuhaus, B.A., Saneii, H.H., Brandt, M.A., Chimoskey, J.E. Atriopeptin II lowers cardiac output in conscious sheep. Am. J. Physiol. 249:R776-R780, 1985.

23. Camargo, M.J.F., Atlas, S.A., Maack, T. Role of

increase glomerular filtration rate in atrial natriuretic factor- induced natriuresis in the rat. Life Sci. 38:2397-2404, 1986.

24. Camargo, M.J.F., Kleinert, H.D., Atlas, S.A., Sealey, J.E., Laragh, J.H., Maack, T. Ca-dependent hemodynamic and natriuretic effects of atrial extract in isolated rat kidney. Am. J. Physiol. 246:F447-F456, 1984.

25. Campbell, W.B., Currie, M.G., Needleman, P. Inhibition of aldosterone biosynthesis by atriopeptins in rat adrenal cells. Clin. Res. 57:113-118,1985.

26. Cantin, M., Genest, J. The heart and the atrial natriuretic factor. Endocr. Rev. 6:107-126, 1985.

27. Capponi, A.M., Lew, P.D., Wurtrich, R., Vallotton, M.B. Effects of atrial natriuretic peptide on the stimulation by angiotensin II of various target cells. J. Hypertension 4:561-565, 1986.

28. Chartier, L., Schiffrin, E.L., Thibault, G. Effect of atrial natriuretic factor (ANF)- related peptides on aldosterone secretion by adrenal glomerulosa cells: Critical role of the ultramolecular disulphide bridge. Biochem. Biophys. Res. Commun. 122:171-174, 1984.

29. Chartier, L., Schiffrin, E.L., Thibault, G., Garcia, R. Atrial natriuretic factor inhibits the stimula-

tion of aldosterone secretion by angiotensin II, ACTH and potassium in vitro and angiotensin II-induced steroidogenesis in vivo. Endocrinology. 115:2026-2028, 1984.

30. Chartier, L., Schiffrin, E.L. Atrial natriuretic peptide inhibits the effect of endogenous angiotensin II on plasma aldosterone in conscious sodium-depleted rats. Clin. Sci. 72:31-35, 1987.

31. Cromlish, J.A., Seidah, N.G., Chrétien M. A novel serine protease (IRCM- serine protease 1) from porcine neurointermediate and anterior pituitary. Lobes isolation, polypeptide chain structure, inhibitory sensitivity and substract specificity. J. Biol. Chem. 261:10850-10858, 1986.

32. Currie, M.G., Geller, D.M., Cole, B.R., Boylan, J.G., Yu Sheng, W., Holmberg, S.W., Needleman, P. Broactive cardiac substances: potent vasorelaxant activity in mammalian atria. Science. 221:71-73, 1983.

33. Currie, M.G., Geller, D.M., Cole, B.R., Siegel, N.R., Fok, K.K., Adams, S.P., Eubanks, S.R., Gallupi, G.R., Needleman, P. Purification and sequence analysis of bioactive atrial peptides (atriopeptins). Science. 223:67-69, 1984.

34. Debinski, W., Gutkowska, J., Kuchel, O., Racz, K.,

Buu, N.T., Cantin, M., Genest, J. ANF-like peptide(s) in the peripheral autonomic nervous system. Biochem. Biophy. Res. Commun. 134:279-284, 1986.

35. De Bold, A.J. Heart atria granularity effects of changes in water-electrolyte balance. Proc. Soc. Exp. Biol. Med. 161:508-511, 1979.

36. De Bold, A.J. Tissue fractionation studies on the relationship between an atrial natriuretic factor and specific granules. Can. J. Physiol. Pharmacol. 60:324-330, 1982.

37. De Bold, A.J., Borenstein, H.B., Veress, A.T., Sonnemberg, H. A rapid and potent natriuretic response to intravenous injection of atrial myocardial extract in rats. Life Sci. 28:89-94, 1981.

38. De Bold, A.J., Raymond, J.J., Bencosme, S.A. Atrial specific microscopic stainning and histochemical reactions. J. Histochem. Cytochem. 26:1094-1102, 1978.

39. De Léan, A., Racz, K., Gutkowska, J., Nguyen, T.T., Cantin, M., Genest, J. Specific receptor-mediated inhibition by synthetic atrial natriuretic factor of hormone-stimulated steroidogenesis in cultured bovine adrenal cells. Endocrinology. 115:1636-1638, 1984.

40. Dietz, J.R. Release of natriuretic factor from rat

heart-lung preparation by atrial natriuretic distension. Am. J. Physiol. 147:R1093-R1096, 1984.

41. Dzau, V.J., Baxter, J.D., Cantin, M., De Bold, A., Ganten, D., Gross, K., Husain, A., Inagami, T., Ménard, J., Poole, S., Robertson, I.I.S., Tang, J., Yamamoto, K. New Engl. J. Med. 316:1278-1279, 1987.
42. Epstein, M. Renal effects of head-out water immersion in man: implications for and understanding of volume homeostasis. Physiol. Rev. 58:529-581, 1978.
43. Epstein, M., Rodger, D.L., Frieland, E., Aceto, R.M., Camargo, M.J.F., Atlas, S.A. Increases in circulating atrial natriuretic factor during immersion-induced central hypervolemia in normal humans. J. Hypertension 4:S93-S99, 1986.
44. Flynn, T.G., Davies, P.L., Kennedy, B.P., De Bold, M.L., De Bold, A.J. Alignment of rat cardionatrin sequences with the preprocardionatrin sequence from complementary DNA. Science. 228:323-325, 1985.
45. Flynn, T.G., De Bold, M.L., De Bold, A.J. The amino acid sequence of an atrial peptide with potent diuretic and natriuretic properties. Biochem. Biophys. Res. Commun. 117:859-865, 1983.
46. Garcia, R., Cantin, M., Thibault, G., Ong, H., Genest, J. Relationship of specific granules to the natriuretic and diuretic activity of rat atria.

Experientia. 38:1071-1073, 1982.

47. Garcia, R., Thibault, G., Cantin, M., Genest, J. Effect of a purified atrial natriuretic factor (ANF) on rat and rabbit vascular strips and vascular beds. Am. J. Physiol. 247:R34-R39, 1984.

48. Garcia, R., Thibault, G., Gutkowska, J., Cantin, M., Genest, J. Changes in regional blood flow induced by atrial natriuretic factor (ANF) in concious rats. Life Sci. 36:1687-1692, 1985.

49. Garcia, R., Thibault, G., Nutt, R.F., Cantin, M., Genest, J. Comparative vasoactive effects on inactive and synthetic atria natriuretic factor (ANF). Biochem. Biophys. Res. Commun. 119:685-688,1984.

50. Gardner, D.G., Deschepper, C.F., Baxter, J.D. The gene for atrial natriuretic factor is expressed in the aortic arch. Hypertension. 9:103-106, 1987.

51. Gardner, D.G., Hane, S., Trachewsky, D., Schenk, D., Baxter, J.D. Atrial natriuretic peptide mRNA is regulated by glucocorticoids in vivo. Biochem. Biophys. Res. Commun. 139:1047-1054, 1986.

52. Gauer, O.H., Henry, J.P. Circulatory basis of fluid volume control. Physiol. Rev. 43:423-481, 1963.

53. Genest, J., Cantin, M. The atrial natriuretic factor:its physiology and biochemistry. In Rev. Phy-

siol. Biochem. Pharmacol. Edited by Innsbruck, H.G., Spring-Verlag, Berlin 110:1-145, 1988.

54. Gilman, A. Guanine nucleotide- binding regulatory proteins and dual control of adenylate cyclase. J. Clin. Invest. 73:1-4, 1984.

55. Glembotski, C.C., Gibson, T.R. Molecular forms of imunoreactive atrial natriuretic peptide released from cultured rat atrial myocytes. Biochem. Biophys. Res. Commun. 132:1008-1017, 1985.

56. Glembotski, C.C., Wildey, G.M., Gibson, T.R. Molecular forms of immunoreactive atrial natriuretic peptide in the rat hypothalamus and atrium. Biochem. Biophys. Res. Commun. 129:671-678, 1985.

57. Greenberg, B.D., Bencen, G.H., Seilhamer, J.J., Lewicki, J.A., Fiddes, J.C. Nucleotide sequence of the gene encoding human atrial natriuretic factor precursor. Nature. 312:656-658, 1984.

58. Gutkowska, J., Horky, K., Thibault, G., Januszewicz, P., Cantin, M., Genest, J. Direct radioimmunoassay of atrial natriuretic factor. Biochem. Biophys. Res. Commun. 122:593-601, 1984.

59. Gutkowska, J., Racz, K., Garcia, R., Thibault, G., Kuchel, O., Genest, J., Cantin, M. The morphine effect on plasma ANF. Eur. J. Pharmacol. 131:91-94, 1986.

60. Hamet, P., Tremblay, J., Pang, S.C., Garcia, R., Thibault, G., Gutkowska, J., Cantin, M., Genest, J. Effect of native and synthetic atrial natriuretic factor on cyclic GMP. Biochem. Biophys. Res. Commun. 123:515-527, 1984.

61. Hayashi, M., Buy, J. Metabolism of atrial natriuretic peptide (ANP) by kidney membranes and isolated tubules. Kidney Int. 31:271, (Abstract), 1987.

62. Heisler, S., Simand, J., Assayag, E., Mehri, Y., Labrie, F. Atrial natriuretic factor does not affect basal, forskolin- and CRF- stimulated adenylate cyclase activity, cAMP formation or ACTH secretion, but does stimulate cGMP synthesis in anterior pituitary. Mol. Cell. Endocrinol. 44:125-131, 1986.

63. Henry, J.P., Gauer, O.H., Reeves, J.L. Evidence of the atrial location of receptors influencing urine flow. Circulation Res. 4:85-90, 1956.

64. Hiruma, M., Ikemoto, F., Yamamoto, K. Rat atrial natriuretic factor stimulates renin release from renal cortical slices. Eur. J. Pharmacol. 125:151-153, 1986.

65. Holtz, J., Stewart, D.J., Elsner, D., Bassenge, E. In vivo peptide-renodilation: minimal potency relative to nitrogycerin in dogs. Life Sci.

39:2177-2184, 1986.

66. Horky, K., Gutkowska, J., Garcia, R., Thibault, G., Genest, J., Cantin, M. Effect of different anesthetics on immunoreactive atrial natriuretic factor concentrations in rat plasma. Biochem. Biophys. Res. Commun. 129:651-657, 1985.

67. Huet, M., Cantin, M. Ultrastructural cytochemistry of atrial muscle cells. II. Characterization of the protein content of specific granules. Lab. Invest. 30:525-532, 1974.

68. Januszewicz, P., Thibault, G., Garcia, R., Gutkowska, J., Genest, J., Cantin, M. Effect of synthetic atrial natriuretic factor on arginine vasopressis release by the rat hypothalamoneurohypophyseal complex in organ culture. Biochem. Biophys. Res. Commun. 134:652-658, 1986.

69. Januszewicz, P., Thibault, G., Gutkowska, J., Garcia, R., Mercure, C., Jolicoeur, F., Genest, J., Cantin, M. Atrial natriuretic factor and vasopressin during dehydration and rehydration in rats. Am. J. Physiol. 251:E497-E501, 1986.

70. Jamieson, J.D., Palade, G.E. Specific granules in atrial muscle cells. J. Cell Biol. 23:151-172, 1964.

71. Johnson, R.A., Jakobs, K.H., Schultz, G. Extraction of the adenylate cyclase activating factor of bovine

sperm and its identification as a trypsin-like protease. J. Biol. Chem. 260:114-121, 1985.

72. Kangawa, K., Fukuda, A., Kubota, I., Hayashi, Y., Matsuo, H. Identification in rat atrial tissue of multiple forms of natriuretic polypeptides of about 3,000 daltons. Biochem. Biophys. Res. Commun. 121:585-591, 1984.

73. Kangawa, K., Fukuda, A., Matsuo, H. Structural identification of beta-and gamma-humans atrial natriuretic polypeptide. Nature 313:394-400, 1985.

74. Katada, T., Ui, M. Direct modification of the membrane adenylate cyclase system by islet-activating protein due to ADP-ribosylation of a membrane protein. Proc. Natl. Acad. Sci. USA. 79:3129-3133, 1982.

75. Keeler, R., Azzarolo, A.M. Effects of atrial natriuretic factor on renal handling of water and electrolytes in rats. Can. J. Physiol. Pharmacol. 61:996-1002, 1983.

76. Kisch, B. Electron microscopy of the atrium of the heart. I. Guinea pig. Exp. Med. Surg. 14:99-112, 1956.

77. Kleinert, H.D., Maack, T., Atlas, S.A., Januszewicz, A., Sealey, J.E., Laragh, J.H. Atrial natriuretic factor inhibits angiotensin- norepinephrine-, and

potassium- induced vascular contractility. Hypertension. 6:I-143-I147, 1984.

78. Kuno, T., Andresen, J.W., Kamisaki, Y., Waldman, S.A., Chang, L.Y., Saheki, S., Leitman, D.C., Nakane, M., Murad, F. Co-purification of an atrial natriuretic factor receptor and particulate guanylate cyclase from rat lung. J. Biol. Chem. 261:5817-5823, 1986.

79. Kurtz, A., Della Bruna, R., Pfeilschifter, J., Taugner, R., Bauer, C. Atrial natriuretic peptide inhibits renin release from juxtaglomerular cells by a cGMP-mediated process. Proc. Natl. Acad. Sci. USA 83:4769-4773, 1986.

80. Lachance, D., Garcia, R., Gutkowska, J., Cantin, M., Thibault, G. Mechanisms of release of atrial natriuretic factor. I. Effect of several agonists and steroids on its release by atrial minces. Biochem. Biophys. Res. Commun. 135:1090-1098, 1986.

81. Lang, R.E., Thoelken, H., Ganten, D., Luft, F.C., Ruskdaho, H., Unger, T.H. Atrial natriuretic factor- a circulating hormone stimulated by volume load. Nature. 314:264-266, 1985.

82. Lappe, R.W., Smits, J.F., Todt, J.A., Debets, J.J., Wendt, R.L. Failure of atriopeptin II to cause arterial vasodilation in the conscious rat. Circ Res.

56:606-612, 1985.

83. Ledsome, J.R., Wilson, N., Rankin, A.J., Courneya, C.A. Time course of release of atrial natriuretic peptide in the anesthetized dog. Can. J. Physiol. Pharmacol. 64:1017-1022, 1986.

84. Leitman, D.C., Agnost, V.L., Tuan, J.J. Atrial natriuretic factor and sodium nitro-prusside increase cyclic GMP in cultured rat lung fibroblasts by activating different forms of guanylate cyclase. Biochem. J. 244:69-74, 1987.

85. Leitman, D.C., Andresen, j., Kund, T., Kamisaki, Y., Ghang, j.K., Murad, F. Identification of multiple binding sites for atrial natriuretic factor by affinity cross linking in cultured endothelial cells. J. Biol. Chem. 261:11650-11655, 1986.

86. Leitman, D.C., Andresen, J.W., Catalano, R.M., Waldman, S.A., Tuan, J.J., Murad, F. Atrial natriuretic peptide binding, cross-linking, and stimulation of cyclic GMP accumulation and particulate guanylate cyclase activity in cultured cells. J. Biol. Chem. 263:3720-3728, 1988.

87. Leitman, D.C., Agnost, V.L., Catalano, R.M., Schroder, H., Waldman, S.A., Bennett, B.M., Tuan, J.J., Murad, F. Atrial natriuretic peptide, oxytocin and vasopressin increase guanosine 3', 5'- mono-

phosphate in LLC-PK$_1$ kidney epithelial cells. Endocrinology 122:1478-1485, 1988.

88. Linden, R.J., Sreeharan, N. Humoral nature of the urine response to stimulàtion of atrial receptors. Quant. J. Exp. Physiol. 66:431-438, 1981.

89. Luft, F.C., Lang, R.E., Aronoff, G.R., Ruskoaho, H., Toth, M., Ganten, D., Sterzel, R.B., Unger, T. Atriopeptin III kinetics and pharmacodynamics in normal and anephric rats. J. Pharmacol. Exp. Ther. 236:416-418, 1986.

90. Luft, F.C., Sterzel, R.B., Lang, R.E., Trabold, E.M., Veelken, R., Ruskoaho, H., Gao, Y., Ganten, D., Unger, T. Atrial natriuretic factor determinations and chronic sodium homeostasis. Kidney Int. 29:1004-1010, 1986.

91. Maack, T., Kleinert, H.D., Renal and cardiovascular effect of atrial natriuretic factor. Biochem. Pharmacol. 35:3357-3361, 1986.

92. Maack, T., Marion, D.N., Camargo, M.J., Kleinert, H.D., Laragh, J.H., Vaughan, E.D. Jr., Atlas, S.A. Effects of auriculin (atrial natriuretic factor) on blood pressure, renal function, and the renin-aldosterone system in dogs. Am. J. Med. 77:1069-1075, 1984.

93. Maki, M., Takayanagi, R., Misono, K.S., Pandey,

K.N., Tibbetts, C., Inagami, T. Structure of rat atrial natriuretic precursor deduced from cDNA sequence. Nature. 309:722-724, 1984.

94. Manning, P.T., Schwartz, D., Katsube, N.C., Holmberg, S.W., Needleman, P. Vasopressin-stimulated release of atriopeptin: endocrine antagonists in fluid homeostasis. Science. 229:395-397, 1985.

95. Marie, J.P., Guillemot, H., Hatt, P.Y. Le degré de granulation des cardiocytes auriculaires. Étude planimétrique au coins des différents apports d'eau et de sodium chez le rat. Pathol. Biol. Paris 4:549-554, 1976.

96. McKenzie, J.C., Tanaka, I., Misono, K.S., Inagami, T. Immunocytochemical localization of atrial natriuretic factor in the kidney, adrenal medulla, pituitary and atrium of rat. J. Histochem. Cytochem. 33:828-832, 1985.

97. McNutt, N.S., Fourcett, D.W. The ultrastructure of the cat myocardium. II. atrial muscle. J. Cell Biol. 42:46-67, 1969.

98. Metzler, D.H., Lee, M.E., Thrasher, T.N., Ramsay, D.J. Increased right or left atria pressure stimulates release of atrial natriuretic peptides in conscious dogs. Endocrinology. 119:2396-2398, 1986.

99. Michener, M.L., Gierse, J.K., Seatharom, R., Fok,

K.F., Olins, P.O., Mai, M.S., Needleman, P. Proteolytic conversion of atriopeptin prohormone. Mol. Pharmacol. 30:552-557, 1986.

100. Misono, K.S., Grammer, R.T., Fukumi, H., Inagami, T. Rat atrial natriuretic factor: isolation, structure and biological activity of four major peptides. Biochem. Biophys. Res. Commun. 123:444-451, 1984.

101. Murthy, K.K., Thibault, G., Garcia, R., Gutkowska, J., Genest, J., Cantin, M. Degradation of atrial natriuretic factor in the rat. Biochem. J. 240:461-469, 1986.

102. Murthy, K.K., Thibault, G., Schiffrin, E.L., Garcia, R., Chartier, L., Gutkowska, J., Genest, J., Cantin, M. Desappearance of atrial natriuretic factor from circulation in the rat. Peptides. 7:241-246, 1986.

103. Napier, M.A., Vandlen, R.L., Albers-Schonberg, G., Nutt, R.F., Brady, S., Lyle, T., Winguist, R., Faison, E.P., Heinel, L.A., Blaine, E.H. Specific membrane receptors for atrial natriuretic factor in renal and vascular tissues. Proc. Natl. Acad. Sci. USA. 81:5946-5950, 1984.

104. Natsume, T., Kardon, M.B., Trippodo, N.C., Januszewicz, A., Pegram, B.L., Frohlich, E.D. Atriopeptin III does not alter cardiac performance in rats. J. Hypertens. 4:477-480, 1986.

105. Nemer, M., Lavigne, J.P., Thibault, G., Gannon, M., Antakly, T. Expression of atrial natriuretic factor gene in heart ventricular tissues. Peptides. 7:1147-1152, 1986.

106. Obana, K., Naruse, M., Inagami, T., Brown, A.B., Naruse, K., Kurimoto, F., Sakurai, H., Demura, H., Shizume, K. Atrial natriuretic factor inhibits vasopressin secretion from rat posterior pituitary. Biochem. Biophys. Res. Commun. 132:1088-1094, 1985.

107. Obana, K., Naruse, M., Naruse, K., Sakurai, A., Demura, H., Inagami, T., Shizume, K. Synthetic rat atrial natriuretic factor inhibits in vitro and in vivo renin secretion in rats. Endocrinology. 117:1282-1284, 1985.

108. Oikawa, S., Imai, M., Veno, A., Tanak, S., Nogushi, T., Nakasato, H., Kangawa, K., Fukuda, A., Matsuo, H. Cloning and sequence analysis of cDNA encoding a precursor for human atrial natriuretic peptide. Nature. 309:724-726, 1984.

109. Palade, G.E. Secretory granules in the atrial myocardium. Anat. Rec. 139:262-274, 1961.

110. Racz, K., Kuchel, O., Cantin, M., De Léan, A. Atrial natriuretic factor inhibits the early pathway of steroid biosynthesis in bovine adrenal cortex. FEBS Lett. 192:19-22, 1985.

111. Ruskoaho, H., Toth, M., Ganten, D., Unger, T.H., Lang, R.E. The phorbol ester induced atrial natriuretic peptide secretion is stimulated by Forskolin and Bay K8644 and inhibited by 8-bromo-cyclic GMP. Biochem. Biophys. Res. Commun. 139:266-274, 1986.

112. Ruskoaho, H., Toth, M., Lang , R.E. Atrial natriuretic peptide secretion: synergistic effect of phorbol ester and A23187. Biochem. Biophys. Res. Commun. 133:581-588, 1985.

113. Sakamoto, M., Nakao, K., Kihara, M., Morii, N., Sugawara, A., Suda, M., Shimokura, M., Kiso, Y., Yamori, Y., Imura, H. Existence of atrial natriuretic polypeptide in kidney. Biochem. Biophys. Res. Commun. 128:1281-1287, 1985.

114. Salazar, F.J., Romero, J.C., Burnett, J.C. Jr., Schryver, S., Granger, J.P. Atrial natriuretic peptide levels during acute and chronic saline loading in conscious dogs. Am. J. Physiol. 251:R499-R503, 1986.

115. Saper, C.B., Standaert, D.G., Currie, M.G., Schwartz, D., Geller, D,M., Needleman, P. Atriopeptin-immunoreactive neurons in the brain: presence in cardiovascular regulatory areas. Science. 227:1047-1049, 1985.

116. Sasaki, A., Kida, O., Kangawa, K., Matsuo, H., Tanaka, K. Involvement of sympathetic nerves in cardio de pressive effects of α-human atrial natriuretic polypeptide (α- hANP) in anesthetized rats. Eur. J. Pharmacol. 120:345-349, 1986.

117. Schiffrin, E.L., Chartier, L., Thibault, G., St-Louis, J., Cantin, M., Genest, J. Vascular and adrenal receptors for atrial natriuretic factor in the rat. Cir. Res. 56:801-807, 1985.

118. Scivoletto, R., Carvalho, M.H. Cardionatrin causes vasodilation in vitro which is not dependent on the presence of endothelial cells. Eur. J. Pharmacol. 101:143-145, 1984.

119. Schwartz, D., Geller, D.M., Manning, P.T., Siegel, N.R., Fok, K.F., Smith, C.F., Needleman, P. Ser-leu-Arg-Arg-atriopeptin III: the major circulating form of atrial peptide. Science. 229:397-400, 1985.

120. Seidah, N.G., Lazure, C., Chrétien, M., Thibault, G., Garcia, R., Cantin, M., Genest, J., Nutt, R.F., Brady, S.F., Lyle, T.A., Palaveda, W.J., Colton, C.D., Ciccarone, T.M., Veber, D.F. Amino acid sequence of homologous rat atrial peptides: natriuretic activity of native and synthetic forms. Proc. Natl. Acad. Sci. USA. 81:2640-2644, 1984.

121. Seidman, C.E., Block, K.D., Klein, K.A., Smith,

J.A., Seidman, J.G. Nucleotide sequences of the human and mouse atrial natriuretic factor genes. 226:1206-1209, 1984.

122. Seidman, C.E., Duby, A.D., Choi, E., Graham, R.M., Haber, E., Homcy, C., Smith, J.A., Seidman, J.G. The structure of rat preproatrial natriuretic factor as defined by a complementary DNA clone. Science. 225:324-326, 1984.

123. Seymour, A.A., Blaine, E.H., Mazack, E.K., Smith, S.G., Stabilito, I.I., Haley, A.B., Napier, M.A., Whinnery, M.A., Nutt, R.F. Renal and systemic effects of synthetic atrial natriuretic factor. Life Sci. 36:33-44, 1985.

124. Share, L., Iitake, K., Crofton, J.T., Brooks, D.P., Duchi, Y., Blaine, E. Central atrial natriuretic factor induces vasopressin release in conscious rats. Fed. Proc. 45:166 (Abstract), 1986.

125. Shenker, Y., Sider, R.S., Ostafin, E.A., Grekin, R.J. Plasma levels of immunoreactive atrial natriuretic factor in healthy subjects and patients with edema. J. Clin. Invest. 76:1684-1698, 1985.

126. Shibasaki, T., Naruse, M., Yamauchi, N., Masuda, A., Imaki, T., Naruse, K., Demura, H., Ling, N., Inagami, T., Shizume, K. Rat atrial natriuretic factor suppresses proopiomelanocortin derived peptides

secretion from both anterior and intermediate lobe cells and growth hormone release from anterior lobe cells of rat pituitary in vitro. Biochem. Biophys. Res. Commun. 135:1035-1041, 1986.

127. Shiono, S., Nakao, K., Morii, N., Yamada, T., Itaoh, H., Sakamoto., Sugawara, A., Saito, Y., Katsuura, G., Imura, H. Nature of atrial natriuretic polypeptide in rat brain. Biochem. Biophys. Res. Commun. 135:728-734, 1986.

128. Skofitsch, G., Jacobowitz, D.M., Eskay, R.L., Zamir, N. Distribution of atrial natriuretic factor-like immunoreactive neurons in the rat brain. Neuroscience. 16:917-948, 1985.

129. Sonnenberg, H., Cupples, W.A., De Bold, A.J., Veress, A.T. Intracellular localization of the natriuretic effect of cardiac atrial extract. Ann. N.Y. Acad. Sci. 372:213 (Abstract), 1981.

130. Sonnenberg, H., Veress, A.T. Cellular mechanism of release of atrial natriuretic factor. Biochem. Biophys. Res. Commun. 124:443-449, 1984.

131. Standaert, D.G., Needleman, P., Saper, C.B. Organization of atriopeptin-like immunoreactive neurons in the central nervous system of rat. J. Comp. Neurol. 253:315:341, 1986.

132. Stephenson, S.L., Kenny, A.J. The hydrolysis of

α-human atrial natriuretic peptide by pig kidney microvillar membranes is inhibited by endopeptidase - 24.11. Biochem. J. 243:183-187, 1987.

133. Stone, R.A., Glembotski, C.C. Immunoreactive atrial natriuretic peptide in the rat eye: molecular forms in anterior uvea and retina. Biochem. Biophys. Res. commun. 134:1022-1028, 1986.

134. Sugiyama, M., Fukumi, H., Grammer, R.T., Misono, K.S., Yabe, Y., Morisawa, Y., Inagami, T. Synthesis of atrial natriuretic peptides and studies on structural factor in tissue specificity. Biochem. Biophys. Res. Commun. 123:338-344, 1984.

135. Takagi, M., Franco-Saenz, R., Mulrow, P.J. Effect of atrial natriuretic factor on the plasma aldosterone response to potassium infusion in rats - in vivo study. Life Sci. 39:359-364, 1986.

136. Tanaka, J., Misono, K.S., Inagami, T. Atrial natriuretic factor in rat hypothalamus, atria and plasma: determination by specific radioimmunoassay. Biochem. Biophys. Res. Commun. 124:663-668, 1984.

137. Thibault, G., Garcia, R., Cantin, M., Genest, J. Atrial natriuretic factor. Characterization and partial purification. Hypertension. 5:I-75-I-80, 1983.

138. Thibault, G., Lazure, C., Schiffrin, E.L., Gutkowska, J., Chartier, L., Garcia, R., Seidah,

N.G., Chrétien, M., Genest, J., Cantin, M. Identification of a biologically active circulating form of rat atrial natriuretic factor. Biochem. Biophys. Res. Commun. 130:981-986, 1985.

139. Tremblay, J., Gerzer, R., Vinay, P., Pang, S.C., Beliveau, R., Hamet, P. The increase in cGMP by atrial natriuretic factor correlates with the distribution of particulate guanylate cyclase. FEBS. Lett. 181:17-22, 1985.

140. Trippodo, N.C., MacPhee, A.A., Cole, F.E., Blakesly, H.L. Partial chemical characterization of a natriuretic substance in rat atrial heart tissue. Proc. Soc. Exp. Biol. Med. 170:502-508, 1982.

141. Villarreal, D., Freeman, R.H., Davis, J.O., Verburg, K.M., Vari, R.C. Renal mechanisms for supression of renin secretion by atrial natriuretic factor. Hypertension. 8:II-28-II-35, 1986.

142. Waldman, S.A., Rapoport, R.M., Fiscus, R.R., Murad, F. Effects of atriopeptin on particulate guanylate cyclase from rat adrenal. Biochem. Biophys. Acta. 845:298-303, 1985.

143. Waldman, S.A., Rapoport, R.M., Murad, F. Atrial natriuretic factor selectively activates particulate guanylate cyclase and elevates cyclic GMP in rat tissues. J. Biol. Chem. 259:14332-14334, 1984.

144. Winquist, R.J., Faison, E.P., Nutt, R.F. Vasodilator profile of synthetic atrial natriuretic factor. Eur. J. Pharmacol. 102:169-173, 1984,

145. Winquist, R.J., Faison, E.P., Waldman, S.A., Schwartz, K., Murad, F., Rapoport, R.M. Atrial natriuretic factor elicits an endothelium-independent relaxation and activates particulate guanylate cyclase in vascular smooth muscle. Proc. Natl. Acad. Sci. USA. 81.7661-7664, 1984.

146. Yandle, T.G., Espiner, E.A., Nicholls, M.G., Duff, H. Radioimmunoassay and characterization of atrial natriuretic peptide in human plasma. J. Clin. Endocrinol. Metab. 63:72-79, 1986.

147. Yandle, T.G., Richards, A.M., Nicholls, M.G., Cuneo, R., Espiner, E.A., Livisey, J.H. Metabolic clearance rate and plasma half-life of alpha-human atrial natriuretic peptide in man. Life Sci. 38:1827-1833, 1986.

148. Yang-Feng, T.L., Floyd-Smith, G., Nemer, M., Drouin, J., Francke, U. The pronatriodilatin gene is located on the distal short arm of human chromosome 1 and on mouse chromosome 4. Am. J. Hum. Genet. 37:1117-1128, 1985.

149. Zamir, N., Haass, M., Dave, J.R., Zukowska-Grojec, Z. Anterior pituitary gland modulates the release of

atrial natriuretic peptide from cardiac atria. Proc. Natl. Acad. Sci. USA. 84:541-545, 1987.

150. Zeidel, M.L., Silva, P., Brenner, B.M., Seifter, J.L. cGMP mediates the effects of atrial peptides on medullary collecting duct cells. Am. J. Physiol. 252:F551-F559, 1987.

151. Zivin, R.A., Condra, J.H., Dixon, R.A.F., Seidah, N.G., Chrétien, M., Nemer, M., Chamberland, M., Drouin, J. Molecular cloning and characterization of DNA sequences encoding rat and human atrial natriuretic factors. Proc. Natl. Acad. Sci. USA 81:6325-6329,1984.

CHAPTER 2

This chapter describes the localization of ^{125}I-ANF binding sites in the rat brain. They are present in both vascular and non-vascular structures of the circumventricular organs, choroid plexus, pia-arachnoid and endothelium of capillaries.

RADIOAUTOGRAPHIC LOCALIZATION OF ^{125}I-ATRIAL NATRIURETIC FACTOR BINDING SITES IN THE BRAIN

This work was published in

Neuroendocrinology (44: 365-372, 1986)

ABSTRACT

Rats were injected through the carotid artery (cephalad direction) with 18.9 µCi of either ^{125}I-atrial natriuretic factor (Arg 101-Tyr 126) alone or together with an excess of unlabeled hormone. At 2 min after injection, all rats were fixed *in vivo* by perfusion and serial sections of the whole brain were processed for light microscope radioautography. The radioautographic reaction produced by ^{125}I-atrial natriuretic factor alone was localized in all circumventricular organs (except the subcommissural organ), the smooth muscle cells and endothelial cells of arteries, arterioles, veins, venules, the endothelial cells of intraparenchymal capillaries and the epithelial cells of the choroid plexus. In rats which received ^{125}I-atrial natriuretic factor plus an excess of unlabeled hormone, the radioautographic reaction was reduced by 70-90%. Binding sites are thus localized in regions of the brain, some of them involved in the central monitoring of blood pressure and osmolarity. In addition, the presence of binding sites in the cerebral vasculature and in the epithelium of the choroid plexus suggests that circulating ANF may play a role in the control of cerebral blood flow and in the production of cerebrospinal fluid.

INTRODUCTION

The myoendocrine cells of the mammalian atria secrete a peptide (atrial natriuretic factor, ANF), whose chemical structure, cDNA and gene are now known (8,11,20,22). The synthetic C-terminal portion of the molecule (Arg 101-Tyr 126) has been shown to produce a variety of effects related to the regulation of blood pressure and salt balance (8,11,20,22). By means of *in vivo* light microscope radioautography, we have localized binding sites for 125I-ANF in pheripheral tissues (4) and these binding sites have been characterized both by radiologand binding and by their effects on second messengers (8,11,20,22). Since ANF is a hormone whose circulating amino acid sequence is now known (36) (Ser 99-Tyr 126) and since an intravascular injection has been shown to affect hypothalamus function (30), it became of interest to localize the putative target cells in the brain which are reached by intravascular delivery. The localization by *in vitro* radioautography of brain ANF receptors (29) and the presence of immunoreactive ANF- containing neurons in several brain structures (17,31) point to a possible central action of the hormone in the control of blood pressure and extracellular fluid balance.

MATERIALS AND METHODS

Preparation of ^{125}I-ANF

^{125}I-ANF was prepared as already described (14) using synthetic ANF (Arg 101-Tyr 126) (kindly provided by Dr.R.Nutt, Merck Sharp and Dohme Research Laboratories) with minor modifications of the chloramine-T method (15). The tracer was purified on a Sepharose 4B anti-ANF affinity column. The immunoglobulins from rabbit plasma immunized with synthetic ANF (Arg 101-Tyr 126) were partially purified by precipitation with 35% saturated ammonium sulfate at 4°C. This was repeated twice and the final precipitate was dissolved in 0.1 M sodium bicarbonate, pH 8.3, containing 0.5 M NaCl and dialyzed against the same buffer. Antibodies were coupled at pH 8.3 to wet cyanogen-bromide-activated Sepharose 4B. A small column of Sepharose 4B anti-ANF was prepared in disposable Pasteur pipettes (bed volume of about 1 ml). The column was equilibrated with 0.15 M NaCl, 0.01 M sodium phosphate, pH 7.4. The radioactive ^{125}I-ANF(100 x 10^6 cpm) was deposited on the column which was washed with the equilibration buffer. Acetic acid (0.1 M) was used for elution. One-milliliter fractions were collected and radioactivity in 10 µl aliquots was mesured in a gamma counter. Fractions containing radioactivity were pooled. Further purification of the radiolabeled tracer was achieved

by HPLC on a μBondapak C_{18} column (0.39 x 30 cm), eluted with a linear gradient of 20-50% acetonitrile with 0.1% trifluoroacetic acid with a slope of 0.5% min and a flow rate of 1 ml/min. One-milliliter eluates were collected. Aliquots of 10 μl from each fraction were counted in a gamma counter. The iodinated peptide eluted at about 30% of acetonitrile. The acetonitrile was evaporated with a nitrogen stream at 4°C for 1 h.

Injection of ^{125}I-ANF

^{125}I-ANF(Arg 101-Tyr 126) (18.9 μCi, ~ 0.035 nmol) in sodium phosphate buffer 0.1 M, pH 5.5, containing 0.1% BSA was injected in a volume of 0.1 ml through a catheter inserted in the left carotid artery of female, 40 g Sprague-Dawley rats, under pentobarbital anesthesia, with the tip in a cephalad direction. For displacement analysis, ANF (Arg 101-Tyr 126) (9 nmol) was mixed with ^{125}I-ANF as above (in a total volume of 0.1 ml) and injected in a single bolus to the rats under the same type of anesthesia.

Exactly 2 min after the injection, the rats were sacrificed by intracardiac perfusion first of Ringer-Locke fluid for exactly 1 min and then with Bouin's fluid for 10 min. The brains were fixed for a further 24 h in the same fixative, dehydrated, embedded in paraffin and serial, coronal, 5 μm sections of the whole brain were done. The sections were stained with periodic acid-Schiff (PAS) and then pro-

cessed for radioautography using Ilford K_5 emulsion, exposed for 1 month and then developed as already described (2,70). After preliminary examination to determine the areas where silver grains were located, they were counted in each tissue of interest at a magnification of x 1,000 using an ocular micrometer. At least 50 squares of 121 μm^2 for each tissue in every animal were assessed in that manner (Table 1).

RESULTS

Following in intracarotid, cephalad injection of 18.9 µCi of ^{125}I-ANF, accumulation of silver grains were seen over the whole cerebral vasculature including the pia-arachnoid, over the choroid plexus and all circumventricular organs (except the subcommissural organ). This radioautographic reaction could be significantly reduced by an excess of cold ANF(9 nmol, Table 1). No meaningful accumulation of silver grains was observed in brain structures localized inside the blood brain barrier (Table 1, frontal cortex, paraventricular nucleus and septum).

Cerebral Vessels and Pia-Arachnoid

An equal intensity of radioautographic reaction was observed in arteries, arterioles, veins, venules and capillaries everywhere in the brain. Silver grains were localized over smooth muscle cells and endothelial cells of the internal carotid branches as well as on the

Table 1. Radioautographic reaction displacement over the rat brain at 2 min after an intracarotid cephalad injection of ^{125}I-ANF

Brain Structure	Silver grains/unit area		
	^{125}I-ANF (n=3)	^{125}I-ANF + cold ANF (n=3)	inhibition %
Pia-arachnoid	17.0 ± 0.8	2.3 ± 0.1	86
Choroid plexus	26.0 ± 0.6	7.7 ± 0.3	70
Area postrema	19.5 ± 0.5	3.4 ± 0.1	82
Subfornical organ	15.3 ± 0.4	1.8 ± 0.1	88
Organum vasculosum laminae terminalis	11.7 ± 0.3	3.4 ± 0.2	71
Subcommissural organ	2.3 ± 0.1	2.4 ± 0.1	-
Frontal cortex (motor area)	1.7 ± 0.2	1.3 ± 0.1	-
Pineal gland	26.0 ± 1.0	2.4 ± 0.1	90
Median eminence	11.8 ± 0.3	2.0 ± 0.1	83
Paraventricular nucleus	2.2 ± 0.1	2.3 ± 0.1	-
Septum	2.5 ± 0.2	2.1 ± 0.1	-

Intracarotid cephalad injection of 18.9 µCi of ^{125}I-ANF (0.035 nmol) was done in both groups. In one group, cold ANF (9 nmol) was injected simultaneously. Exactly 2 min after the injection, the rats were perfused through the left cardiac ventricle, first with 40 ml of Ringer-Locke solution and then with Bouin's fluid for 10 min. All values are the mean ± SEM of at least 50 units areas (121 µm^2) in each of 3 rats.

FIGURES 1 AND 2

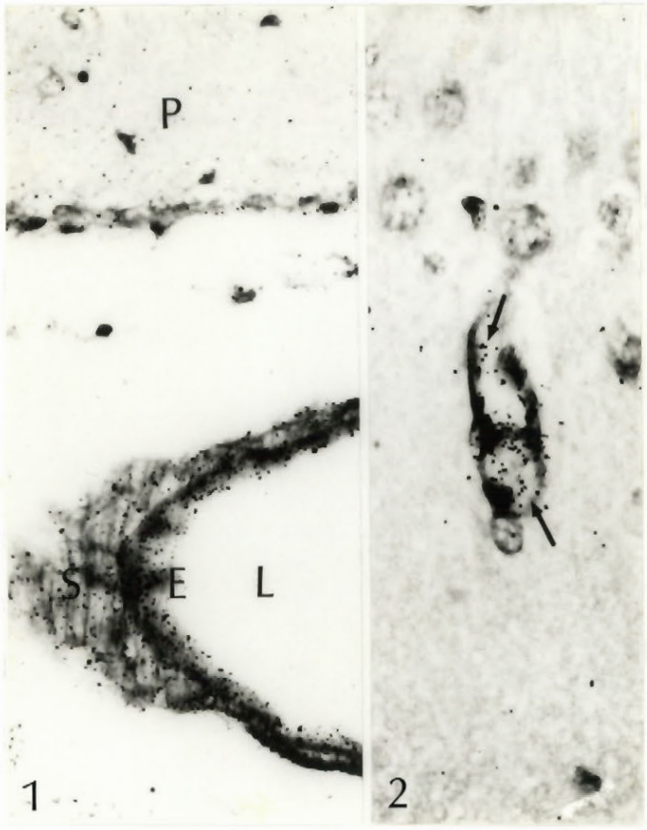

Fig. 1. Coronal section of the brain of a rat 2 min after injection of ^{125}I-ANF. Silver grains are localized on smooth muscle cells (S) and on endothelial cells (E) of a subarachnoid artery at the level of the amygdala cortex. L= Lumen; P = cerebral parenchyma. X 400.

Fig. 2. Coronal section of the cortex of rat injected with ^{125}I-ANF alone. Silver grains (arrows) are localized on the endothelium of a capillary. X 630.

pia-arachnoid vessels (Fig.1) and on the endothelium of capillaries (Fig.2). The brain parenchyma surrounding the vessels was unlabeled. In sections where the choroid plexus was present, silver grains were localized on the pia-arachnoid of the brain fissures, on the choroid plexus capillaries and on the veins of the venous sinuses. The radioautographic reaction was greatly diminished in rats receiving an excess of cold hormone together with ^{125}I-ANF (Table 1).

Choroid Plexus

The choroid plexus of the 3rd, 4th and lateral ventricles of rats injected with ^{125}I-ANF was heavily labeled. Silver grains were homogeneously distributed on the single layer of flattened epithelial cells as well as on the endothelium of capillaries (Fig.3). The radioautographic reaction was considerably reduced on the choroid plexus of rats which received an excess of cold ANF together with ^{125}I-ANF (Fig.4, Table 1).

Circumventricular Organs

Organum vasculosum of the Lamina terminalis. The external zone rich in capillaries loops and the internal parenchymal zone of the organum vasculosum of the lamina terminalis (38) were consistently labeled (Fig.5, Table 1). The radioautographic pattern and the intensity of labeling were similar over several sections of this organ.

FIGURES 3 AND 4

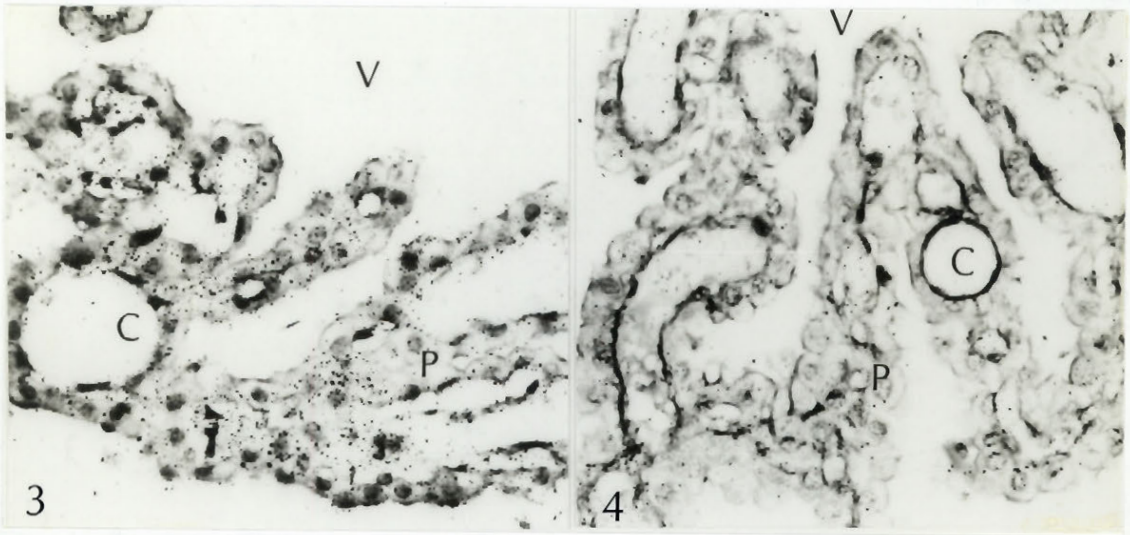

Fig. 3. Coronal section at the level of the 3rd ventricle (V). After injection of ^{125}I-ANF alone, silver grains are distributed on the epithelial cells (P) and on the choroid plexus capillaries (C). X 400.

Fig. 4. In the choroid plexus of a rat receiving ^{125}I-ANF, plus an excess of cold ANF, the radioautographic reaction is consistently reduced. P = Epithelial cells; C = capillaries; V = 3 rd ventricle. X 400.

The injection of ^{125}I-ANF together with an excess of cold ANF considerably reduced the number of silver grains over both internal and external zones (Fig.6, Table 1).

Mediam Eminence. Silver grains were homogeneously distributed over both internal and external zone of the median eminence although the nerve fibers were more heavily labeled than blood vessels (Fig.7). the radioautographic pattern observed in figure 7 was similar in sections localized either rostrally or caudally. The median eminence of rats which received an injection of ^{125}I-ANF together with an excess of cold ANF had their radioautographic reaction almost completely abolished (Fig.8, Table 1).

Subfornical Organ. The vasculature and the parenchyma of the subfornical organ were consistently labeled (Fig.9). From serial sections of the organ it was observed that silver grains were more numerous in the central region followed by caudal one. In the caudal region, the capillaries continuous to the choroid plexus that penetrate the parenchyma were also labeled. A less intense labeling was observed in the rostral region. A co-injection of ^{125}I-ANF with an excess of unlabeled ANF reduced the radioautographic reaction by 88% (Fig.10, Table 1).

Subcommissural Organ. The two layers of the subcommissural organ were not consistently labeled. Even though few silver grains were present on the pars

FIGURES 5 AND 6

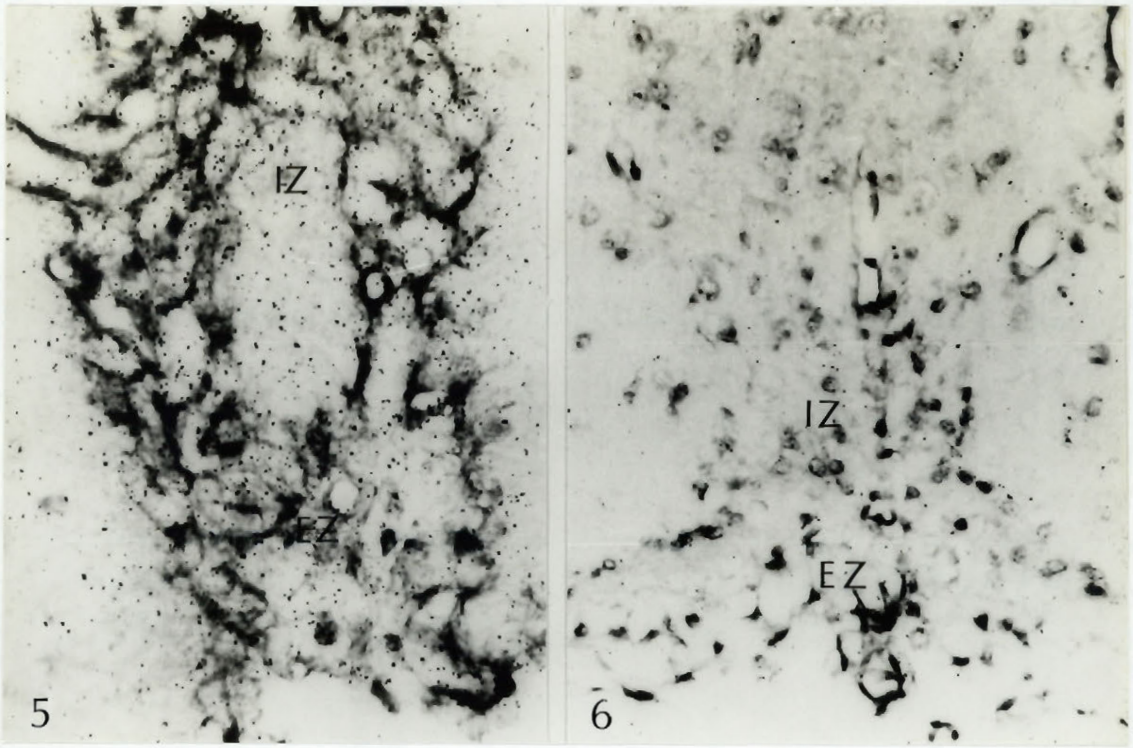

Fig. 5. Coronal section at the level of the organum vasculosum of the laminae terminalis. Silver grains are present on the parenchymal cells of the internal zone (IZ) and on the capillaries of the external zone (EZ) of a rat injected with ^{125}I-ANF alone. X 630.

Fig. 6. Coronal section at the level of the organum vasculosum of the lamina terminalis. The radioautographic reaction is consistently reduced in rats injected with an excess of unlabeled ANF. IZ = Internal zone; EZ = external zone. X 400.

FIGURES 7 AND 8

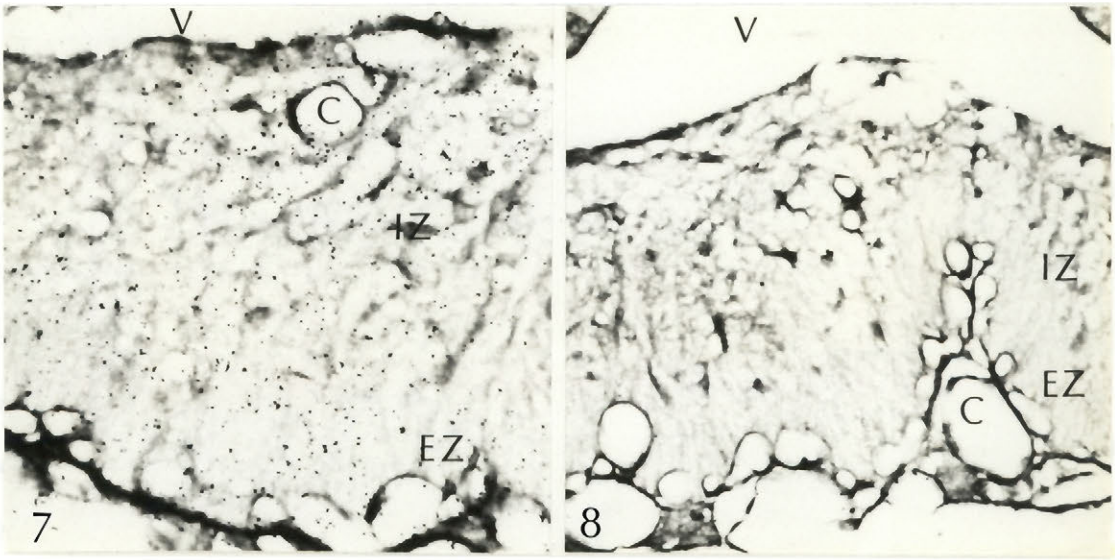

Fig. 7. In the median eminence of a rat injected with ^{125}I-ANF alone, silver grains are distributed on both internal (IZ) and external zone (EZ) and on endothelium of capillaries (C). V = 3rd ventricle. X 630.

Fig. 8. The median eminence of a rat receiving an excess of cold ANF is almost completely unlabeled. IZ = Internal zone; EZ = external zone; C = capillaries; V = 3rd ventricle. X 400.

ependymalis and hypendymalis, an excess of cold ANF did not displace them (Table 1). Here again, this structure was followed from the more rostral to the caudal sections and the radioautographic pattern was not found to change.

Pineal Gland. As observed in figure 11, the distribution of silver grains on the pineal gland was not homogeneous. Here, the radioautographic reaction seemed to follow the regular lobulation of parenchymal cells constituted mostly of pinealocytes. This pattern of reaction was identical in all sections made from the whole gland. The blood vessels were labeled. In the pineal gland of rats injected with an excess of cold ANF, the radioautographic reaction was significantly reduced (Fig.12, Table 1).

Area postrema. Silver grains were localized over the endothelium of capillaries and the parenchymal cells (not shown) similarly to that described for the central region of the subfornical organ. The examination of serial sections revealed that the pattern of labeling was identical throughout. Displacement of the radioautography reaction was observed in the area postrema of rats injected with an excess of cold ANF (Table 1).

FIGURES 9 AND 10

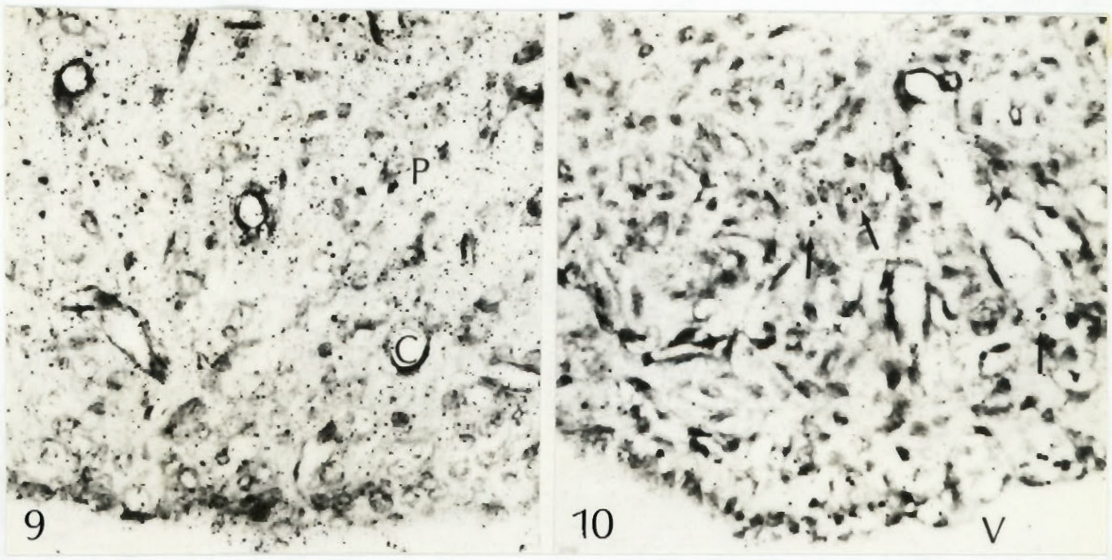

Fig. 9. Coronal section of the central region of the subfornical organ of a rat injected with ^{125}I-ANF alone. Silver grains are localized over parenchymal cells (P) as well as on the endothelium of capillaries (C). X 400.

Fig.10. Reduced radioautographic reaction observed over the subfornical organ of rat injected with ^{125}I-ANF together with an excess of cold ANF. V = ventricle. X 400. Most of the black dots observed are PAS-positive glycoproteins (arrows) and not silver grains.

FIGURES 11 AND 12

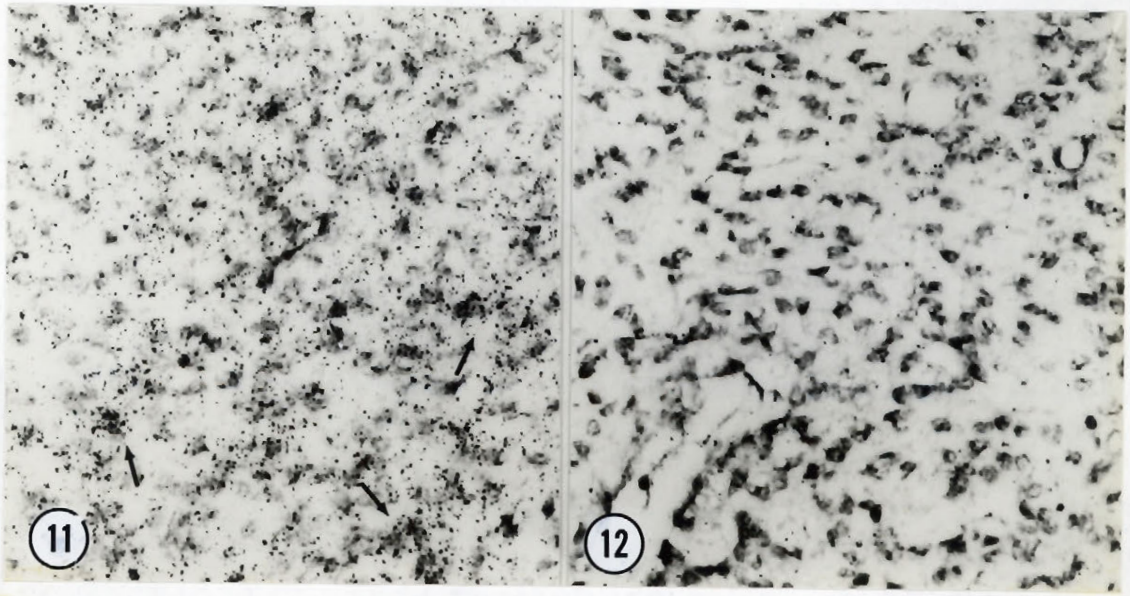

Fig.11. Pineal gland of rat injected with ^{125}I-ANF. Silver grains are localized in patches over groups of pinealocytes (arrows). X 400.

Fig.12. Pineal gland of rat injected with ^{125}I-ANF together with an excess of cold ANF. Only a few silver grains are observed over the parenchyma. X 400.

DISCUSSION

The presence of a radioautographic reaction on several brain regions lacking the blood-brain barrier and in cerebral vessels, which is consistently reduced by concomitant injection of an excess of unlabeled ANF, suggests that silver grains localized binding sites for the circulating hormone and confirms and extends *in vitro* radioautographic studies which have localized ANF receptors in the subfornical organ, area postrema and choroid plexus (29). We have now shown the exact localization of ANF bindings sites in these structures and also in the organum vasculosum of the lamina terminalis. The failure to localize ANF binding sites *in vivo* in brain regions inside the blood-brain barrier where receptors have been demonstrated *in vitro* (29) suggests that ANF does not penetrate the brain at 2 min after injection. Whether ANF may penetrate the brain at longer time intervals awaits further investigations.

Previous light microscope radioautography has localized binding sites for ANF in endothelial cells and smooth muscle cells of arteries, veins, venules and in endothelial cells of capillaries in the adrenal, kidney and liver (4). Radioligand binding and second messengers studies have characterized receptor for ANF positively coupled to guanylate cyclase and negatively to adenylate cyclase in aorta,

renal artery homogenates (1) and in cultured smooth muscle cells and endothelial cells of aorta (32). The presence of ANF binding sites in the brain vasculature may suggest that this hormone is implicated in the regulation of cerebral blood flow as has been proposed for the circulation in peripheral tissues (8,11,20,22). Adenylate cyclase (25) as well as guanylate cyclase (24) are present in pia-arachnoid and cerebral microvessels and both have been implicated as second messengers in the potent relaxing effect of ANF on precontracted arteries by angiotensin II (ANG II) and norepinephrine (8,20,22).

Since the endothelium of the cerebral microvessels has been implicated as a regulator of salt and water transport in the brain (3), the presence of ANF binding sites in cerebral endothelial cells suggests that the blood-brain barrier could be, as it may by ANG II (35), modulated by the former peptide.

The secretory epithelium of the choroid plexus, where part of the cerebrospinal fluid is produced (10), has been shown to be under neuroendocrine control as suggested by the presence of hormonal receptors in the epithelium (19). The localization of ANF binding sites on the epithelial cells of the choroid plexus suggests, here again, that ANF may be involved in the control of cerebrospinal fluid formation.

ANF binding sites appear to be present in several organs

of the brain lacking the blood-brain barrier (median eminence, organum vasculosum of the lamina terminalis, subfornical organ and area postrema). Intravenous injections of ANF have been shown to inhibit the release of vasopressin after dehydration and hemorrage in rats (30). The localization of ANF binding sites in the median eminence, after an intravascular injection, may suggest that, at least in part, this inhibitory effect may take place at this level. Nerve terminals containing vasopressin have been found in both external and internal zones of the median eminence (33). The presence of ANF binding sites in the organum vasculosum of the lamina terminalis, in the subfornical organ and area postrema, not only in the capillaries of these structures but also in parenchymal cells, suggest that ANF may be implicated in the modulation of blood pressure and extracellular fluid volume (6,28). Since these regions can be reached by components of the general circulation and because the circulatory form of ANF has now been characterized, it will be of interest to find out if these regions are sensitive to alterations in the circulating levels of ANF.

Although there is no direct evidence of the participation of the pineal gland in the control of salt homeostasis and blood pressure, receptors fo ANG II (34) and immunoreactive renin (16), ANG II (23) and vasopressin (26) have been demonstrated in this organ. On the other hand, there is good

evidence that the pineal gland is implicated in the regulation of the neurosecretory activity of the hypothalamo-hypophysial system through the release of indoles, in particular melatonin (27). Whether the presence of ANF binding sites in pinealocytes may predict a role for ANF in the modulation of pineal function remains to be determined.

Investigations performed during the last two years have shown that ANF is a powerful antagonist of the effect of ANG II on arterial contraction (13), secretion of aldosterone (9) and cortisol (12) and glomerular contraction (5). The finding that intraventricular injection of ANF inhibits the dipsogenic effect of ANG II (21) and the presence of ANG II receptors in the cerebral microvessels (35) and circumventricular organs (34,37) suggests that ANF may inhibit some of the central nervous system effects of ANG II as well.

Finally, the presence of immunoreactive ANF in brain regions inside the blood-brain barrier (17,31) as well as receptors (29) and the localization of ^{125}I-ANF binding sites in circumventricular organs that can be reached by intravascular delivery raises the possibility that the possible central control of blood pressure and fluid homeostasis by ANF may be modulated via peripheral and central sources of ANF production. These are further confirmed by the observations that hypothalamic functions can be affected by peripheral (30) and central injections (21) of

ANF as well as in cultured hypothalamo-neurohypophysial complex (18).

REFERENCES

1. Anand-Srivastava, MB., Franks, D.J., Cantin, M., Genest, J. Atrial natriuretic factor inhibits adenylate cyclase activity. Biochem. Biophys. Res. Commun. 121:855-862, 1984.
2. Benchimol, S., Cantin, M. Ultrastructural radioautography of synthesis and migration of proteins and catecholamines in the rat adrenal medulla. Cell Tiss. Res. 225: 293-314, 1982.
3. Betz, A.L. Epithelial properties of brain capillary endothelium. Fed. Proc. 44:2614-2615, 1985.
4. Bianchi, C, Gutkowska, J., Thibault, G., Genest, J., Cantin, M. Radioautographic localization of ^{125}I-atrial natriuretic factor (ANF) in rat tissues. Histochemistry 82:441-452, 1985.
5. Bianchi, C., Gutkowska, J., Thibault, G., Garcia, R., Genest, J., Cantin, M. Distinct localization of atrial natriuretic factor and angiotensin II binding sites in the glomerulus. Am. J. Physiol. 251:F594-F602, 1986.
6. Brody, M.J., Johnson, A.K. Role of the antero-ventral third ventricule region in fluid and electrolyte balance, arterial pressure regulation, and hypertension. In Frontiers in neuroendocrinology, edited by Martini,

D., Ganong, F. pp. 249-292. Raven Press, New York, 1980.

7. Cantin, M., Ballak, M., Beuzeron-Mangina, J., Anand-Srivastava, M.B., Tautu, C. DNA synthesis in cultured adult cardiocytes. Science 214:569-570, 1981.
8. Cantin, M., Genest, J. The heart and the atrial natriuretic factor. Endocr. Rev. 6:107-127, 1985.
9. Chartier, L., Schiffrin, E.L., Thibault, G. Effect of atrial natriuretic factor (ANF)-related peptides on aldosterone secretion by adrenal glomerulosa cells critical role of the intramolecular disulfide bond. Biochem. Biophys. Res. Commun. 122:171-174, 1984.
10. Davson, H. Physiology of the cerebrospinal fluid Little, Brown & Co., Boston, 1967.
11. De Bold, A.J. Atrial natriuretic factor a hormone produced by the heart. Science 230:767-770, 1985.
12. De Léan, A., Racz, K., Gutkowska, J., Nguyen, T.T., Cantin, M., Genest, J. Specific receptor mediated inhibition by synthetic atrial natriuretic factor of hormone-stimulated steroidogenesis in cultured bovine adrenal cells. Endocrinology 115:1636-1637, 1984.
13. Garcia, R., Thibault,G., Cantin, M., Genest, J. Effect of a purified atrial natriuretic factor on rat and rabbit vascular strips and vascular beds. Am. J. Physiol. 247:R34-R39, 1984.

14. Gutkowska, J., Thibault, G., Januszewicz, P., Cantin., M., Genest., J. Direct radioimmunoassay of atrial natriuretic factor. Biochem. Biophys. Res. Commun. 122:593-600, 1984.

15. Greenwood, F.C., Hunter, W.L., Glover, J. The preparation of ^{131}I-labeled human growth hormone of high specific radioactivity. Biochem. J. 89:114-123, 1963.

16. Hauliea, I., Branisteanu, D.D., Rosea, A., Stratone, A., Berbelur, V., Balon, G., Ionescu, L. A renin-like activity in pineal gland and hypophysis. Endocrinology 96:508-510, 1975.

17. Jacobowitz, D.M., Skofitsch, G., Keiser, H.R., Eskay, R.L., Zamir, N. Evidence for the existence of atrial natriuretic factor-containing neurons in rat brain. Neuroendocrinology 40:92-94, 1984.

18. Januszewicz, P., Thibault, G., Garcia, R., Gutkowska, J., Genest, J., Cantin, M. Effect of synthetic atrial natriuretic factor on arginine vasopressin release by the rat hypothalamo-neurohypophysial complex in organ culture. Biochem. Biophy. Res. Commun. 134:652-658, 1986.

19. Lorenzo, A.V., Wisnton, K.R., Welch, K., Adler, R.R., Granholm, L. Evidence of prolactin receptors in the choroid plexus and a possible role in water balance in neonatal brain. S. Kinderchir. 38:68-70, 1983.

20. Maack, T., Camargo, M.J.F., Kleinert, H.D., Laragh, J.H., Atlas, S.A. Atrial natriuretic factor structure and functional properties. Kidney Int. 27:607-615, 1985.

21. Nakamura, M., Katsura, G., Nakao, K., Imura, H. Antidipsogenic action of α-human atrial natriuretic polypeptide administered intraventricularly in rats. Neurosci. Lett. 581-586, 1985.

22. Needleman, P., Adams, S.P., Cole, B.R., Currie, M.G., Geller, D.M., Michener, M.L., Saper, C.B., Schwartz, D., Standaert, D.G. Atriopeptins as cardiac hormones. Hypertension 7:469-482, 1985.

23. Negro-Vilar, A., Sanchez-Franco, F., Samson, W. Failure to detect radioimmunoassayable arginine vasotocin in mammalian pineals. Brain Res. Bull. 4:789-791, 1979.

24. Palmer, G.C. Distribution of guanylate cyclase in rat cerebral cortex neuronal, glial, capillary, pia-arachnoid and synaptosomal fractions plus choroid. Neuroscience 6:2547-2553, 1981.

25. Palmer, G.C., Palmer S.J. Adenylate cylclase sensitivity to catecholamines and forskolin in rat pia-arachnoid and cerebral microvessels. Neuropharmacology 22:213-219, 1983.

26. Pevet, P., Reinharz, A., Dogterom, J. Neurophysins, vasopressin and oxytocin in the bovine pineal gland. Neurosci. Lett. 16:301-306, 1980.

27. Preslock, J.P. The pineal gland basic implications and clinical correlations. Endocr. Rev. 5:282-308, 1984.

28. Phillips, M.I., Hoffman, W.E., Bealer, S.L. Dehydration and fluid balance central effects of angiotensin. Fed. Proc. 41:2520-2527, 1982.

29. Quirion, R., Dalpe, M., De Léan, A., Gutkowska, J., Cantin, M., Genest, J. Atrial natriuretic factor (ANF) binding sites in brain and related structures. Peptides J. 5:1167-1172, 1984.

30. Samson, W.K. Atrial natriuretic factor inhibits dehydration and hemorrage-induced vasopressin release. Neuroendocrinology 40:277-279, 1985.

31. Samson, W.K. Dehydration-induced alterations in rat brain vasopressin and atrial natriuretic factor immunoreactivity. Endocrinology 117:1279-1281, 1985.

32. Schenk, D.B., Johnson, L.K., Schwartz, K., Sista, H., Scarborough, R.M., Lewicki, J,A. Distinct atrial natriuretic factor receptors sites on cultured bovine aortic smooth muscle and endothelial cells. Biochem. Biophys. Res. Commun. 127:433-442, 1985.

33. Silverman, A.J., Zimmerman, E.A. Magnocellular neurosecretory system. Annu. Rev. Neurosci. 6:357-380, 1983.

34. Speth, R.C., Harik, S.I., Gehlert, D.R., Chernicky, C.L., Barnes, K.L., Ferrario, C.M. Angiotensin II

receptor localization in the canine CNS. Brain Res. 326: 137-143, 1985.

35. Speth, R.C., Harik, S.I. Angiotensin II receptor binding sites in brain microvessels. Proc. Natl. Acad. Sci. USA 82:6340-6343, 1985.

36. Thibault, G., Lazure, C., Schiffrin, E.L., Gutkowska, J., Chartier, L., Garcia, R., Seidah, N.G., Chretien, M., Genest, J., Cantin, M. Identification of a biologically active circulating form of rat atrial natriuretic factor. Biochem. Biophys. Res. Commun. 130:981-986, 1985.

37. Van Houten, M., Schiffrin, L., Mann, J.F.E., Posner, B., Boucher, R. Radioautographic localization of specific binding sites for blood borne angiotensin II in the rat brain. Brain Res. 186:480-485, 1980.

38. Weindl, A., Sofroniew, M.V. Relation of neuropeptides to mammalian circumventricular organs. In Neurosecretion and brain peptides, edited by Martini, D., Reichlin, G., Blick, J. pp. 303-320 Raven Press, New York, 1981.

CHAPTER 3

In Chapter 2 and in the section on "Localization of ANF binding sites" we have demonstrated putative target cells in the rat brain and peripheral tissues by light microscope radioautography *in vivo*. We now describe their ultrastructural localization in the rat kidney. This chapter is divided into two main sections: Section A discusses the distribution of ANF binding sites in renal glomeruli and the effects of ANF on Angiotensin II induced contraction of isolated glomeruli. Section B elaborates the distribution of binding sites in the outer and inner medulla of the rat kidney.

SECTION A

DISTINCT LOCALIZATION OF ATRIAL NATRIURETIC FACTOR AND ANGIOTENSIN II BINDING SITES IN THE GLOMERULUS

This work was published in

Am. J. Physiol. 251: F594-F602, 1986.

ABSTRACT

A comparative study of the localization of ^{125}I-labeled atrial natriuretic factor (ANF) and ^{125}I-labeled angiotensin II (ANG II) binding sites in the glomerulus of the rat, after an intravascular injection, has been done by ultrastructural radioautography. ^{125}I-ANF binding sites are localized predominantly on the podocytes of the visceral epithelium (63%) followed by the endothelium of capillaries (14%), the parietal epithelium (13%), and finally mesangial cells (10%). In a comparative study, it was confirmed that ^{125}I-ANG II uptake is localized predominantly on mesangial cells (60%) followed by epithelial visceral cells (23%) and the endothelium of capillaries (16%). Using isolated rat glomeruli, it was confirmed that ANG II decreases glomerular size (maximum effect of 15%) with an apparent half maximum effective concentration (EC_{50})between 10^{-9} and 10^{-8} M. Although ANF alone has no apparent effect on glomerular size, it inhibits the contractile effect of ANG II with a half maximum inhibitory concentration (IC_{50})between 10^{-11} and 10^{-10} M. These results suggest that an intraglomerular mechanism other than glomerular arteriolar resistance may be involved in the modulation of glomerular filtration rate by ANF. The presence of ^{125}I-ANF uptake mainly in foot

processes of visceral epithelial cells of glomeruli *in vivo* and the inhibition of ANG II decrease in glomerular size by ANF *in vitro* raise the possibility that ANF may regulate the ultrafiltration coefficient by two mechanisms: modulation of glomerular permeability, and surface area.

INTRODUCTION

Atrial Natriuretic Factor (ANF) is a peptide secreted by the myoendocrine cells of atria, whose chemical structure, c-DNA and gene are now known (9). Previous light microscope radioautographic studies have localized ^{125}I-ANF in the renal arteries and arterioles, glomerular capillaries, vasa recta of outer and inner medulla, and veins of the kidney (7). Studies on dog isolated glomeruli, proximal tubules, Henle's loops, and collecting ducts have established that the greatest number of receptors is localized in glomeruli with a total absence of measurable receptor level in proximal tubules and a much lesser amount in distal tubules and collecting ducts (11). After exposure of various isolated renal structures to ANF, the greatest increase in cyclic guanosine 5'-monophosphate (cGMP) (due to stimulation of particule guanylate cyclase) was found in glomeruli, with lesser increments in distal tubules and collecting ducts and no change in proximal tubules (9), whereas

contradictory results were obtained regarding inhibition of adenylate cyclase activity by ANF (Ref.33, and M.B. Anand-Srivastava, P. Vinay, J. Genest, and M. Cantin, unpublished observations). Although a tubular effect cannot be ruled out, these observations suggest that diuresis and natriuresis produced by ANF are mostly mediated by hemodynamic changes with a major impact on the glomerulus itself. The aim of the present study was therefore to localize ^{125}I-ANF binding sites by ultrastructural radioautography in vivo. For control and comparative purposes, parallel experiments were conducted with ^{125}I-labeled angiotensin II (ANG II) for which receptors are well known to be localized on mesangial cells (23). Finally, the effects of ANF on isolated glomeruli in vitro were studied with and without the presence of ANG II, which is well known to decrease glomerular diameter in such isolated preparations (31).

MATERIALS AND METHODS

Preparation of ^{125}I-ANF ^{125}I-ANF was prepared as already described (16) using synthetic Arg 101-Tyr 126 ANF (obtained through the courtesy of Dr. R. Nutt, Merck Sharp & Dohme Research Laboratories, West Point, PA) with minor modifications of the chloramine-T method (14). The tracer was purified on a Sephadex 4B anti-ANF affinity column. Further

purification of the radiolabeled tracer was achieved by high-performance liquid chromatography on a μBondapak C_{18} column (0.39 x 30 cm) and eluted with a linear gradient of 20-50% acetonitrile with 0.1% trifluoroacetic acid with a slope of 0.5% per min and a flow rate of 1 ml/min. The monoiodinated peptide eluted at 30% of acetonitrile. The acetonitrile was evaporated with a nitrogen stream for a period of 1 h at 4°C before the injection.

Preparation of ^{125}I-ANG II

^{125}I-ANG II was prepared as already described (15) by the chloramine-T method (14) and purified by partition chromatography on Sephadex G-25.

Injection of ^{125}I-ANF

^{125}I-ANF (18.9 μCi, ~ 0.054 nmol) in sodium phosphate buffer (0.1 M, pH 5.5) containing 0.1% bovine serum albumin (BSA) was injected in a volume of 0.1 ml through a catheter inserted in the left carotid artery of female Sprague-Dawley rats (40 g body wt) under pentobarbital anesthesia so that its tip reached the aortic lumen. For displacement analysis, either 9 nmol (10 μl) of ANF (Arg 101-Tyr 126), adrenocorticotropic hormone $ACTH^{1-24}$, or bradykinin were mixed with ^{125}I-ANF as above and injected in a single bolus to the rats under the same type of anesthesia.

Injection of ^{125}I-ANG II

^{125}I-ANG II (67.6 μCi ~ 0.037 nmol) was injected in the same way to rats of the same sex, breed, and body weight. For displacement analysis, either 5 nmol of saralasin (Sar^1-Ala^8-ANG II) or the angiotensin III inhibitor des-Asp^1-Ile^8-ANG II were infused through the jugular vein during 30 min before the injection of ^{125}I-ANG II, as above.

Preparation for Radioautography

At 2 min after injection of either ^{125}I-ANF (n = 6) or ^{125}I-ANG II (n = 6), the rats were killed by intracardiac perfusion first with Krebs solution for exactly 1 min and then with 2% glutaraldehyde buffered with cacodylate HCl (0.1 M, pH 7.4) for 10 min. The kidneys were removed, and the cortex and outer and inner medulla were dissected. The radioactivity of a portion of each renal zone was evaluated in a LKB 1272 Clinigamma, and then these tissues were fixed for a further period of 1 h at 4°C. After this period, they were washed in cacodylate buffer with 2% sucrose, posfixed in 2% osmium tetroxide buffered with Veronal acetate, and embedded in Araldite as already described (5,8). Semithin sections (1 μm) as well as thin sections (silver-gold interference color) were made from the same blocks of tissue with a Reichert (OMU_2) ultramicrotome. Unstained semithin sections were coated with Ilford K_5 emulsion as already

described (5,8). Thin sections were placed on glass slides coated with Parlodion, stained with 2% uranyl acetate (10 min) followed by 1% lead citrate (2 min), and then coated with a thin carbon film. They were then coated with Ilford L_4 emulsion for electron microscope radioautography. Semithin sections were exposed for 1 month and developed as already described (5,8). This sections were exposed for 2 months and developed with the Agfa Gevaert physical developer for compact grains, which affords a better resolution (19). Semithin sections were poststained with 1% toluidine blue.

Ultrastructure Localization of ^{125}I-ANF and of ^{125}I-ANG II

Renal glomeruli were scanned at a magnification of X 7,880, and photographs were taken wherever grains were present. More than 400 grains were thus localized for each peptide.

Preparation of Isolated Glomeruli

Renal cortices were obtained from kidneys of 200-g Sprague-Dawley rats killed by decapitation. Glomeruli were isolated by centrifugation as described by Fong and Drummond (13). Isolated glomeruli were suspended in Krebs solution at 4°C and oxigenated with 95% O_2-5% CO_2 before each experiment. Samples of each glomerular suspension were

analysed before each experiment, and it was observed that tubular fragments and blood cells represented <5% of the preparation. Unencapsulated glomeruli represented 80-90% of the total glomerular population.

Glomerular Contraction Experiment

Twenty microliters of isolated glomeruli (105 ± 32 glomeruli) were incubated in a Petri dish (3 ml) containing various concentrations of ANG II with or without synthetic ANF (Arg 101-Tyr 126), in a final volume of 500 µl of Krebs solution containing 1% BSA at 22°C. Control experiments were prepared in the absence of these hormones. Pictures (X80) were taken between 10 and 11 min after the addition of the hormones using a phase-contrast microscope (Leitz, Federal Republic of Germany) equipped with a motor-driven camera, developed, and projected perpendicularly to a screen that made up a final magnification of X800. The area occupied by each unencapsulated glomerulus was estimated by the formula $\pi \cdot d_1 \cdot d_2 / 4$, where π is a constant (3.1416), d_1 is the greater diameter, and d_2 is the diameter perpendicular to d_1 passing through the center of the glomerulus. Glomerular diameters were measured with a graduated (in mm) caliper. Thus an index of glomerular size was obtained.

In Vitro Light Microscope Radioautography

Forty microliters of glomeruli isolated as above were incubated in an Eppendorf tube (1.5 ml) containing 30,000 counts/min of ^{125}I-ANF alone (n = 2) or with various concentrations of unlabeled ANF (n = 2) in a final volume of 200 µl of Krebs solution plus 1% BSA. After 10 min of incubation (22°C), 1 ml of cold Krebs solution was added, and the preparation was centrifuged (Eppendorf 3200) for 2 min. The supernatant was discarded, and the pellet was resuspended in 1 ml of the same solution and processed as above. The remaining pellet was processed for light microscope radioautography, after 2 h fixation in 2% glutaraldehyde and embedded in Araldite, as described above. Similar experiments were performed with 70,000 counts/min of ^{125}I-ANG II alone (n = 2) or with 10^{-6} M unlabeled hormone (n = 2).

RESULTS

Displacement of Radioactivity

Table I summarizes the effects of an injection of an excess of cold ANF, of ACTH$^{1-24}$, or of bradykinin on the uptake by the kidney of ^{125}I-ANF 2 min after the injection. The most potent inhibitor of uptake in the renal cortex was cold ANF, followed by a 2.5-times-less-potent effect of bradykinin, whereas ACTH$^{1-24}$ had no effect. Neither

Table 1. Displacement response analysis of radioactive content (cpm/mg of fixed tissue) in kidney 2 min after injection of ^{125}I-ANF with and without various hormonal peptides

Kidney	none	ANF	%	ACTH$^{1-24}$	%	bradykinin	%
Co	3,542	1,640	54	3,570		2,890	21
Om	1,438	713	50	1,475		1,375	4
Im	1,847	847	54	1,726	7	1,902	

Intra-aortic injection of the various peptides was done under pentobarbital anesthesia. Exactly 2 min after injection, the rats were perfused through the left cardiac ventricle first with 40 ml of Krebs solution, then with 2% glutaraldehyde for 10 min. Radioactivity of tissues was then measured in a LKB 1272 Clinigamma. Doses: ^{125}I-labeled atrial natriuretic factor ANF, 18.9 µCi (~0.054 nmol); ANF, adrenocorticotropic hormone ACTH$^{1-24}$, and bradykinin, 9 nmol each. Co: cortex; Om: outer medulla; Im: inner medulla.

Table 2. Displacement response analysis of radioactive content (cpm/mg of fixed tissue) in kidney 2 min after injection of ^{125}I-ANG II with and without competitive antagonists

Kidney	none	Sar^1-Ala^8-ANG II	%	des-Asp^1-Ile^8-ANG II	%
Co	9,974	2,161	78	3,460	65
Om	7,132	2,609	63	4,765	33
Im	4,539	2,528	44	4,937	

Intrajugular infusion (30 min) of angiotensin II (ANG II) inhibitors was done under pentobarbital anesthesia. Exactly 2 min after injection of ^{125}I-ANG II, the rats were perfused through the left cardiac ventricle first with 40 ml of Krebs solution, then with 2% glutaraldehyde for 10 min. Radioactivity of tissues was then measured in a LKB 1272 Clinigamma. Doses: ^{125}I-ANG II, 67.6 µCi (~ 0.037 nmol); Sar^1-Ala^8-ANG II and des-Asp^1-Ile^8-ANG II, 5 nmol each. Co: Cortex; Om: outer medulla; Im: inner medulla.

$ACTH^{1-24}$ nor bradykinin could mimic the inhibitory effect of cold ANF on the displacement of radioactivity in the outer and inner medulla.

Table 2 shows the effects of two competitive antagonists of ANG II. Whereas Sar^1-Ala^8-ANG II was a potent inhibitor of radioactive uptake in all renal zones analyzed, des-Asp^1-Ile^8-ANG II had no inhibitory effect in the inner medulla.

Radioautographic Localization

Light microscopy in vivo. After the injection of ^{125}I-ANF, silver grains followed the countour of the capillaries. No preferential localization over mesangial cells or over epithelial parietal cells was observed (Fig. 1). The radioautographic reaction on glomeruli could be completely displaced by an excess (9 nmol) of cold ANF, whereas in the same sections silver grains were still present over the proximal tubular lumen and brush border (Fig. 2). The concomitant injection of either $ACTH^{1-24}$ or of bradykinin had no effect on either the number or the localization of silver grains over the glomeruli and proximal tubular lumina.

The radioautographic pattern observed after the injection of ^{125}I-ANG II confirms earlier observations that localized this labeled hormone over the glomerular mesangial

FIGURES 1 AND 2

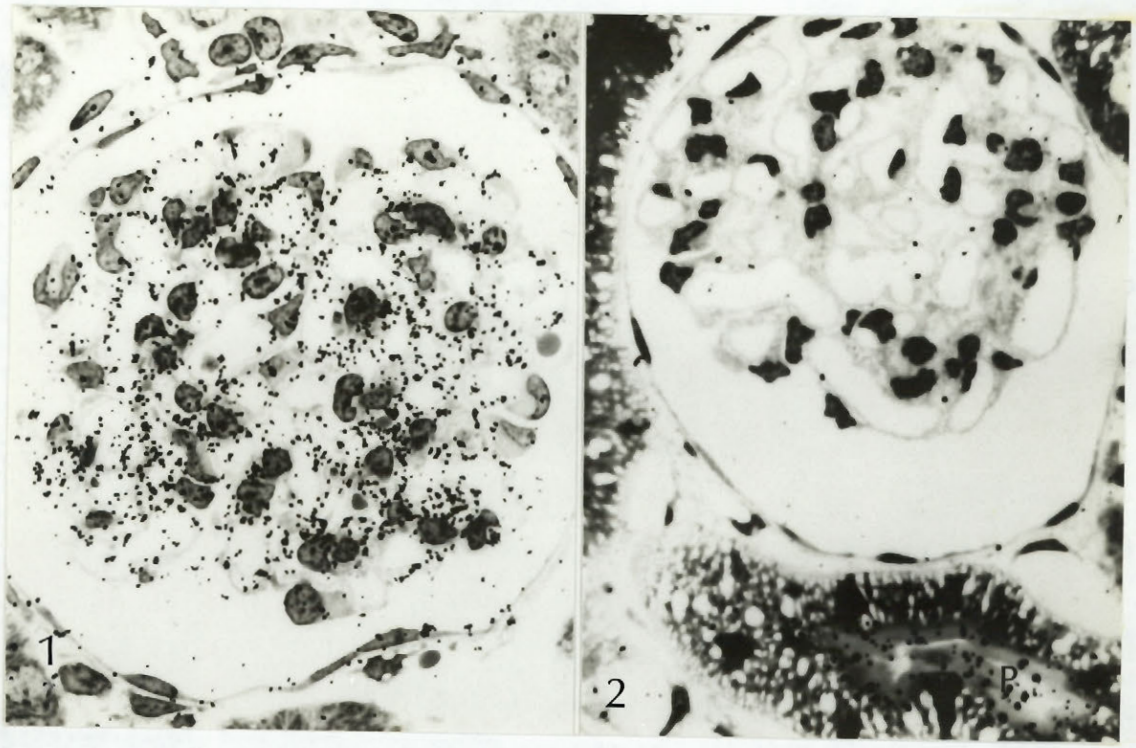

Fig. 1. Glomerulus after injection of ^{125}I-labeled atrial natriuretic factor. Silver grains follow contour of glomerular capillaries. Radioautograph of semithin section poststained with toluidine blue. Magnification, X 1,000.

Fig. 2. Glomerulus after injection of ^{125}I-labeled atrial natriuretic factor with an excess of atrial natriuretic factor. Whereas silver grains are almost totally absent over glomerular structures, they are still present over lumen and brush border of proximal tubules (P). Radioautograph of semithin section poststained with toluidine blue. Magnification, X 1,000.

FIGURES 3 AND 4

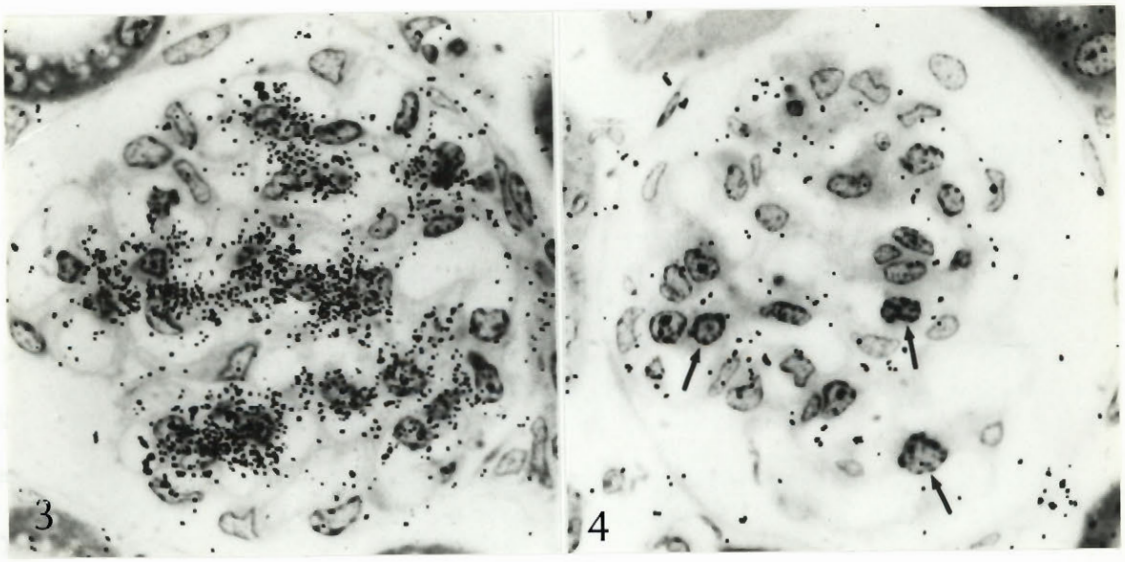

Fig. 3. Glomerulus after injection of ^{125}I-labeled angiotensin II. Silver grains are localized in clusters over axial region of glomerulus. Radioautograph of semithin section poststained with toluidine blue. Magnification, X 1,000.

Fig. 4. Glomerulus after injection of ^{125}I-labeled angiotensin II (ANG II) following 30 min infusion with saralasin (Sar^{1}-Ala^{8}-ANG II). Note paucity of silver grains located over mesangial cells (arrows). Radioautograph of semithin section poststained with toluidine blue. Magnification, X 1,000.

FIGURES 5 AND 6

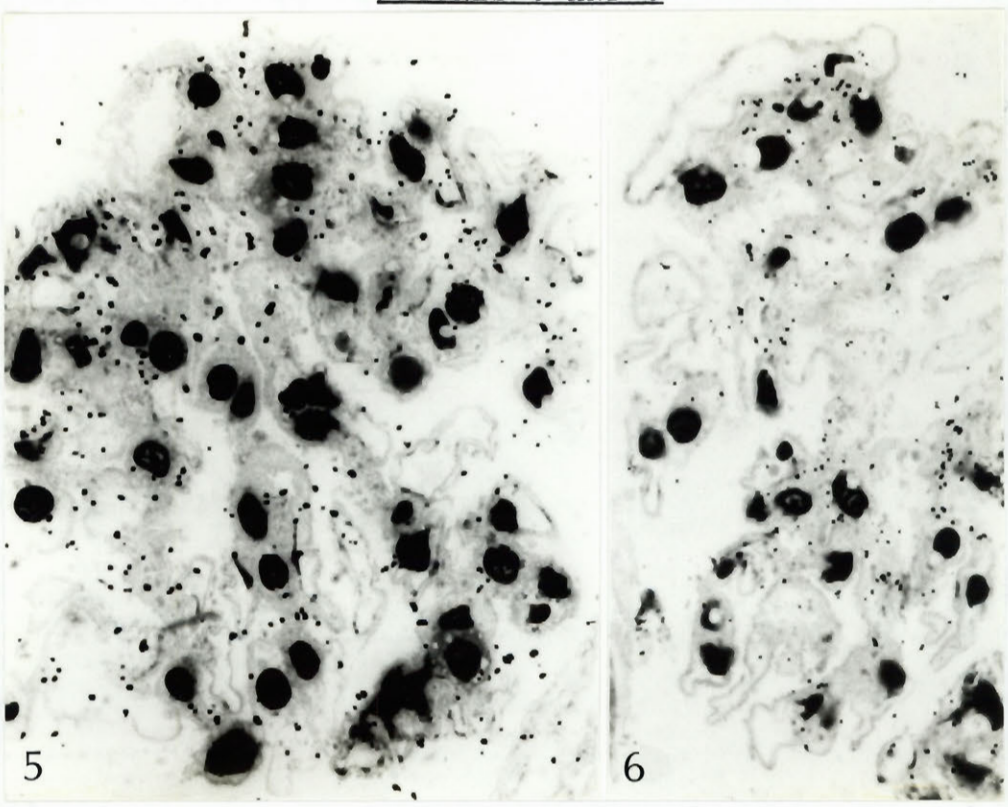

Fig. 5. Isolated glomerulus exposed to 30,000 counts/min of ^{125}I-labeled atrial natriuretic factor for 10 min at 22°C. Silver grains were distributed along entire glomerular section. Radioautograph of semithin section poststained with toluidine blue. Magnification, X 1,000.

Fig. 6. Isolated glomerulus exposed to 70,000 counts/min of ^{125}I-labeled angiotensin II for 10 min at 22°C. Silver grains were particularly numerous on some glomerular regions. Radioautograph of semithin section poststained with toluidine blue. Magnification, X 1,000.

capillaries were labeled to a much lesser extent (14 and 13%, respectively) (Table 3), followed by 10% over mesangial cells. The basal membrane of glomeruli was not labeled, and the radioautographic background was practically nil, as can be ilustrated by the absence of silver grains over capillary lumina and intercellular spaces (Figs. 7-9).

Electron microscopic localization of ^{125}I-ANG II. The majority of silver grains was localized over mesangial cells (Figs. 10 and 11, and Table 3). Although mesangial cells alone accounted for 60% of all the silver grains analyzed over the glomeruli (Table 3), 23% of silver grains were observed over the epithelial visceral cells (Fig. 10 and Table 3) and 16% over the endothelial cells of the capillaries, whereas epithelial parietal cells were practically unlabeled (1%). Here again, the lumen of capillaries as well as the intercellular spaces were free of radioautographic reaction (Figs. 10 and 11). The basement membrane was not labeled (Fig. 10).

Effect of ANG II and ANF on Isolated Glomeruli

As can be seen in Fig. 12, ANG II alone significantly decreased the index of glomerular size at concentrations of 10^{-7} and 10^{-6} M. The effect appeared to be concentration dependent from 10^{-9} to 10^{-7} M and then reached a plateau. There was a maximal decrease of 15% at the concentration

FIGURES 7, 8 AND 9

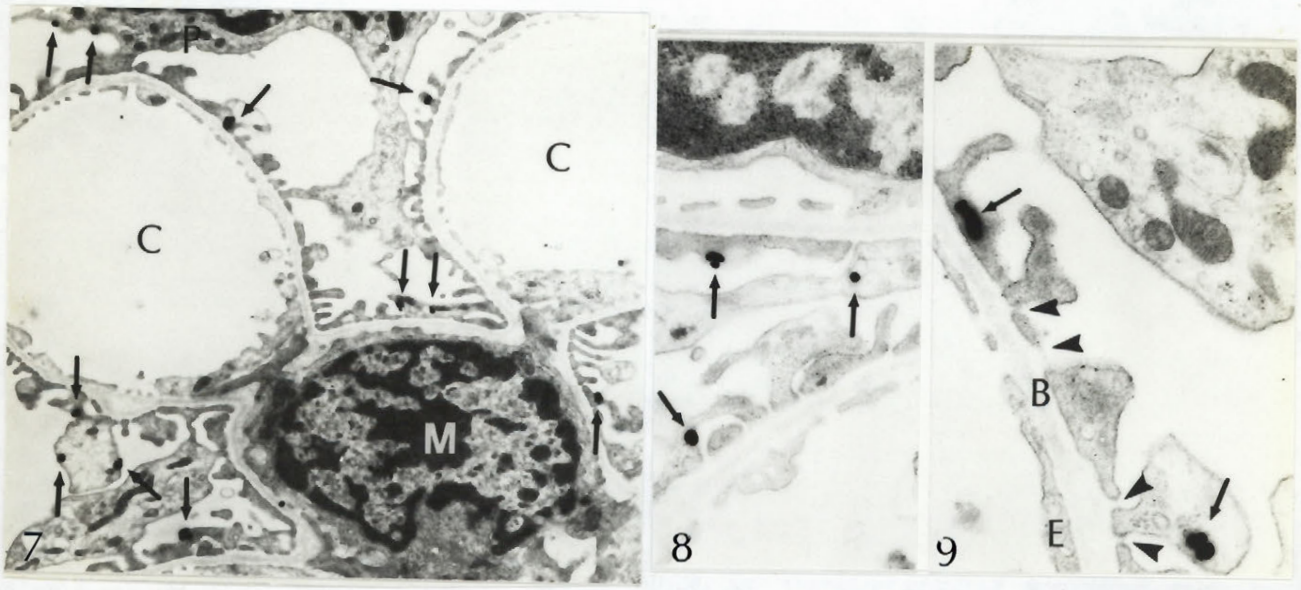

Fig. 7. Electron microscope radioautograph of glomerulus. Part of glomerulus after injection of ^{125}I-labeled atrial natriuretic factor is shown. Note silver grains over podocytes (arrows) of epithelial visceral cells (P). M, mesangial cell; C, capillary lumen. Magnification, X 7,880.

Fig. 8. Electron microscope radioautograph of glomerulus. Detail of glomerulus after injection of ^{125}I-labeled atrial natriuretic factor is shown. Silver grains are located over podocytes of epithelial cells (arrows). Magnification, X 18,390.

Fig. 9. Electron microscope radioautograph of glomerulus. Detail of glomerulus after injection of ^{125}I-labeled atrial natriuretic factor is shown. Silver grains are located over podocytes of epithelial cell (arrows). Slit diaphragm is indicated by arrow heads. E, endothelium; B, basement membrane. Magnification, X 25,430.

TABLE 3. Distribution of silver grains over glomerular cells

Cell Type	^{125}I-ANF	%	^{125}I-ANG II	%
Epithelial parietal	57	13	4	1
Epithelial visceral	272	63	103	23
Endothelial	63	14	73	16
Mesangial	43	10	275	60
No. of silver grains	435	100	455	100

Values were determined by ultrastructural radioautography 2 min after intra-aortic injection of either ^{125}I-labeled atrial natriuretic factor (ANF) or ^{125}I-labeled angiotensin II (ANG II). Between 55 and 60 electron microscope radioautographs for each peptide were taken over the renal glomeruli wherever silver grains were present (final magnification, X 7,880). Silver grains overlaying each of the glomerular cells were scored and expressed as a percentage of the total silver grains analyzed.

FIGURES 10 AND 11

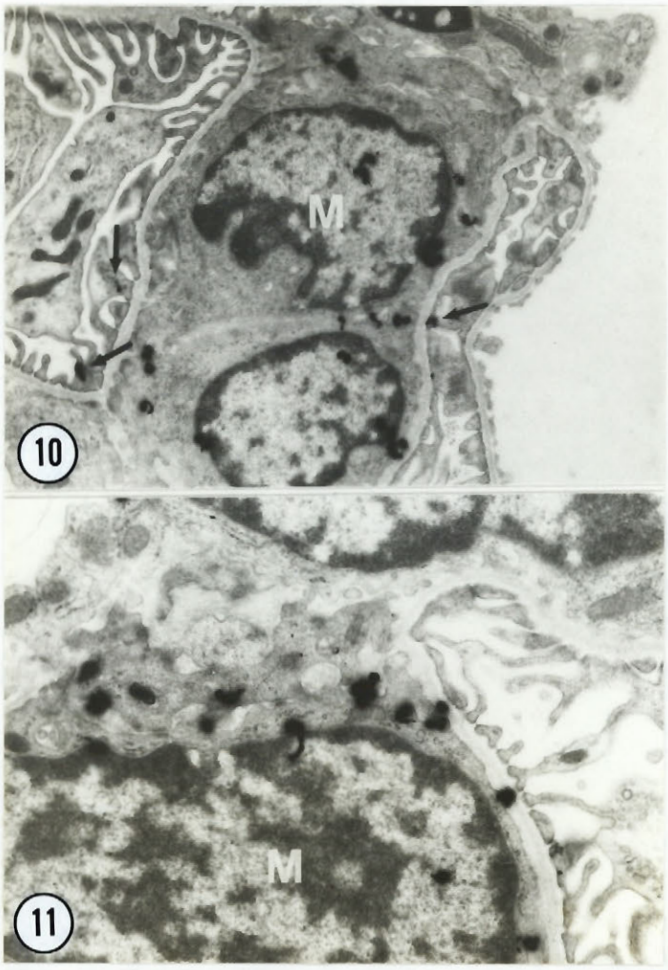

Fig. 10. Electron microscope radioautograph of glomerulus. Part of glomerulus after injection of ^{125}I-labeled angiotensin II is shown. Silver grains are mostly localized over mesangial cells (M). Three grains (arrows) are located over podocytes of visceral epithelial cells. Magnification, X 7,780.

Fig. 11. Electron microscope radioautograph of glomerulus. Detail of glomerulus after injection of ^{125}I-labeled angiotensin II is shown. Most silver grains are located at periphery of a mesangial cell (M). Magnification, X 13,030.

(EC_{50}) between 10^{-9} and 10^{-8} M. ANF alone had significant effect on glomerular size index at concentrations ranging from 10^{-11} to 10^{-6} M. In contrast, when ANF was added to ANG II, the decrease in glomerular size index observed after addition of ANG II alone was abolished. This inhibitory effect of ANF was concentration dependent with an apparent IC_{50} between 10^{-11} and 10^{-10} M (Fig.13).

DISCUSSION

The radioactive uptake of ^{125}I-ANG II after an intravascular injection, and the proportion of the displacement obtained in the cortex and outer and inner medulla of the kidney by the prior perfusion of ANG II antagonists correlates with the distribution of ANG II receptors as observed by other techniques. The highest concentration of ANG II receptors is localized in the cortex and outer medulla with a low concentration in the inner medulla (22). Although tissues fixed by perfusion contained variable amounts of nondisplaceable uptake, radioautograms did not generate silver grains, probably because part of the nondisplaceable uptake is lost during the radioautographic processing. The radiactive losses occur mainly during the fixation period, before embedding, and they may represent up to 30% of the total radioactive uptake (7). The demonstra-

FIGURES 12 AND 13

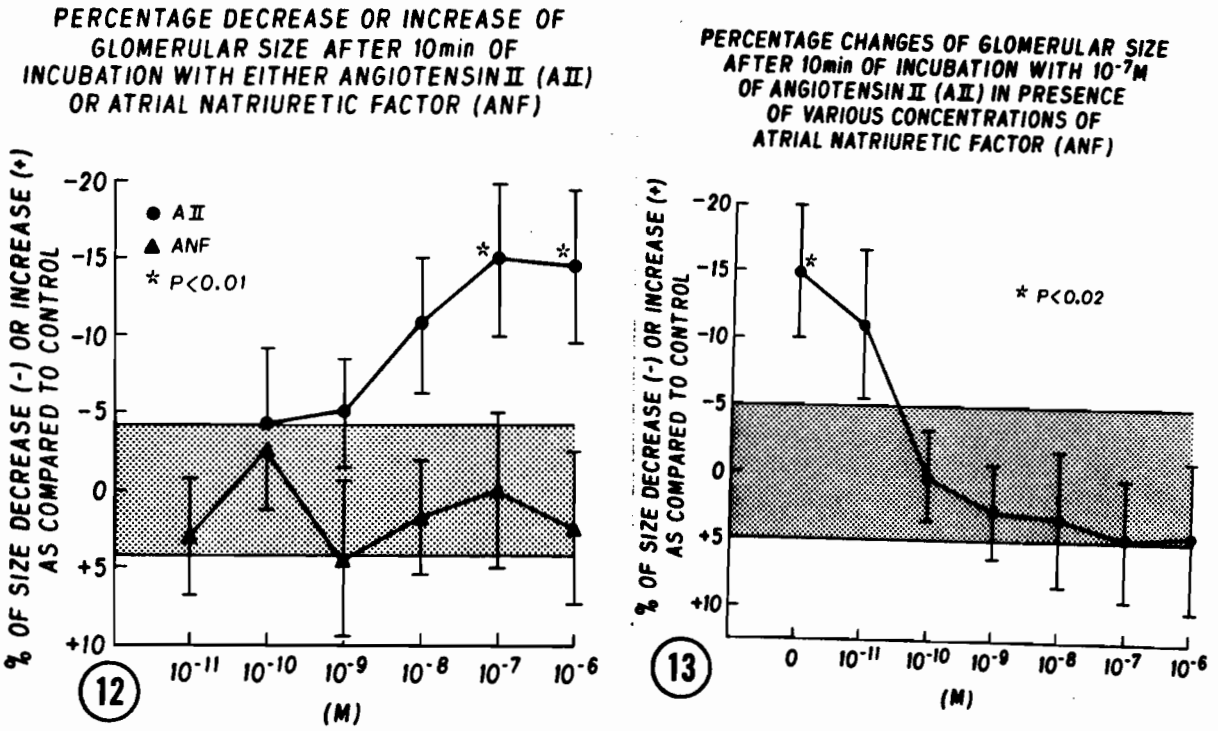

Fig. 12. Isolated rat glomeruli were suspended in an oxygenated Krebs solution and incubated for 10 min at 22°C alone (control) or with various concentrations of either angiotensin II (AII) or atrial natriuretic factor (ANF). At 10-11 min, glomeruli were photographed (n = 90) and their size estimated. Changes in size were plotted as percentage from control (dotted area). Points and bars are means ± SE of at least 3 separate experiments. Significance was assumed for $P < 0.05$ using Dunnett's test for multiple comparisons to control.

Fig. 13. Isolated rat glomeruli were suspended in an oxygenated Krebs solution and incubated for 10 min at 22°C alone (control) or with various concentrations of atrial natriuretic factor plus 10^{-7} M angiotensin II. At 10-11 min, glomeruli were photographed (n = 70) from control (dotted area). Points and bars are means ± SE of at least 3 separate experiments. Significance was assumed for $P < 0.05$ using Dunnett's test for multiple comparisons to control.

tion that ^{125}I (6) and tyrosine-H^3 (23) do not generate silver grains on radioautograms in the kidney, when injected intravascularly, suggest that free iodine and tyrosine molecules are not cross linked by glutaraldehyde. Thus the displacement of the radioautographic reaction over glomeruli by specific ANG II antagonists confirms that ^{125}I-ANG II binding sites are localized in the glomeruli. Furthermore, the localization of 60% of silver grains on mesangial cells by electron microscope radioautography demonstrates that binding sites for ANG II are localized mainly on these cells.

Using an identical technique, the amount of radioactive uptake of ^{125}I-ANF at 2 min after an intravascular injection and the displacement obtained with the concomitant injection of unlabeled ANF and not by ACTH or bradykinin correlate with the distribution of ^{125}I-ANF receptors in isolated nephron segments of the dog kidney (11). The fact that excess of cold ANF produced only 50% inhibition of radioactive uptake in the kidney indicates that an appreciable amount of the radioactivity in this organ is not associated with high-affinity sites. The inhibition produced by simultaneous injection of ^{125}I-ANF and bradykinin may be due to the blood pressure lowering effect of the latter

(24). Because this decrease in uptake was not detectable in the radioautograms and was not accompanied by a decrease in the number of silver grains localized over glomeruli or proximal tubules, it is probable that it may represent a diffuse decrease in the radioactive uptake in the cortex. The almost complete displacement of radioautographic reaction on the glomeruli by an excess of unlabeled ANF, but not on proximal tubules that do not appear to possess receptors for ^{125}I-ANF (11), strongly suggest that binding sites for ^{125}I-ANF are thus localized on the glomeruli by radioautography *in vivo*. This is confirmed by the *in vitro* results.

The localization of silver grains mainly on foot processes of epithelial cells at the ultrastructural level is in agreement with the radioautographic pattern observed at the light microscope level by both *in vivo* and *in vitro* techniques. Silver grains are also found in smaller amounts on endothelial (15%) and mesangial (10%) cells, which is not surprising; previous radioautographic studies have localized binding sites for ^{125}I-ANF in endothelial cells and smooth muscle cells of arteries, arterioles, veins, and venules in the kidney (7), and specific receptors have been characterized on cultured endothelial and smooth muscle cells (28). Their presence correlates with cGMP production (28). Thus the increase in particulate guanylate cyclase activity {with

a subsequent rapid and massive (50-fold) rise in cGMP} (9) and the decrease in adenylate cyclase activity (Anand-Srivastava et al., unpublished observations) observed after exposure of isolated glomeruli to ANF are likely to be due to interaction of ANF with epithelial visceral cells. Both cyclic adenosine 5'-monophosphate (cAMP) and cGMP have been localized by immunohistochemistry on the foot processes of epithelial visceral cells (12), and adenylate cyclase is present on their surface (27). However, in a recent report, Ballermann et al. (3) have demonstrated that cultured rat glomerular mesangial cells (but not epithelial cells) expressed receptors for ANF that correlate with an increase in cGMP. On the other hand, human glomerular epithelial cells in culture (but not mesangial cells) show an increase in cGMP levels when stimulated by ANF (R. Ardaillou, personal communication). Whether these discrepancies are due to differences in ANF receptor expression in cultured cells has to be determined.

The mechanism by which ANF induces diuresis and natriuresis has not been elucidated. Although hemodynamic changes and increase in GFR have been implicated as the major factors of ANF action in the kidney (4,9,10,21), inhibition of proximal tubular reabsorption, or redistribution of blood flow without changes in GFR have also been

observed (9,21). In a preliminary report, it has suggested that ANF increases glomerular filtration rate (GFR) by a concomitant afferent vasodilation and a mild efferent vasoconstriction (17). Likewise, the effects of ANG II in the kidney are not fully elucidated. ANG II markedly lowers cAMP in glomeruli but has no effect on cGMP (32). ANG II decreases GFR probably by a decrease in the ultrafiltration coefficient (K_f), despite an increase in postglomerular resitance (18). It has been suggested that, in addition to an effect of ANG II on arteriolar resistance, ANG II may modulate, by contraction of mesangial cells (18), the glomerular surface area available for filtration and thus the K_f. The presence of ANF receptors in isolated glomeruli may suggest some similar mechanisms. Morphological (20,25,26,30) and functional data (1,2) tend to indicate that the k_f may be modulated by the foot processes of the visceral epithelial cells of the glomeruli. The presence of 125I-ANF binding sites in the foot processes suggests that this vasoactive hormone may indeed be involved. In fact, the foot processes contain a large quantity of action filaments with concentrations of heavy meromyosin at their base near the insertion of the slit diaphragms (2). Microtubules are also abundant. Exposure of glomeruli to cytochalasins known to inhibit the contractile capacity of f-actin alters the

shape of foot processes from short processes with broad bases to taller processes with narrow bases (1,2). Analogous changes are produced by poisoning the microtubular system (1). Changes of the foot process shape may modulate the number or patent "pores" and the length of the slit diaphragms, which could influence the k_f (1). Changes of foot process shape may also change the filtration surface area or the resistance to convective water flow through interdigitating foot process.

Inhibition of ANG II-induced decrease in glomerular size could also increase k_f. Inhibition of ANG II-induced decrease in glomerular size by ANF, at picomolar concentrations, may have important physiological and physiopathological implications, since the influence on k_f of substances such as PTH, prostaglandins, and a variety of hormones seems to be mediated by increased cAMP formation and consequent release of renin with local ANG II formation (18,29).

REFERENCES

1. Andrews, P.M. Investigations of cytoplasmic contractile and cytoskeletal elements in the kidney glomerulus. Kidney Int. 20:549-562, 1981.

2. Andrews, P.M., Coffey, A.K. Cytoplasmic contractile elements in glomerular cells. Federation Proc. 42:3046-3052, 1983.

3. Ballermann, B.J., Hoover, R.L., Karnovsky, M., Brenner, B.M. Physiologic regulation of atrial natriuretic peptide receptors in rat renal glomeruli. J. Clin. Invest. 76:2049-2056, 1985.

4. Beasley, D., Malvin, R.L. Atrial extracts increase glomerular filtration rate in vivo. Am. J. Physiol. 248:F24-F30, 1985.

5. Benchimol, S., Cantin. M. Ultrastructural radioautography of synthesis and migration of proteins and catecholamines in the rat adrenal medulla. Cell. Tiss. Res. 225:293-314, 1982.

6. Bergeron, J.J.M., Rachubinski, R., Searle, N., Borts, D., Sikstron, R., Posner, B.I. Polypeptide hormones receptors in vivo: demonstration of insulin binding to adrenal gland and gastrointestinal epithelium by quantitative radioautography. J. Histochem. Cytochem. 28:824-835, 1980.

7. Bianchi, C., Gutkowska, J., Thibault, G., Garcia, R.,

Genest, J., Cantin, M. Radioautographic localization of ^{125}I-atrial natriuretic factor (ANF) in rat tissues. Histochemistry 82:441-452, 1985.

8. Cantin, M., Ballack, M., Beuzeron-Mangina, J., Anand-Srivastava, M.B., Tautu, C. DNA synthesis in cultured adult cardiocytes. Science 214:569-570, 1981.
9. Cantin, M., Genest, J. The heart and the atrial natriuretic factor. Endocr. Rev. 6:107-127, 1985.
10. Chou-Long, H., Lewicki, J., Johnson, L.K., Cogan, M.G. Renal mechanism of action of rat atrial natriuretic factor. J. Clin. Invest. 75:769-773, 1985.
11. De Léan, A., Vinay, P., Cantin, M. Distribution of atrial natriuretic factor receptors in dog kidney fractions. FEBS Lett. 193:239-242, 1985.
12. Dousa, T.P., Barnes, L.D., Ong, S.H., Steiner, A.L. Immunohistochemical localization of 3':5'-cyclic AMP and 3':5'-cyclic GMP in rat and cortex: effect of parathyroid hormone. Proc. Natl. Acad. Sci USA 74:3569-3573, 1977.
13. Fong, J.S.C., Drummond, K.N. Method for preparation of glomeruli for metabolic studies. J. Lab. Clin. Med. 71:1034-1039, 1968.
14. Greenwood, F.C., Hunter, W.L., Glover, J.J. The preparation of ^{131}I-labeled human growth hormone of high specific radioactivity. Biochem. J. 89:114-123, 1963.
15. Gutkowska, J., Lis, M., Cantin, M., Genest, J. Solid-

phase radioimmunoassay of tonin in extracts of submandibular glands of rats treated chronically with isoproterenol. Proc. Soc. Exp. Biol. Med. 170:165-171, 1982.

16. Gutkowska, J., Thibault, G., Januszewicz, P., Cantin, M., Genest, J. Direct radioimmunoassay of atrial natriuretic factor. Biochem. Biophys. Res. Commun. 122:593-601, 1985.

17. Ichikawa, I., Dunn, B.R., Troy, J.L., Maack, T., Brenner, B.M. Influence of atrial natriuretic peptide on glomerular microcirculation in vivo (Abstract) Clin. Res. 33:487A, 1985.

18. Kon, V., Ichikawa, I. Hormonal regulation of glomerular filtration. Ann. Rev. Med. 36:315-331, 1985.

19. Kopriwa, B.M., Levine, G.M., Nadler, N.J. Assessment of resolution by half distance values for tritium and radioiodine in electron microscopic radioautographs using Ilford L_4 emulsion. Developed "solution Physical" or D-19b methods. Histochemistry. 80:519-522, 1984.

20. Landis, E.M., Pappenheimer, J.R. Exchange of substances through the capillary walls. In Handbook of Physiology. Circulation, edited by Hamilton, W.F., Dow, P. Washington, DC. Am. Physiol. Soc., sect. 2, vol. 2, pp.961-1034, 1983.

21. Maack, T., Camargo, M.J.F., Kleinert, H.D., Laragh, J.H., Atlas, S.A. Atrial natriuretic factor:structure and functional properties. Kidney Int. 27:607-615, 1985.

22. Mendelsohn, F.A.O., Aguilera, G., Saavedra, J.M., Quirion, R., Catt, K. Characterization and regulation of angiotensin II receptors im pituitary, circumventricular organs and kidney. Clin. Exp. Hypertens. Part A Theory Pract. 5:1081-1097, 1983.

23. Osborne, M.J., Droz, B., Meyer, P., Morel, F. Angiotensin II: renal localization in glomerular mesangial cells by autoradiography. Kidney Int. 8:245-254, 1975.

24. Roblero, J., Ryan, M., Stewart, J.M. Assay of kinins by their effects on blood pressure. Res. Commun. Chem. Pathol. Pharmacol. 6:207-212, 1973.

25. Rodewald, R., Karnowsky, M.J. Porous substructure of the glomerulus slit diaphragms in the rat and mouse. J. Cell. Biol. 60:23-33, 1974.

26. Ryan, C.B., Heim, S.J., Karnowsky, M.J. Glomerular permeability to proteins: effect of hemodynamics factors in the distribution of endogenous immunoglobulin and exogenous catalase in the rat glomerulus. Lab. Invest. 37:415-427, 1976.

27. Sato, T., Garcia-Bunuel, R., Brandes, D. Ultrastructural cytochemical localization of adenylate cyclase in the rat nephron. Lab. Invest. 30:222-229, 1974.

28. Schenk, D.B., Jonhson, L.K., Schwartz, K., Sista, H., Scarborough, R.M., Lewicki, J.A. Distinct atrial natriuretic factor receptor sites on cultured bovine aorta smooth muscle and endothelial cells. Biochem. Biophys.

Res. Commun. 127:433-442, 1985.

29. Schlondorff, D., Yoo, P., Alpert, B.E. Stimulation of adenylate cyclase in isolated rat glomeruli by prostaglandins. Am. J. Physiol. 235: F458-464, 1978.

30. Shea, S.M., Morrison, A.B. A sterological study of the glomerular filter in the rat. Morphometry of the slit diaphragm and basement membrane. J. Cell Biol. 67:436-443, 1975.

31. Sraer, J.D., Sraer, J., Ardaillou, R., Minoune, O. Evidence for renal glomerular receptors for angiotensin II. Kidney Int. 6:241-246, 1974.

32. Torres, U.E., Nortdrup, T.E., Edwards, R.M., Shah, S.U., Dousa, T.P. Modulation of cyclic nucleotides in isolated rat glomeruli. Role of histamine carboxylcholine, parathyroid hormone and angiotensin II. J. Clin. Invest. 62:1334-1343, 1978.

33. Umemura, S., Smyth, D.D., Pettinger, W.A. Lack of inhibition by atrial natriuretic factor on cyclic AMP levels in single nephron segments and the glomerulus. Biochem. Biophys. Res. Commun. 127:943-949, 1985.

SECTION B

LOCALIZATION OF ^{125}I ATRIAL NATRIURETIC FACTOR (ANF) BINDING SITES IN RAT RENAL MEDULLA. A LIGHT AND ELECTRON MICROSCOPE RADIOAUTOGRAPHIC STUDY

This work was published in

J. Histochem. Cytochem. 35:149-153, 1987

ABSTRACT

Using light and electron microscope autoradiography *in vivo*, the localization of ^{125}I-(Arg 101-Tyr 126) atrial natriuretic factor (ANF)-binding sites was studied in the renal medulla of rats. At the light microscopic level, the radioautographic reaction was mainly distributed in patches in the outer medulla, and followed the tubular architecture in the innermost part of the inner medulla. At the electron microscopic level, binding sites were mainly found in the outer medullary descending vasa recta and inner medullary collecting ducts. These results suggest that, in rats, the renal medulla may participate in the natriuresis and diuresis produced by ANF through vascular and tubular effects; the former by changing medullary blood flow at the level of descending vasa recta and the latter by acting on electrolyte and water transport at the level of collecting ducts.

INTRODUCTION

The myoendocrine cells of atria secrete a peptide (atrial natriuretic factor, ANF) which produces rapid, short-lived, and massive diuresis and natriuresis (8,9,12). It is now established that the circulating form of ANF in rat is the 28 amino acid C-terminal moiety (Ser 99-Tyr 126) of the propeptide (22). The mechanism(s) and sites of the

effect along the nephron are not known. In vivo studies in dogs and rats have suggested that both hemodynamic changes (2,7,11) and specific interactions of ANF with proximal (21) or distal (6) segments of the nephron may be reponsible for the observed natriuresis.

Studies in dog isolated glomeruli, proximal tubules, Henle's loops, and collecting duct membranes have stablished that most receptors are localized in glomeruli, none are measurable in proximal tubules, and a much lesser number are found in distal tubules and collecting ducts (13). Solubilized receptors have been characterized in isolated rat glomeruli (10). After exposure of various isolated renal structures to ANF, the greatest increase in cGMP (resulting from stimulation of particulate guanylate cyclase) was found in glomeruli, with lesser increases in distal tubules and collecting ducts and no change in proximal tubules (23). Similarly,the greatest inhibition of adenylate cyclase activity was found in glomeruli, with no change in proximal tubules and smaller decreases in distal tubules and collecting ducts (1). Exposing isolated tubular populations to ANF also did not produce any measurable metabolic changes (oxigen consumption, substrate utilization) (24).

Light and electron microscope radioautographic studies (4,5) have shown that glomerular epithelial visceral cells (podocytes) seem to be the main target for ANF in the renal

cortex, together with arteries, arterioles, veins, and venules (4). The present study describes the ultrastructural distribution of binding sites in the renal medulla of rats 2 min after an intra-aortic injection of ^{125}I-ANF. We have observed that medullary binding sites for ^{125}I-ANF are localized mainly in descending vasa recta of the outer medulla and collecting ducts of the inner medulla.

MATERIALS and METHODS

Preparation of ^{125}I-ANF

^{125}I-ANF was prepared as already described (15) using synthetic Arg 101-Tyr 126 ANF with minor modifications of the chloramine-T method (14). The monoiodinated peptide was purified on a Sephadex 4B anti-ANF affinity column by HPLC as already described (15). The acetonitrile was evaporated with a nitrogen stream for a period of 1 hr at 4°C before the injection.

Injection of ^{125}I-ANF

0.054 nmol of ^{125}I-ANF (Arg 101-Tyr 126) (~ 1700 µCi/µg; ~ 18.9 µCi) in 0.1 M sodium phosphate buffer, pH 5.5, containing 0.1% BSA was injected in a total volume of 0.1 ml through a catheter inserted in the left carotid artery (directed to the aorta) of 40-g female Sprague-Dawley rats, under pentobarbital anesthesia. For displacement analysis, 10 µl of either ANF (Arg 101-Tyr 126; from 1.5 to 18 nmol),

$ACTH^{1-24}$(9 nmol) of bradykinin (9 nmol) were mixed with ^{125}I-ANF as above and injected as a single bolus into rats under identical conditions.

Preparation for Radioautography

Glutaraldehyde Fixation. At 2 min after injection of ^{125}I-ANF either alone or with an excess of unlabeled ANF, the rats were killed by intracardiac perfusion with Kreb's solution for 1 min followed by 2% glutaraldehyde buffered with cacodylate HCl (0.1 M, pH 7.4) for 10 min. The kidneys were removed and outer and inner medulla dissected.

The radioactivity present in a fragment of each renal zone was evaluated in an LKB 1270 gamma counter (LKB, Rockville, MD), and the fragments were then fixed for a further period of 1 h at 4°C. After this period, they were washed in cacodylate buffer with 2% sucrose, post-fixed in 2% osmium tetroxide buffered with veronal acetate, and embedded in Araldite as already described (8). Both semithin sections (1 μm) and thin sections (silver-gold interference color) were cut from the same blocks of tissue with a Reichert (OMU_2) ultramicrotome. Unstained semithin sections were coated with Ilford K_5 emulsion (ILford; Basildon, Essex, UK) as already described (8). Thin sections were placed on glass slides, coated with Parlodion (Baker Chemicals, Phillipsburg, NJ), stained with 2% uranyl acetate (10 min) followed by 1% lead citrate (2 min), and then coated

with a thin carbon film followed by Ilford L_4 emulsion (ILford) for electron microscope radioautography (3). Semithin sections were exposed for 1 month and developed as already described (8). Thin sections were exposed for 2 months and developed with Agfa Gevaert physical developer (Agfa Gevaert; Leverkusen, FRG) for compact grains, wich affords better resolution (17). Semithin sections were post-stained with 1% toluidine blue.

Bouin's Fixation. To allow the observation of ^{125}I-ANF binding sites in the whole kidney on the same autoradiogram, four rats of the same breed, weight, and sex were injected with 18.9 µCi (0.054 nmol) of ^{125}I-ANF either alone (n=2) or with an excess (9 nmol) of unlabeled ANF (n=2) as above. At 2 min after injection, the rats were perfused with Kreb's solution for 1 min followed by Bouin's fluid for 10 min. The kidneys were removed, fixed for a further 24 hr in the same fixative, and embedded in paraffin, and coronal sections (5 µm) were processed for light microscope autoradiography as described above.

Localization of ^{125}I-ANF

Light microscopy. Unstained paraffin sections of the whole kidney (5 µm) were examined with dark-field ilumination, and semithin sections from the outer and inner medulla were observed with a Zeiss light microscope.

FIGURE 1

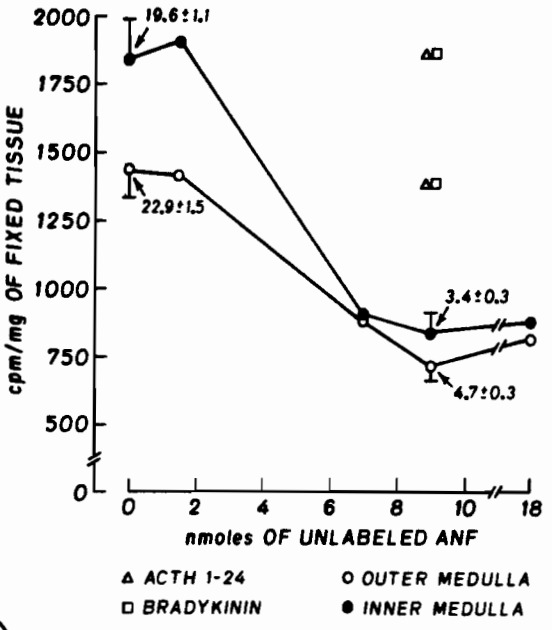

(1)

Fig. 1. Effect of unlabeled ANF, bradykinin, and $ACTH^{1-24}$ on renal medullary uptake after an intra-aortic injection of 0.054 nmol of ^{125}I-ANF 2 min after injection. Each point is from one experiment except when bars are present, which are from six different experiments. Numbers represent mean ± SE of silver grains counted on semithin sections (2500 μm^2) from outer and inner medulla and on the whole region of the innermost part of the inner medulla. Tissues were fixed with glutaraldehyde and the radioactivity content evaluated as described in Materials and Methods.

Electron Microscopy. Outer and inner medullas were scanned in a Jeol 1200 EX electron microscope at a magnification of 10,000, and photographs were taken wherever silver grains were present. More than 600 grains were thus analyzed on printed micrographs at a final magnification of 21,180.

RESULTS

Displacement of Radioactivity

Figure 1 summarizes the uptake of ^{125}I-ANF by the kidney in the presence of either unlabeled ANF, ACTH$^{1-24}$, or bradykinin 2 min after injection. The most potent inhibitor of uptake in the renal outer and inner medulla was 9 nmol of unlabeled ANF, whereas ACTH$^{1-24}$ and bradykinin were ineffective.

Light Microscopy

Radioautographs generated from both paraffin sections of whole kidney and semithin sections of outer and inner medulla showed that silver grains were not homogenously distributed. The concentration of silver grains seemed to follow the localization of vasa recta bundles in the outer medulla (Figure 2a). In rats receiving an excess of unlabeled ANF, silver grains were almost completely absent on vasa recta bundles, whereas the number of silver grains on brush border of P_3 segments of proximal tubules did not change (Figure 2b). In the inner medulla, silver grains were more homogenously distributed and seemed to follow the

FIGURE 2

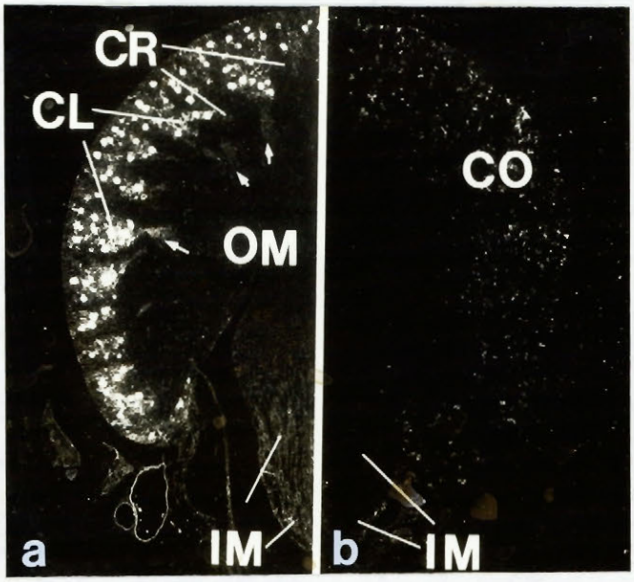

Fig. 2. (a) Coronal section of the kidney of rats injected with 0.054 nmol of ^{125}I-ANF. Silver grains (white) are localized on the cortical labyrinths (glomeruli and vasculature) (CL) and absent on medullary rays (tubular structures) (CR). In the outer medulla (OM) silver grains are localized on vasa recta bundles (arrows). In the inner medulla (IM) silver grains are localized predominantly in the innermost part. (b) Coronal section of kidney of rat injected with 0.054 nmol of ^{125}I-ANF plus 9 nmol of unlabeled ANF. Silver grains localized in the cortex (CO) are more diffusely distributed. Vasa recta bundles are no longer labeled in the outer medulla (OM) and silver grains are absent in the inner medulla (IM). Original maginifications X 10.

tubular architecture (Figure 2a). In rats receiving an excess of unlabeled ANF, the radioautographic reaction was almost completely absent (Figure 2b).

Table 1. Ultrastructural Localization of Silver Grains in the Renal Medulla after Injection of ^{125}I-ANF

Structure	Outer medulla		Inner medulla	
	No. of grains	%	No. of grains	%
Vasa recta	266	70	49	15
Thin loop of Henle	16	4	66	21
Thick loop of Henle	44	12	-	-
Interstitial cell	-	-	62	19
Collecting duct	52	14	143	45
Total	380	100	320	100

Between 100 and 150 electron microscope radioautographs per medullary zone were taken over the renal wherever silver grains were present (final magnification, X 21,180). Silver grains overlying tissue were scored and expressed as a percentage of the total grains counted.

Electron Microscopy

An the electron microscopic level, tubular and vascular structures in the outer and inner medulla were characterized morphologically according to Kriz and Kaissling (19). Most

silver grains were localized on bundles of vasa recta (70%) at the outer medulla (Table 1). Silver grains on vasa recta were observed mainly in descending branches (Figure 3a,b and Table 1). Both endothelium and pericytes were labeled (Figure 3b). In the outer medulla, a smaller percentage of silver grains was also observed on collecting ducts, thick loops of Henle, and finally thin loops of Henle (Table 1). At the inner medulla, however, silver grains were mainly observed on collecting duct epithelium, followed by thin loops of Henle, interstitial cells, and capillary endothelium (Table 1 and Figure 3c-f).

DISCUSSION

The localization of the labeled ANF that is displaced by increasing concentrations of unlabeled ANF but not by bradykinin or $ACTH^{1-24}$ suggests that binding sites for ANF are present in the outer and inner medulla of the rat kidney. The displacement of the radioactivity uptake seems to be dose-dependent with a maximum inhibition of ~50% and ~54% in the outer and inner medulla respectively. Although an appreciable amount of the radioactivity in the medulla was not displaceable, the radioautographic reaction was very weak in renal sections of rats injected with an excess of unlabeled hormone, suggesting that radioactivity losses occurred during the processing of radioautographs. The nature of

these losses is not known but it may represent 30% of the total radioactivity uptake in the cortex, outer and inner medulla (4) and occurred mainly during the 2 hr and 24 hr periods of glutaraldehyde and Bouin's fixations respectively. The presence of an radioautographic reaction in renal cortex of rats injected with labeled and unlabeled ANF is mostly due to the presence of nondisplaceable radioactivity uptake that was fixed by glutaraldehyde at the level of proximal tubule brush border (4). The presence of a radioautographic reaction on cortical rays after injection of unlabeled ANF results from the presence of silver grains on P3 segments of proximal tubule brush border, which also accounts for the presence of nondisplaceable uptake. Either glutaraldehyde or Bouin's fixation revealed that the localization of ANF binding sites is identical. Autoradiographs from paraffin sections allowed a view of the localization of binding sites, but it did not permit detailed morphological analysis. Such difficulties have been encountered using <u>in vitro</u> radioautographic techniques (16,18,20). These limitations result both from the complexity of the rat medulla, wich is composed of a complex network of vascular and tubular elements, and from the poor resolution of the light microscope. The electron microscope made it possible to obtain a more precise localization of

FIGURE 3

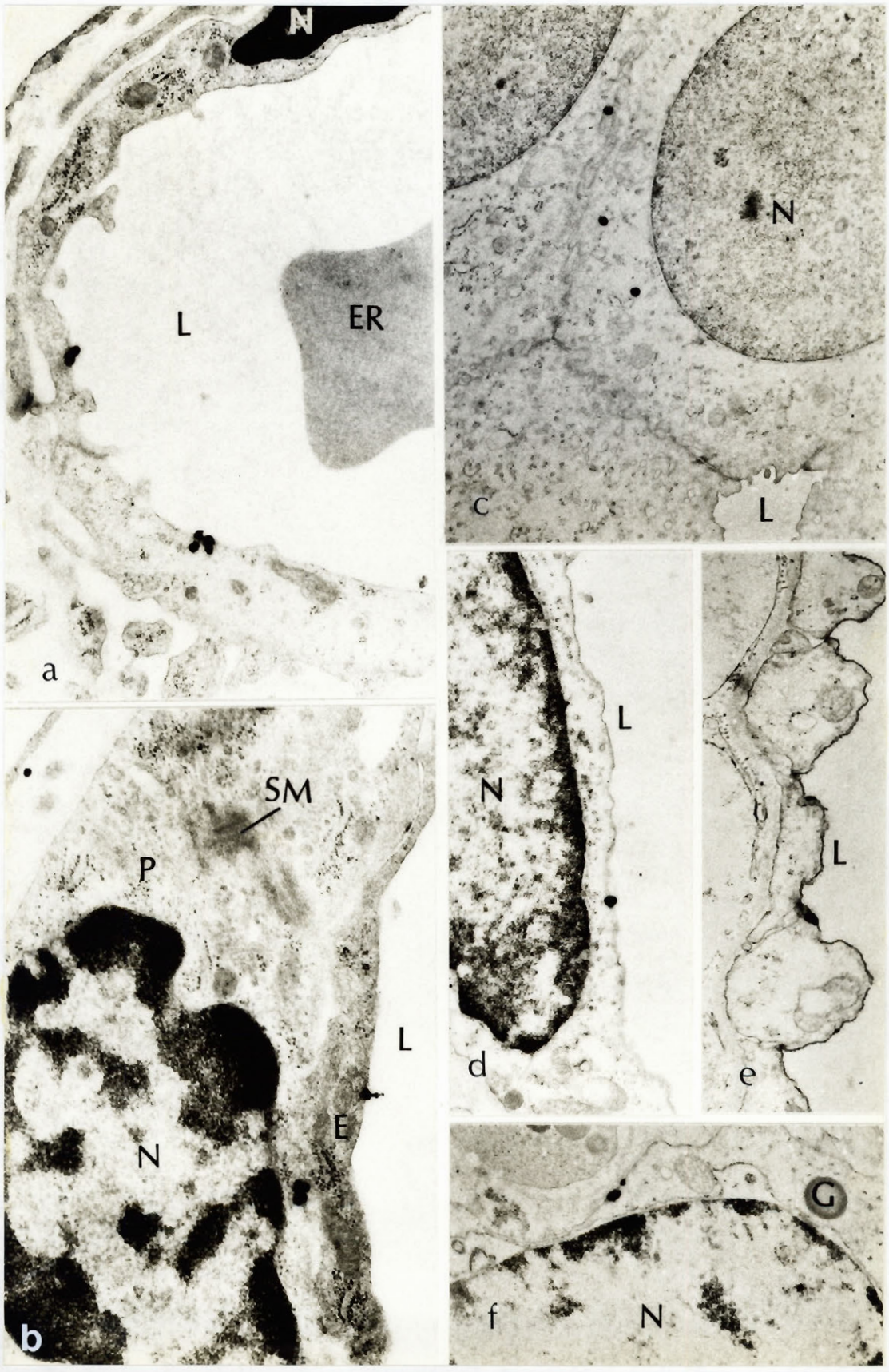

Fig. 3. Electron microscope radioautographs from renal medulla of rats injected with 0.054 nmol of ^{125}I-ANF. Silver grains (black dots) are localized on endothelial cells (E) (a,b) and pericytes (P) (b) of descending vasa recta of the outer medulla. In the inner medulla (c-f) silver grains are localized on collecting ducts (c), vasa recta (d), descending thin limb of long loop of Henle (e), and interstitial cell (f). N, nuclei; L, lumen; SM, smooth muscle; G, granules; ER, etythrocytes. Original magnifications: a, b X 19,000; c X 9,000; d,f X 11,000; e X 14,000.

ANF binding sites because of its higher resolution (80 nm) associated with the morphological characteristics of each structure. With the elecron microscope, silver grains were mainly found on descending vasa recta in outer medulla and on collecting ducts. Although silver grains were also present on the brush border of outer medulla proximal tubules, these grains were not analyzed because no displacement was caused by a concomitant injection of an excess of unlabeled ANF, which suggests that these silver grains do not represent binding sites. The presence of binding sites for ANF in vasa recta and collecting tubules lends support to physiological studies that suggest a vascular and tubular effect of ANF in promoting diuresis and natriuresis. The presence

of ANF binding sites mainly in the descending vasa recta of the outer medulla, in both endothelial cells and pericytes, is in close agreement with these observations. Medullary blood flow may be adjusted by modulation of descending vasa recta diameter at the level of the outer medulla (19). The presence of ANF binding sites on pericytes strongly suggests such effects. The presence of smaller percentage of binding sites on medullary collecting tubules and thick loop of Henle suggests that ANF may also affect these structures. A relatively low concentration of ANF receptors has been characterized in isolated thick loops of Henle (13) together with a response of putative second messengers (1,23). In the inner medulla, binding sites for ANF are more widespread, and are concentrated over collecting ducts. These results are in agreement with a tubular effect of ANF at this level. The presence of binding sites in interstitial cells, thin loops of Henle, and capillaries points to an effect on these structures as well. It is interesting to note that inner medullary collecting ducts or Bellini's ducts seem to present more binding sites for ANF and that thin loops of Henle are also labeled at the inner medulla, suggesting that if a tubular effect is present, it will occur in the innermost part of the inner medulla. The presence of binding sites in inner medullary thin loops of Henle suggests that they represent long loops.

REFERENCES

1. Anand-Srivistava, M.B., Vinay, P., Genest, J., Cantin, M. Effect of atrial natriuretic factor on adenylate cyclase nephron segments. Am. J. Physiol. 251:F417-F423, 1986.
2. Besley, D., Malvin, R.L. Atrial extracts increase glomerular filtration rate in vivo. Am. J. Physiol. 248:F24-F30, 1985.
3. Benchimol, S., Cantin, M. Ultrastructural radioautography of synthesis and migration of proteins and catecholamines in the rat adrenal medulla. Cell Tissue Res. 225:293-314, 1982.
4. Bianchi, C., Gutkowska, J., Garcia, R., Thibault, G., Cantin, M., Genest, J. Localization of ^{125}I-atrial natriuretic factor in rat tissues. Histochemistry 82:441-452, 1985.
5. Bianchi, C., Gutkowska, J., Thibault, G., Garcia, R., Genest, J., Cantin, M. Distinct localization of atrial natriuretic factor and angiotensin II binding sites in the glomerulus. Am. J. Physiol. 251:F594-F602, 1986.
6. Borenstein, H.B., Cupples, W.A., Sonnenberg, H., Veress, A.T. The effect of a natriuretic atrial extract on renal haemodynamics and urinary excretion in anaesthetized rats. J. Physiol. 334:133-140, 1983.
7. Camargo, M.J.F., Kleinert, D., Atlas, S.A., Sealey,

J.F., Laragh, J.H., Maack, T. Ca-dependent hemodynamic and natriuretic effects of atrial extract in the isolated perfused kidney. Am. J. Physiol. 246:F447-456, 1984.

8. Cantin, M., Ballack, M., Beuzeron-Mangina, J., Anand-Srivastava, M.B., Tautu, C. DNA synthesis in cultured adult cardiocytes. Science 214:569-571, 1981.
9. Cantin, M., Genest, J. The heart and the atrial natriuretic factor. Endocrine Rev. 6:107-126, 1985.
10. Carrier, F., Thibault, G., Schiffrin, E.L., Garcia, R., Gutkowska, J., Cantin, M., Genest, J. Partial characterization and solubilization of receptors for atrial natriuretic factor in rat glomeruli. Biochem. Biophys. Res. Commun. 132:666-673, 1985.
11. Chou-Long, H., Lewicki, J., Johnson, L.K., Cogan, M.G. Renal mechanism of action of rat atrial natriuretic factor. J. Clin. Invest. 75:769-773, 1985.
12. De Bold, A.J. Atrial natriuretic factor: a hormone produced by the heart. Science 230:767-770, 1985.
13. De Léan, A., Vinay, P., Cantin, M. Distribution of atrial natriuretic factor receptors in dog kidney fractions. FEBS Lett. 193:239-242, 1985.
14. Greenwood, F.C., Hunter, W.L., Glover, J.J. The preparation of ^{131}I-labelled human growth hormone of high specific radioactivity. Biochem. J. 89:114-123,1963.

15. Gutkowska, J., Thibault, G., Januszewicz, P., Cantin, M., Genest, J. Direct radioimmunoassay of atrial natriuretic factor. Biochem. Biophys. Res. Commun. 12:593-601, 1985.

16. Healy, D.P., Fanestil, D.D. Localization of atrial natriuretic peptide binding sites within the rat kidney. Am. J. Physiol. 250:F573-578, 1986.

17. Kopriva, B.M., Levine, G.M., Nadler, N.J. Assessment of resolution by half distance values for tritium and radioiodine in electron microscopic radioautographs using Ilford L4 emulsion. Developed "solution physical" or D-19b methods. Histochemistry 80:519-522, 1984.

18. Koseki, C., Hayashi, Y., Torikai, S., Furuya, M., Ohnuma, N., Imai M. Localization of binding sites for α-rat atrial natriuretic polupeptide in rat kidney. Am. J. Physiol. 250:F210-216, 1986.

19. Kriz, W., Kaissling, B. Structural organization of the mammalian kidney. In the kidney: physiology and pathophysiology, edited by Seldin, D.W., Giebish, G. New York, Raven Press, 1985, 265.

20. Murphy, K.M.M., McLaughlin, L.L., Michener, M.L., Needleman, P. Autoradiographic localization of atriopeptin III receptors in rat kidney. Eur. J. Pharmacol. 111:291-292, 1985.

21. Sonnenberg, H.J., Cupples, W.A., De Bold, A.J., Veress, A.T. Intrarenal localization of the natriuretic effect

of cardiac atrial extract. Can. J. Physiol. Pharmacol. 60:1149-1152, 1982.

22. Thibault, G., Lazure, C., Schiffrin, E.L., Gutkowska, J., Chartier, L., Garcia, R., Seidah, N.G., Chretien, M., Genest, J., Cantin, M. Identification of a biologically active circulating form of rat atrial natriuretic factor. Biochem. Biophys. Res. Commun. 130:981-986, 1985.

23. Tremblay, J., Gerzer, R., Vinay, P., Pang, S.C., Beliveau, R., Hamet, P. The increase of cGMP by atrial natriuretic factor correlates with the distribution of particulate guanylate cyclase. FEBS Lett. 181:17-22, 1985.

24. Vinay, P., Manillier, C., Lalonde, L., Thibault, G., Boulanger, Y., Gougoux, A., Cantin, M. Comparative effects of ANF and various diuretics on isolated nephron segments of dogs and rats. Kidney Int. 31:946-955, 1987.

CHAPTER 4

This chapter discusses the localization of ANF binding sites in the eye. These binding sites are negatively coupled to adenylate cyclase.

LOCALIZATION AND CHARACTERIZATION OF SPECIFIC RECEPTORS FOR ATRIAL NATRIURETIC FACTOR IN THE CILIARY PROCESSES OF THE EYE.

This work was published in
Curr. Eye Res. 4:283-293, 1986.

ABSTRACT

By light and electron microscope radioautography *in vivo*, competitive binding sites for (Arg 101 - Tyr 126) ^{125}I-atrial natriuretic factor were localized mostly on the "pigmented" epithelium of the rat ciliary process. Further investigation using isolated ciliary processes from rabbits demonstrated the presence of specific receptors for ^{125}I-atrial natriuretic factor. In addition, synthetic atrial natriuretic factor inhibited basal and stimulated adenylate cyclase activity.

These results demonstrate for the first time the presence of specific receptors for atrial natriuretic factor in the ciliary processes which are negatively coupled to adenylate cyclase. The possible role of this peptide in the control of intraocular pressure is suggested.

INTRODUCTION

Recently a biologically active peptide, atrial natriuretic factor (ANF), has been isolated from rat atria, sequenced, and synthetized (31). By immunocytochemistry this peptide was localized in atrial secretory granules (5). ANF was found to be the C-terminus of a much larger molecule (pre, pro and connecting peptide) made up of 152 amino acids (25, 27, 33, 35, 36) The synthetic peptide (Arg 101-Tyr 126) was found to posses a great variety of biological effects such as diuresis and natriuresis (13, 17, 31) vasodilation

with inhibition of the arterial contraction produced by norepinephrine and angiotensin II (18), inhibition of aldosterone and cortisol hypersecretion from the adrenal (10, 11, 14, 15) and modulation of arginine vasopressin secretion from the posterior pituitary (23). This peptide inhibits basal and stimulated adenylate cyclase activity in a variety of target tissues (1, 2, 3) and increases cGMP levels in blood, urine and renal cortical cells in culture (21) and particulate guanylate cyclase activity in isolated glomeruli, thick loops of Henle and collectiong tubules (34). Specific receptors for this synthetic fragment have been characterized in the aorta, mesenteric artery, adrenal zona glomerulosa and zona fasciculata of beef adrenal cortex (10, 11, 14, 15). Competitive binding sites for ^{125}I-ANF have been localized by radioautography in a great variety of rat tissues including the epithelial cells of the rat ciliary body (4). Since the epithelium of the ciliary body is implicated in the control of aqueous humor formation in the eye, and because ANF has been implicated in salt and water homeostasis, we extended our investigation to this particular tissue. The present experiments combined light and electron microscope radioautography, radioligand binding studies and adenylate cyclase activity determinations which have been, up to now, of crucial importance in the localization and characterization of receptors for ANF in putative target

tissues (6).

By means of these techniques it was demostrated that high affinity receptors for ANF (negatively coupled to adenylate cyclase) are mostly localized on the plasma membrane of basilar infoldings of the ciliary process epithelium facing the blood supply ("pigmented" layer). These results raise the possibility that ANF may also be implicated in sodium/water homeostasis in the eyes as well.

MATERIALS AND METHODS

Materials

The following products were purchased from Sigma Chemical Co. (St. Louis, MO): GTP, ATP, cAMP, ACTH, epinephrine, norepinephrine, dopamine, isoproterenol. Forskolin was obtained from Calbiochem-Behring Corp., (San Diego, CA). ANF (Arg 101-Tyr 126) was a gift from Dr. R.Nutt of Merck Sharp & Dohme Research Laboratories (West Point, PA). Bradykinin was purchased from Beckman Instruments, Inc. (Palo Alto, CA). (α^{32}P) ATP was obtained from Amersham Corp. (Arlington Heights, IL).

Preparation of ^{125}I-ANF

^{125}I-ANF was prepared as already described (20) using synthetic ANF (Arg 101-Tyr 126) with minor modifications of the chloramine-T method (22). The tracer was purified on sepharose 4B anti-ANF affinity column followed by HPLC on a μ Bondapack C_{18} column (0.39 x 30 cm).

Injection of ^{125}I-ANF

Freshly purified ^{125}I-ANF (18.9 µCi; ~ 0.035 nmoles) in sodium phosphate buffer 0.1 M, pH 5.5 containing 0.1% BSA was injected in a volume of 0.1 ml through a catheter implanted in the left carotid artery and directed to the aorta of female, 60 g B.W., Sprague-Dawley albino rats (n=4), under pentobarbital anesthesia. For displacement analysis, 9 nmoles of either ANF (Arg 101-Tyr 126) (n=4), bradykinin (n=2) or ACTH$^{1-24}$ (n=2) was mixed with ^{125}I-ANF as above and injected in a single bolus to rats of the same breed, weight and sex.

At 2 min after injection of ^{125}I-ANF alone or in combination with either ANF, bradykinin or ACTH$^{1-24}$, the rats were sacrificed by intracardiac perfusion first of Kreb's solution for 30 seconds followed by glutaraldehyde 2% buffered with cacodylate HCL (0.1 M; pH 7.4) for 10 min. The right eyes were enucleated and the radioactive content evaluated in a LKB 1270 Rack gamma II counter. After counting, the eyes were divided in two halves by a coronal section and fixed for a further period of one hour. The ciliary processes were then isolated from the anterior segment of the eye and their radioactive content evaluated as above. The ciliary processes were kept at 4°C in cacodylate buffer plus 2% sucrose and embedded in Araldite as already described (7) after post-fixation with 2% osmium tetroxide

buffered with Veronal acetate. During all phases of embedding, the radioactivity losses never exceeded 15% of the initial counts.

Light microscope radioautography

Semithin sections (1 µm) of the isolated ciliary processes were done in a Reichert (OMU2) ultramicrotome equipped with a glass knife, coated with Ilford K5 emulsion, exposed for one month and developed as already described (7, 8, 9). The sections were then stained with 1% toluidine blue and visualized with a Zeiss light microscope.

Electron microscope radioautography

Thin sections (silver-gold interference color) were cut using the same ultramicrotome equipped with a diamond knife. They were placed on glass slides coated with Parlodion and stained with 2% uranyl acetate (pH 7.4) for 10 min followed by 1% lead citrate for 3 min. A thin layer of carbon was evaporated over each slide and they were then dipped in L4 Ilford emulsion as already described (7). The slides were exposed for 2 months (4°C), developped with Agfae/Gevaert solution physical developer as already described (24) and examined, after having been placed on copper grids coated with formvar, in a Jeol 1200 EX electron microscope. The distance from the center of each silver grain (total of 351) to the nearest cell surface of the "pigmented" epithelium cells of the ciliary process was measured with a graduated

caliper (mm) and a x 10 magnifying glass from forty five radioautographs (final magnification of x 21,180). In this evaluation, the Half-Distance (H.D.) was calculated using a 10 H.D. cut off as described by Salpeter (29).

Isolation of rabbit ciliary processes

Female albino rabbits (2 to 2.5 kg) were anesthetized by intravenous injection of sodium pentobarbital. The rabbits were perfused through the left cardiac ventricle with Kreb's solution for 1 min to wash out the blood from the eyes and then enucleated and chilled in ice-cold Kreb's solution before dissection of the ciliary processes. A circumferential incision close to the limbus was done, the anterior segment was isolated and the vitreous as well as the lens removed. The remaining anterior preparation was placed, cornea down, in a Petri dish. The Petri was filled with fresh ice-cold Kreb's solution and, under a dissecting microscope, the ciliary processes were freed from their attachments to the iris, cut and pooled in a tube containing fresh ice-cold Kreb's solution. Each group of 4 rabbits (for a total of 32 rabbits) yielded about 80 mg of isolated ciliary processes. A sample (20 mg) was taken and its purity and integrity examined by light microscopy from 5 µm sections, of paraffin-embedded tissue fixed in Bouin's fluid and stained with hemotoxylin-eosin.

Radioligand binding studies

Fresh isolated ciliary processes from rabbits were homogenized in 20 nM $NaHCO_3$, 1 mM EDTA and membranes were prepared by centrifugation at 40,000 g for 10 min. at 4°C. The final pellet was ressuspended in 50 mM Tris-HCl, pH 7.4, 0.5% BSA, 0.1 mM EDTA. ^{125}I-ANF (30,000 CPM) was incubated at 25°C for 60 min. in 1 ml of the same buffer containing 60 µg of protein of ciliary process membranes with various concentrations of unlabeled ANF. Membrane bound ^{125}I-ANF was then separated by filtration on FG/C glass fiber filters followed by washing with 24 ml of cold buffer and the ^{125}I-ANF retained in the filter was mesured in a gamma counter (80% efficiency). The competition curves were analyzed with a four-parameter logistic equation (16).

Adenylate cyclase activity determination

Fresh rabbit ciliary processes were placed in ice-cold buffer containing 10 mM Tris and 1 mM EDTA (pH 7.5). The tissue was homogenized in the same buffer with a teflon-glass homogenizer and then used for adenylate cyclase determination. Adenylate cyclase activity was determined as already described (1, 2, 3). Incubations were initiated by addition of the particulate fraction (50 µg - 80 µg of protein) to the reaction mixture which had been thermally equilibrated for 2 min at 37°C. Reactions were conducted in

Table 1. Effect of either ANF, bradykinin or $ACTH^{1-24}$ on the radioactive uptake (cpm/mg of fixed tissue) of ^{125}I-ANF by the eye [1]

Fixed tissue	Whole eye	Anterior segment without ciliary processes, lens and vitreous	Posterior segment	Ciliary processes
None	102 ± 4[2]	100 ± 3	120 ± 8	2,050 ± 148
ANF	68 ± 2	98 ± 4	118 ± 9	680 ± 82
%	33	2	2	67[3]
Bradykinin	98 ± 3	105 ± 3	117 ± 7	1,980 ± 127
%	4	-	2.5	3
ACTH	107 ± 4	110 ± 5	113 ± 6	2,100 ± 110
%	-	-	6	-

1. The animals were injected through the left carotid artery with 18.9 µCi of ^{125}I-ANF either alone (n=4) or in combination with 9 nanomoles of cold ANF (n=4), bradykinin (n=2) or $ACTH^{1-24}$ (n=2) in a total volume of 0.1 ml 2 min after injection they were sacrified by intracardiac infusion of Ringer-Locke fluid (30 sec) and then of 2% glutaraldehyde (10 min). The right eye was enucleated and processed as described.
2. Mean ± S.E.
3. $p < 0.05$

triplicate for 10 min at 37°C. Reactions were terminated by addition of 0.6 ml of 120 mM zinc acetate. cAMP was purified by co-precipitation of other nucleotides with $ZnCO_3$ and subsequent chromatography by the double column system as described by Saloman et al. (28). Under the assay conditions used, adenylate cyclase activity was linear with respect to protein concentration and time of incubation. Protein was determined as described by Lowry et al (26) with crystalline bovine serum albumin as standard.

RESULTS

^{125}I-ANF uptake in the eye

As shown in Table 1, the radioactive uptake at 2 min after an intracarotid injection of 18.9 µCi of ^{125}I-ANF was concentrated in the ciliary processes of the eye. This structure alone concentrated about 20 times more ^{125}I-ANF than the anterior and the posterior segments. An injection of 9 nmoles of unlabeled ANF together with 18.9 µCi of 125I-ANF inhibited the radioactive uptake in whole eye (33%) (which corresponds to 68% in the isolated ciliary processes) while injections of 9 nmoles of either bradykinin of $ACTH^{1-24}$ had no effect on the radioactive uptake in the eye's segments (anterior and posterior) and in the isolated ciliary processes (Table 1).

FIGURES 1 AND 2

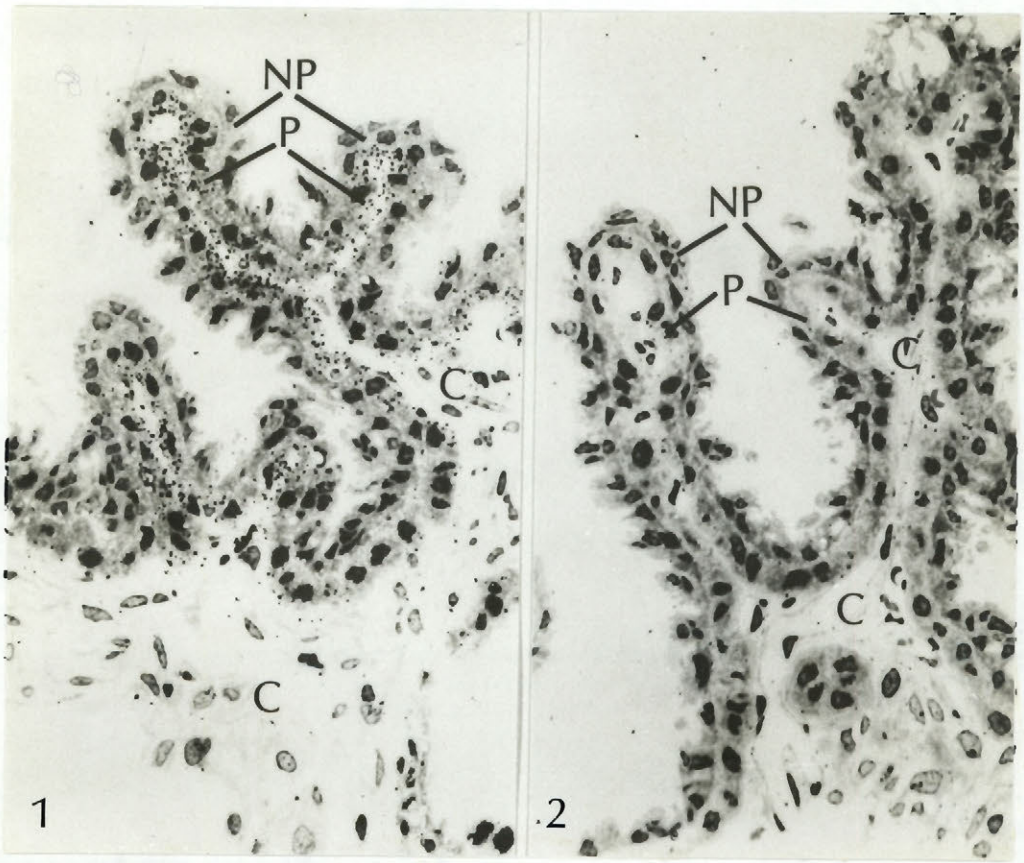

Fig. 1. Light microscope radioautograph of a semithin section of rat ciliary process 2 min after injection of 18.9 µCi of ^{125}I-ANF. Silver grains are localized almost exclusively over the "pigmented" epithelium (P). Capillaries (C); non-pigmented epithelial cells (NP). (Toluidine blue, X 400).

Fig. 2. Light microscope radioautograph of a semithin section of rat ciliary process 2 min after injection of 18.9 µCi of ^{125}I-ANF together with 9 nmoles of ANF. Silver grains are absent over the "pigmented" epithelium (P), non-pigmented epithelium (NP) and capillaries (C). (Toluidine blue, X 400).

FIGURES 3 AND 4

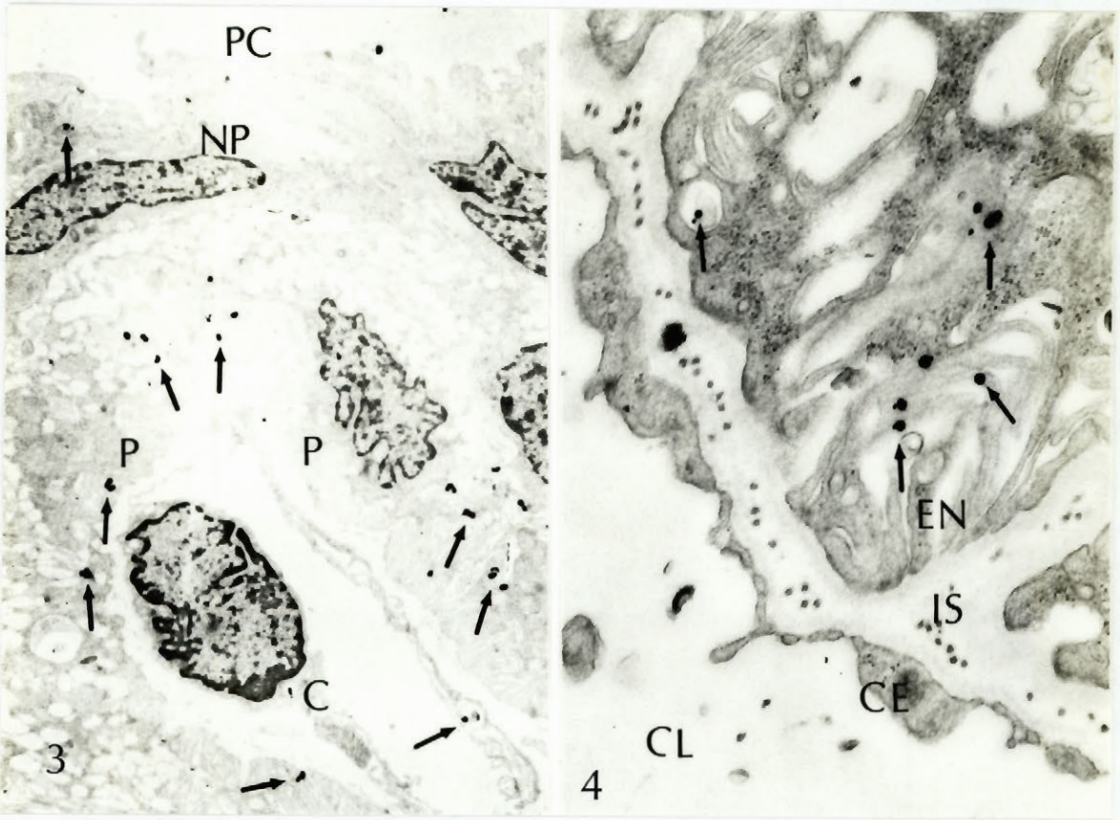

Fig. 3. Electron microscope radioautograph of rat ciliary process 2 min after injection of 18.9 μCi of ^{125}I-ANF alone. Silver grains (arrows) are localized on the basal membrane of "pigmented" epithelial cells (P). Non-pigmented epithelium (NP), posterior chamber (PC), Cappilary (C) (X 4,400).

Fig. 4. Electron microscope radioautograph of the basilar portion of a "pigmented" epithelial cell. There is a close relationship between silver grains (arrows) and the membrane infoldings (EN). Capilllary endothelium (CE), interstitial space (IS), capillary lumen (CL) (X 21,200).

Light and electron microscope radioautography

Light microscope radioautography of the eye showed that silver grains were localized over the "pigmented" epithelium of the ciliary processes (pars plicata) (Fig.1 and Table 2). A weak radioautographic reaction was also observed on non-pigmented cells, vascular stroma and "pigmented" cells (pars plana). The injection of ^{125}I-ANF together with 9 nmoles of unlabeled ANF almost completely inhibited the radioautographic reaction over these cells (Fig.2).

At the electron microscopic level (resolution of ~ 80 nm) (24), silver grains were mainly associated with the basal infoldings of the "pigmented" epithelial layer (Figs. 3 and 4 and Table 3). Analysis of the distribution of 351 silver grains over the "pigmented" epithelial cells showed that they are associated with the plasmalemma of the basal foldings. Intracellular silver grains were more numerous than the extracellular ones and sometimes found over coated vesicles near the cell surface (Figs. 5-7). Most of the grains (59%) overlay the plasmalemma. Assuming that the plasmalemma represents a "line source", an H.D. of 52 nm was found for all grains located within 10 H.D. from the source.

Isolated ciliary processes of rabbit eyes

Light microscope examination of rabbit preparations of

Table 2. Effect of unlabeled atrial natriuretic factor (ANF) on the distribution of silver grains in the eye of rats injected with ^{125}I-ANF

Eye Structure	Silver grains/unit area (121 μm²) (light microscope radioautography)	
	^{125}I-ANF	^{125}I-ANF + ANF
Ciliary body:		
Non-pigmented cells	2.14 ± 0.56*	1.16 ± 0.21***
"Pigmented cells"	31.92 ± 2.88	1.53 ± 0.26**
Vascular stroma	2.45 ± 0.36	1.53 ± 0.26***
Retina and choroid:		
Nerve fiber layer	1.56 ± 0.32	1.00 ± 0.30
Ganglion cells	1.53 ± 0.32	1.12 ± 0.25
Inner plexiform layer	1.68 ± 0.20	1.79 ± 0.19
Bipolar cells	1.21 ± 0.26	1.06 ± 0.17
Rods and cones	1.53 ± 0.30	1.43 ± 0.23
"Pigmented" epithelium	3.81 ± 0.37	1.67 ± 0.13***
Choriocapillaries	1.87 ± 0.36	1.58 ± 0.15

* All values are mean ± SE of at least 20 unit areas in each of two rats.
** $p < 0.001$
*** $p < 0.05$

ciliary processes revealed that ~ 80% of the isolated material was made up of ciliary processes with their two layers of epithelium and vascular stroma (Fig.8). The rest was made up of fragment of muscles and of ciliary processes. These preparations were used in radioligand binding and adenylate cyclase studies.

Radioligand binding

As shown in Fig. 9, The ^{125}I-ANF binding to ciliary precesses membranes had a PK (-log Kd) of 10.4 ± 0.2 (39 ± 8 pM) and a maximum binding capacity (R or Bmax) of 28 ± 4 fmol/mg of protein; competition curve analysis revealed the presence of one class of high affinity receptors.

Adenylate cyclase activity

In order to determine if the ANF receptors in ciliary process are also coupled to adenylate cyclase as has been demostrated in other target tissues (1, 2, 3) the effect of ANF adenylate cyclase activity was studied and the results are shown in Fig. 10. ANF inhibited adenylate cyclase activity in a concentration dependent manner with an apparent ki between 10^{-9} to 10^{-8} M. The maximal inhibition observed was about 20%. However, the extent of inhibition of adenylate cyclase by ANF was more evident in a frozen preparation of ciliary process homogenate (basal enzyme activity 53 ± 1; ANF 10^{-9} M: 40 ± 1; 10^{-7} M: 33 ± 6; 10^{-6} M: 29 ± 1 pmol cAMP/mg protein/10 min).

FIGURES 5 AND 6

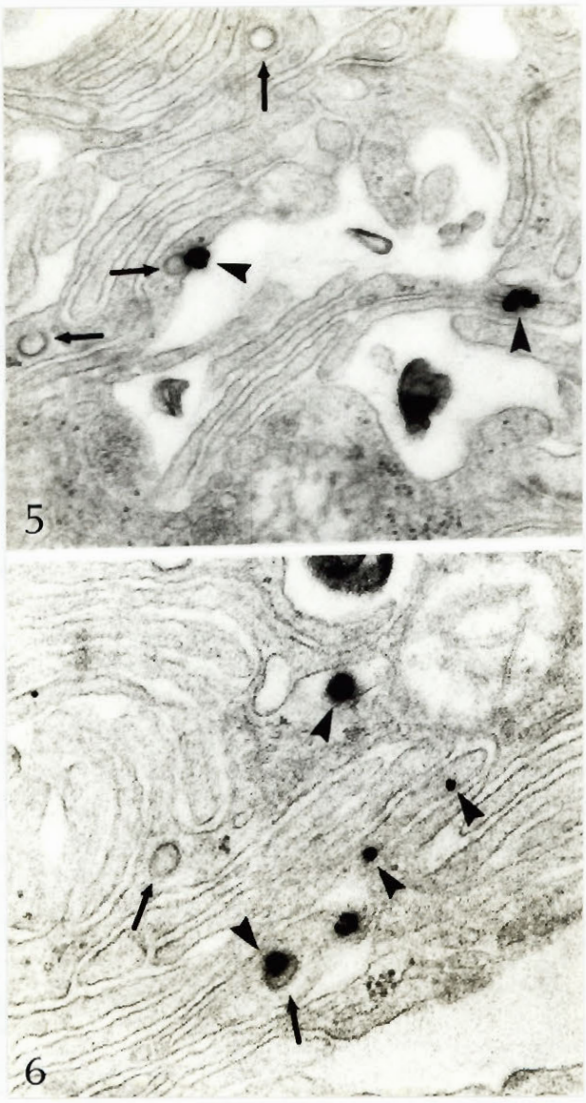

Figs. 5 and 6. Silver grains (arrowheads) are localized predominantly near the cell surface of the basilar infolding of the "pigmented" epithelial cells of the ciliary process. Some silver grains are also observed over coated vesicles (arrows). 5. (X 25,000). 6. (X 42,000).

FIGURE 7

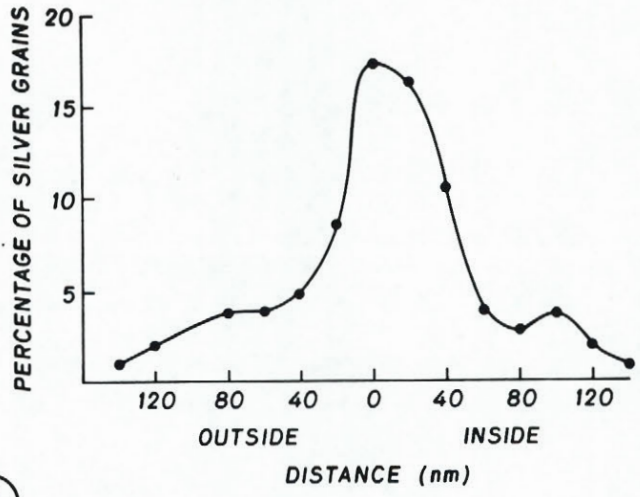

7

Fig. 7. Percentage of silver grains plotted against the distance (20 nm intervals) from the plasmalemma of the "pigmented" cells of the ciliary process. Silver grains are localized on the cell surface with a slight intracellular predominance. Intracellular silver grains are concentrated at a distance of between 20 and 40 nm from the plasmalemma.

The increased inhibition of adenylate cyclase by ANF in frozen preparations may be due to the possibility that more ANF receptors interact with the adenylate cyclase system. Nonetheless, all these results suggest that ANF receptors are present in ciliary process which are negatively coupled to adenylate cyclase. Various hormones such as epinephrine, isoproterenol, norepinephrine and dopamine stimulated adenylate cyclase to various degrees (98, 84, 57 and 40% respectively) and ANF inhibited but did not abolish, the stimulatory reponses of these hormones. In addition, forskolin

which stimulates adenylate cyclase by a receptor independent mechanism was also able to stimulate enzyme activity by about 600% and this was also inhibited by ANF (Fig. 11). When frozen preparation was used to study the effect of ANF on agonist-stimulated adenylate cyclase activity, the stimulations by isoproterol and forskolin were smaller (25% as compared to 84% by isoproterenol and 240% as compared to 600% by forskolin) but these stimulations were almost completely abolished by 10^{-7} M ANF (data not shown).

DISCUSSION

The radioactive uptake at 2 min after the intraaortic injection of ^{125}I-ANF, which was inhibited by cold ANF, suggests that silver grains observed on the "pigmented" epithelial layer of the ciliary process (pars plicata) of the rat represent receptor sites for ANF. Neither bradykinin that has several effects in the perfused eyes of rabbits (12) nor ACTH which increases the concentration of proteins in aqueous humor, probably through disruption of the blood-aqueous barrier (32), were able to displace the radioactive uptake and the radioautographic reaction. As observed at the light and electron microscopic levels, the only structure in the eye that was consistently labeled was the basilar

Table 3. Distribution of silver grains on the ciliary processes at 2 min after injection of ^{125}I-ANF. Electron microscope radioautography.

Ciliary process structure	number of silver grains	%
Non-pigmented cells	35	8
"Pigmented" cells	377	85
Vascular stroma	31	7
Total	443	100

Between 15 and 20 electron micrographs were analysed at a final magnification of X 8.800. Silver grains overlying the ciliary processes were directed scored and expressed as a percentage of total of silver grains analysed.

infoldings of the "pigmented" epithelial cells of the ciliary process and this was confirmed by morphometry at the ultrastructural level. The H.D. of 52 nm we obtained for distribution of silver grains over the plasmalemmal area of the basilar infoldings of "pigmented" epithelial cells suggests that this structure is the main source of radiation. The resolution we obtained is comparable to previous reports

using a similar technique (24) and can be explained by the fact that resolution is improved when specimens are stained with uranium and lead after post-osmication (29). H.D. is the distance from a predetermined thin radioactive line source where 50% of the silver grains are located. The H.D. estimates the resolution of the electron microscope radioautography (~ 80 nm) (24). Since close values are obtained by analysis of H.D. to a given structure (in this study the cell surface of the "pigmented" cells), the results suggest that the line source in this particular experiment (at 2 min after injection) is the cell surface and therefore the exclusive localization fo silver grains is in the "pigmented" cells. Extrapolating for the light microscope radioautographs, all grains localized on "pigmented" cells are on the plasmalemma even though is not evident since considerable scatter of the radioautographic reaction occurs at light microscopy (29).

The presence of silver grains over coated vesicles suggest that ^{125}I-ANF is internalized in these cells (19). In fact, light microscope radioautography has shown that silver grains seem to be progressively internalized at later time intervals after injection (4). The presence of 8% and 7% of silver grains on non-pigmented and vascular stroma respectively as observed at the ultrastructural level.

FIGURE 8

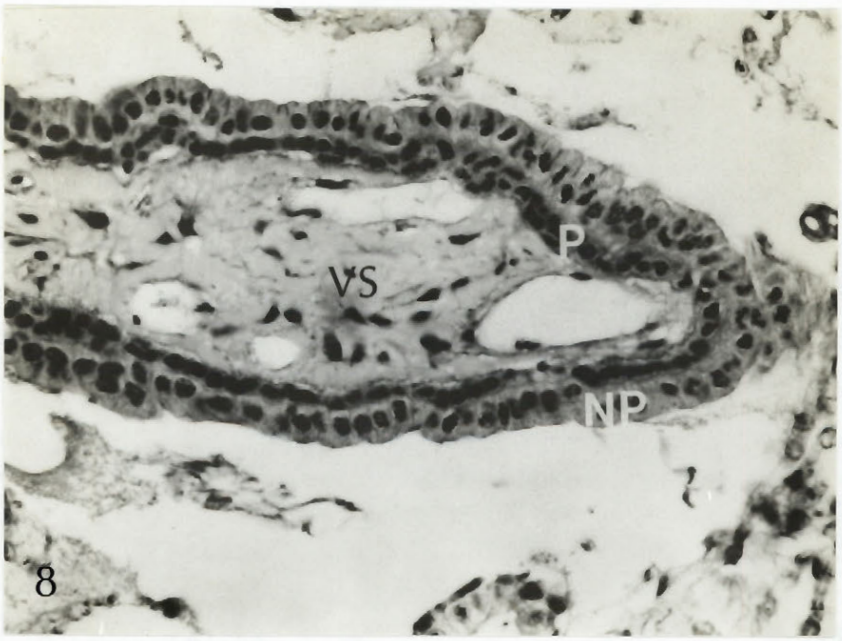

Fig. 8. Rabbit ciliary process used for binding and adenylate cyclase activity studies. The ciliary process architecture is well preserved and is constituted of both layers of epithelial cells ("pigmented" (P); non-pigmented (NP)) as well as of the vascular stroma (vs). (Hematoxylin, X 400).

suggests that binding sites to ^{125}I-ANF may also be present in these cells.

Radioligand binding studies have characterized high affinity specific receptors for ^{125}I-ANF in the ciliary processes of rabbits which correlates very well with ANF receptors in already known target cells (10, 11, 14, 15). The fact that these receptors have affinities very close to the concentration of circulating immunoreactive ANF in plasma (6) raises the possibility that they may be of physiological relevance. The presence of a small percentage

FIGURE 9

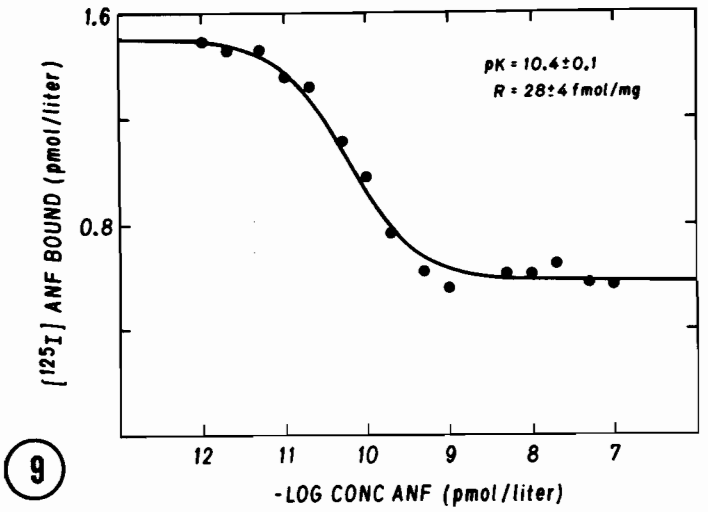

Fig. 9. Inhibition of synthetic ^{125}I-ANF binding to isolated ciliary process membranes by unlabeled ANF. These results are mean ± SE of three experiments.

of binding sites in the vascular stroma and non-pigmented cells suggests that receptors may also be present in these structures as well.

The inhibition of adenylate cyclase by ANF in isolated ciliary processes of rabbits suggests that ANF receptors are negatively coupled to adenylate as has been shown in other target tissues (1, 2, 3).

The small inhibition of adenylate cyclase by ANF in fresh homogenates of ciliary processes as compared to other target tissues may be due to the fact that we are dealing with a few receptors coupled to adenylate cyclase. When frozen preparations were used, the extent of inhibition was

increased significantly. This may be due to the possibility that more receptors are exposed and acessible for the interaction of ANF with adenylate cyclase. Since cAMP has been implicated as a regulator of aqueous humor formation (36), it is possible that a putative effect of ANF in the eyes may be mediated through inhibition of adenylate cyclase.

If an effect of ANF in the eyes is present, as suggested by the present study, evaluation of intraocular pressure and aqueous humor dynamics will be of obvious importance.

FIGURE 10

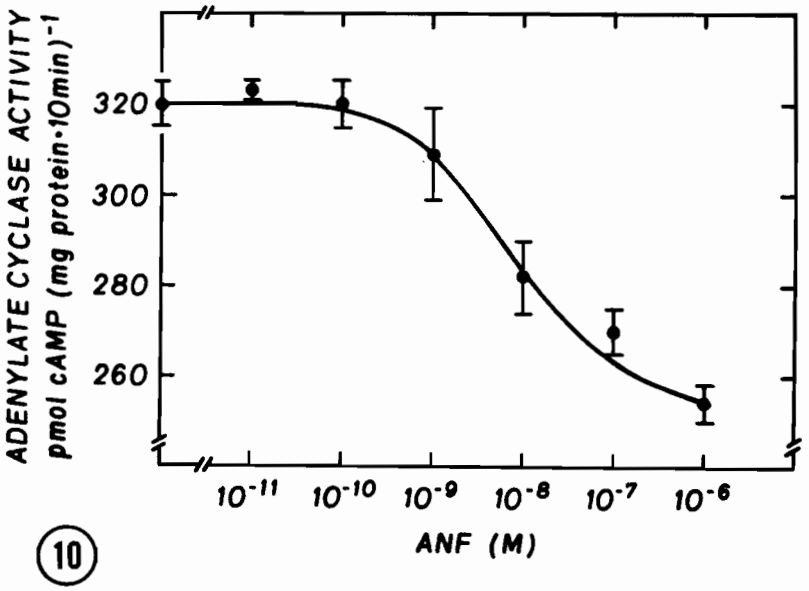

Fig.10. Effect of various concentrations of synthetic ANF on basal adenylate cyclase activity in isolated ciliary process homogenates. Values are means ± SE of triplicate determinations from one of three different experiments.

FIGURE 11

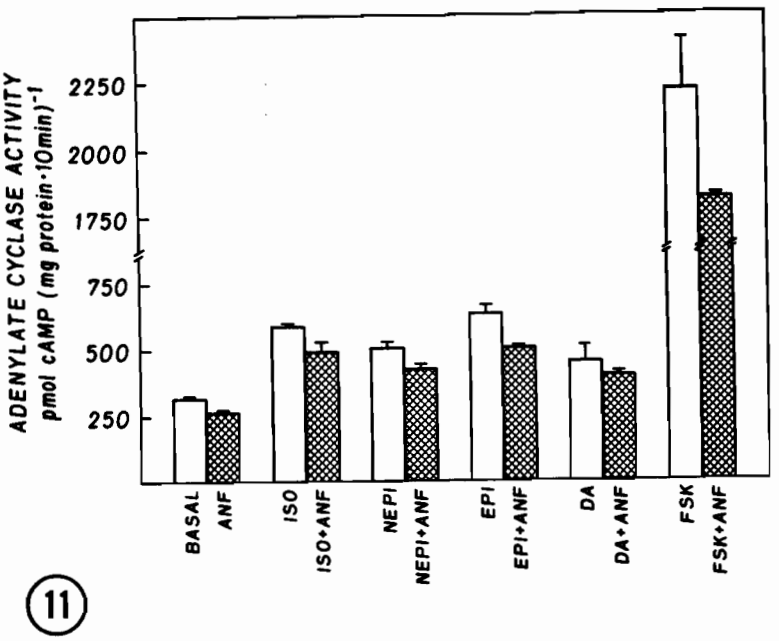

Fig.11. Effect of ANF on basal or stimulated adenylate cyclase activity by various agonists in isolated ciliary process homogenates. Adenylate cyclase was determined in the absence or the presence of 50 µM isoproterenol (ISO), 50 µM norepinephrine (NEP), 50 µM epinephrine (EPI), 100 µM dopamine (DA) and 50 µM forskolin (FSK) alone or in combination with 10^{-7} M of atrial natriuretic factor (ANF). Values are means ± SE of triplicate determinations from one of three experiments.

REFERENCES

1. Anand-Srivastava, M.B., Cantin, M., Genest, J. Inhibition of pituitary adenylate cyclase by atrial natriuretic factor. Life. Sci. 36:1873-1879, 1985.
2. Anand-Srivastava, M.B., Franks, D.B., Cantin, M., Genest, J. Atrial natriuretic factor inhibits adenylate cyclase activity. Biochem. Biophys. Res. Commun. 121:855-862, 1984.
3. Anand-Srivastava, M.B., Genest, J., Cantin, M. Inhibitory effect of atrial natriuretic factor on adenylate cyclase activity in adrenal cortical membranes. FEBS Lett. 181:199-202, 1985.
4. Bianchi, C., Gutkowska, J., Garcia, R., Thibault, G., Genest, J., Cantin, M. Radioautographic localization of ^{125}I-atrial natriuretic factor (ANF) in rat tissues. Histochemistry 82:441-452, 1985.
5. Cantin, M., Gutkowska, J., Thibault, G., Milne, R.W., Ledoux, S., MinLi, S., Chapeau, C., Garcia, R., Genest, J. Immunucytochemical localization of atrial natriuretic factor in the rat heart and salivary glands. Histochemistry 87:113-127, 1984.
6. Cantin, M., Genest, J. The heart and the atrial natriuretic factor. Endrocrine Reviews 6:107-127, 1985.
7. Cantin, M., Ballak, M., Beuzeron-Mangina, J., Anand-Srivastava, M.B., Tatu, C. DNA synthesis in cultured

adult cardiocytes. Science 214: 569-570, 1981.

8. Cantin, M., Benchimol, S. Localization and characterization of carbohydrates in adrenal medullary cells. J. Cell. Biol. 65:463-479, 1975.

9. Cantin, M., Solymoss, B., Benchimol, S., Desormeaux, Y., Langlais, S., Ballak, M. Metaplastic and mitotic activity of the ischemic (Endocrine) kidney in experimental hypertension. Am. J. Path. 96:545-566, 1979.

10. Chartier, L., Schiffrin, E., Thibault, G. Atrial natriuretic factor inhibitos the stimulation of aldosterone secretion by angiotensin II, ACTH, and potassium in vitro and angiotensin II- induced steroidogenesis in vivo. Biochem. Biophys. Res. Commun. 122:171-174, 1984.

11. Chartier, L., Schiffrin, E., Thibault, G., Garcia, R. Effect of atrial natriuretic factor (ANF)-related peptides on aldosterone secretion by adrenal glomerulosa cells: critical role of the intramolecular disulphide bond. Endocrinology 115:2026-2028, 1984.

12. Cole, D.F., Unger, W.G. Action of bradykinin on intraocular pressure and pupillary diameter. Ophthal. Res. 6:308-314, 1974

13. De Bold, A.J., Borenstein, H.B., Veress, A.T., Sonnenberg, H. A rapid and potent natriuretic response to intravenous injection of atrial myocardial extracts in rat. Life Sci. 28:89-94, 1981.

14. De Léan, A., Racz, K., Gutkowska, J., Nguyen, T.T., Cantin, M., Genest, J. Specific receptor mediated inhibition by synthetic atrial natriuretic factor of hormone-stimulated steroidogenesis in culture bovine adrenal cells. Endocrinology, 115:1636-1637, 1984.

15. De Léan, A., Gutkowska, J., McNicoll, N., Schiller, P. W., Cantin, M., Genest, J. Characteristics of specific receptors for atrial natriuretic factor in bovine adrenal zona glomerulosa. Life Sci. 25:2311-2318, 1985.

16. De Léan, A., Munson, P.J., Rodbard, D. Simultaneous analysis of families of sigmoidal curves: application to bioassay, radioligand assay, and physiological dose-response curves. Am. J. Physiol. 235:E-97-E-102, 1978.

17. Garcia, R., Thibault, G., Gutkowska, J., Hamet, P., Cantin, M., Genest, J. Effect of chronic infusion of synthetic atrial natriuretic factor (ANF 8-33) in conscious, two kidney, one clip hypertensive rats. Proc. Soc. Exp. Biol. Med. 178:155-159, 1985.

18. Garcia, R., Thibault, G., Cantin, M., Genest, J. Effect of a purified atrial natriuretic factor on rat and rabbit vascular strips and vascular beds. Am. J. Physiol. 247:R-34-R-39, 1984.

19. Goldstein, J.L., Anderson, R.G.W., Brown, M.S. Coated pits, coated vesicles, and receptor-mediated endocytosis. Nature 279:679-685, 1979.

20. Gutkowska, J., Horky, K., Thibault, G., Januszewicz, P., Cantin, M., Genest, J. Direct radioimmunoassay of atrial natriuretic factor. Biochem. Biophys. Res. Commun. 122:593-601, 1984.

21. Hamet, P., Tremblay, J., Pang, S.C., Carrier, F., Thibault, G., Gutkowska, J., Cantin, M., Genest, J. Effect of native and synthetic atrial natriuretic factor on cyclic GMP. Biochem. Biophys. Res. Commun. 123:515-527, 1985.

22. Hunter, W.M., Greenwood, F.C. Preparation of iodine-131 labelled human growth hormone of high specific activity. Nature 194:495-496, 1962.

23. Januszewicz, P., Gutkowska, J., De Léan, A., Thibault, G., Garcia, R., Genest, J., Cantin, M. Synthetic atrial natriuretic factor induces release (possibly receptor mediated) of vasopressin from rat posterior pituitary. Proc. Soc. Exp. Biol. Med. 178:321-325, 1985.

24. Kopriva, B.V., Levine, G.M., Nadler, N.J. Assessment of resolution by half distance values for tritium and radioiodine in electron microscopic radioautographs using Ilford L_4 emulsion developed "solution physical" or D-19b methods. Histochemistry 87:519-522, 1984.

25. Lazure, C., Seidah, N.G., Chrétien, M., Thibault, G., Garcia, R., Cantin, M., Genest, J. Atrial pronatriodilatin: a precursor for natriuretic factor and cardiodilatin. FEBS Lett. 172:80-86, 1984.

26. Lowry, O.H., Rosebrough, N.J., Farr, A.L., Randall, R.J. Protein measurement with the folin phenol reagent. J. Biol. Chem. 193:265-275, 1951.

27. Maki, M., Takayanagi, R., Misono, K.S., Pandey, K.N., Tibbetts, C., Inagami, T. Structure of rat atrial natriuretic factor precursor deduced from cDNA sequence. Nature 309:722-724, 1984.

28. Salomon, Y., Londos, C., Brodsell, M. A highly sensitive adenylate cyclase assay. Anal. Biochem. 58:541-548, 1974.

29. Salpeter, M.M., Fertuck, H.C., Salpeter, E.E. Resolution in electron microscope autoradiography. III. Iodine-125, the effect of heavy metal staining, and a reassessment of critical parameters. j. Cell. Biol. 72:161-173, 1977.

30. Sears, M., Mead, A. A major pathway for the regulation of intraocular pressure. International Ophthalmology 6:201-212, 1983.

31. Seidah, N.G., Lazure, C., Chrétien, M., Thibault, G., Garcia, R., Cantin, M., Genest, J, Nutt, R.F., Brady, S.F., Lyle, T.A., Paleveda, W.J., Colton, C.D., Cicerone, T.M., Veber, D.F. Amino acid sequence of homologous rat atrial peptides: natriuretic activity of native and synthetic forms. Proc. Natl. Acad. Sci. USA 81:2640-2644, 1984.

32. Starka, J., Hampl, R., Simeickovia, A., Obenberger, J., Drouhault. Changes induced in rabbit plasma and aqueous

humor by $ACTH^{4-10}$ and $ACTH^{1-24}$. Endocrinol. Exp. 19:25-28, 1985.

33. Thibault, G., Garcia, R., Cantin, M., Genest, J., Lazure, C., Seidah, N.G., Chrétien, M. Primary structure of a high Mr. Form of rat atrial natriuretic factor. FEBS Lett. 167:352-356, 1984.

34. Tremblay, J., Gerzer, R., Vinay, P., Pang, S.C., Béliveau, R., Hamet, P. The increase of cGMP by atrial natriuretic factor correlates with the distribution of particulate guanylate cyclase. FEBS Lett. 181:17-22, 1985.

35. Yamanaka, M., Greenberg, B., Johnson, L., Seilhamer, J., Brewer, M., Friedman, T., Miller, J., Atlas, S., Laragh, J., Lewicki, J., Fiddes, J. Cloning and sequence analysis of the C-DNA for the rat atrial natriuretic factor precursor. Nature 309:719-722, 1984.

36. Zivin, R.A., Condra, J.H., Dixon, Seidah, N.G., Chrétien, M., Nemer, M., Chamberland, M., Drouin, J. Molecular cloning and characterization of DNA sequences encoding rat and human atrial natriuretic factor. Proc. Natl. Acad. Sci. USA 81:6325-6329, 1984.

CHAPTER 5

ANF binding sites are also present in the small intestine. Identical and complementary results are obtained with either *in vivo* or *in vitro* radioautography.

ATRIAL NATRIURETIC FACTOR BINDING SITES IN THE JEJUNUM

This work was submitted to

Am. J. Physiol. (in revision, 1988).

ABSTRACT

We have studied the localization and the characterization of atrial natriuretic factor (ANF) binding sites by radioautographic techniques. Quantitative *in vitro* radioautography with a computerized microdensitometer demonstrated the presence of high affinity, low capacity ^{125}I-ANF (99-126) binding sites (Kd: 48 pM; Bmax: 63 fmol/mg of protein) mainly in the villi of 20 µm slide-mounted transverse sections of the rat jejunum. Competition curves showed IC_{50}s of 55 and 1560 pM for ANF (99-126) and ANF (103-123) repectively. *In vivo* electron microscope radioautography showed that 80% of the silver grains were localized on the lamina propria fibroblast-like cell, 18% on mature enterocytes and 2% on capillaries. Bradykinin and ACTH did not compete with ANF binding. These results demonstrate that ANF binding sites in the rat jejunum possess the pharmacological characteristics of functional ANF receptors encountered in other rat tissues and ultrastructural radioautographs showed their cellular distribution. Taken together, these results demonstrate the presence and the localization of specific binding sites for ANF in the jejunal villi of the rat small intestine.

INTRODUCTION

Atrial natriuretic factor (ANF) is a family of polypeptide hormones produced by atrial and ventricular cardiocytes and stored in specific secretory granules. It circulates at a picomolar concentration mainly as a biologically active 28 AA C- terminal ANF (99-126) of the prohormone ANF (1-126). ANF has widespread actions in animals and humans, modulating the renal excretion of water and salts, decreasing blood pressure and inhibiting renin and aldosterone secretion (for reviews see 1,6,10). In the gastrointestinal tract, ANF stimulates cGMP production from rat small intestine (30), possesses binding sites in the bovine small intestine (24), inhibits the absorption of water in the teleost intestine (21), increases salt secretion in isolated shark rectal gland (25) and either increases (13) or decreases (23) water absorption in the rat small intestine. Thus, the presence of 125I-ANF (101-126) binding sites in the rat duodenum, jejunum and ileum (3) suggest the presence of putative functional receptors for ANF. In the present studies, quantitative *in vitro* radioautography corroborated with a *in vivo* electron microscope radioautography were applied in an attempt to stablish the pharmacological characteristics and the cellular distribution of ^{125}I-ANF (99-126) binding sites in the rat jejunum.

MATERIALS AND METHODS

Reagents

Phosphoramidon, phenylsulfonyl fluoride (PMSF), leupeptin, pepstatin, bovine serum albumin (BSA) and bacitracin were purchased from Sigma, USA; ethylenidiaminetetraacetic acid (EDTA) and $MnCl_2$ were from Fisher, USA; aprotinin and OCT compound from Miles, Canada; ANF (Ser 99-Tyr 126) was from Bio-Méga Inc., Canada; bradykinin was from Protein Research Foundation, Japan; ANF (Ser 103-Ser 123) was from Peninsula, USA; X-ray films (Hyperfilm-H^3), ^{125}I-micro-scales (^{125}I-standards) and Na-I^{125} from Amersham, Canada. The microtome cryostat (Bright Instruments, model OTF) was from Haker, USA. Other chemicals were of the highest purity available from commercial sources.

Monoidination of ANF

^{125}I-ANF (99-126) was obtained by the lactoperoxydase method using Na-I^{125} as already described (18). The purification of the monoiodinated form was achieved by high performance liquid chromatography (HPLC) as previously described (3). The specific activity was 3600 dpm/fmol.

In vitro radioautography

Female Sprague-Dawley rats weighing 200-250 g (Charles River, St-Constant, Québec) were decapitated and the jejunum dissected and immediately frozen-mounted (-30°C) in cryostat

shucks with OCT compound. Consecutive cryostat sections (20 µm) were obtained at 18°C and mounted (two per slide) near the edge of pre-cleaned gelatin-coated microscope slides, dried under vacuum at 4°C for two hours and stored into sealed boxes with dessicant at -70°C until used. Saturation curves were carried out by pre-incubation of consecutive slide-mounted sections for 10 min in 50 mM Tris-HCl (pH 7.5) containing 0.5% BSA at room temperature followed by incubation for 90 min with the same buffer plus: 10^{-6} M phosphoramidon, 10^{-6} M leupeptin, 10^{-6} M pepstatin, 10^{-4} M EDTA, 10^{-4} M PMSF, 200 UIK/ml aprotinin, 5 mM $McCl_2$ and 1% bacitracin with increasing concentrations of ^{125}I-ANF (99-126) from 15 to 220 pM. Non-specific binding was estimated from parallel incubations containing in addition 10^{-7}M of ANF (99-126). Competition curves were carried out with 30 pM of ^{125}I-ANF (99-126) and several concentrations of either ANF (99-126) or ANF (103-123). Some slides were also incubated with 10^{-6} M ACTH or bradykinin. After incubation, the slides were washed 2 X 10 min in Tris-HCl buffer with 0.5% BSA at 4°C and dried on a hot plate (60°C). The labeled slide-mounted sections were-mounted in cardboard together with ^{125}I-standards, apposed to X-rays films and exposed at room temperature from 1 to 6 days. The X-ray films were developed with undiluted Kodak D19b developer for 4 min at 20°C, washed in water for 1 min and fixed in Kodak Ectaflo fixer (dilution

1:3) for 4 min.

Depletion and degradation of ^{125}I-ANF

Aliquots (0.5 ml) were obtained before and after incubations of the tissue sections in the buffers containing the lowest and the highest concentrations of either ^{125}I-ANF (saturation curves) or ANF (displacement curves). The aliquots were adicified with 0.5 ml of 0.1 M acetic acid and stored at -20°C until used (~ 3 days). The degree of radioligand depletion and degradation were determined respectively by the radioactivity content of the aliquots and their HPLC elution profile.

^{125}I-Standards

The standards were either commercially available ones (^{125}I-micro scales) or prepared from kidney homogenates as follows: Six kidneys from normal Sprague-Dawley rats were homogenized using a polytron (set 10 for 2 min) and divided in 10 equal aliquots in Beckman microfuge tubes (diam. 5 mm^2). ^{125}I-ANF (20 µl was added to each tube to obtain different concentrations of radioactivity. The homogenates containing radioactivity were mixed with a Vortex for 5 min and frozen on dry ice. Twenty µm sections were done in the same cryostat as above and the amount of radioactivity and the protein content per section measured in a LKB gamma counter and by the method of Bradford (27) respectively.

Microdensitometry

The microdensitometer consisted of a microcomputer SY 286/310 multibys INTEL, a video camera Hitashi (KP-130V), a Nikkon objective (micro-Nikkor 55 mm 1:2.8), a video processor Matrox (MIP-512) and a video monitor Mitsubishi RGB (C3419LPR). A joystic coupled to the monitor allows the positioning of windows on the radioautographic images to select the areas to be analyzed. Optical densities readings from the radioautographic images were preceded by the acquisition of the standard curve for optical densities of the X-ray film. The equation which describes the linear segment of the sigmoid curve allowed the conversion of optical densities to dpm/mg of standard. Knowing the specific activity of the radioligand, dpm is transformed to fmol, generating fmol/mg of standard.

Analysis of binding

The saturation curves were analyzed by the program SCATFIT (8), to obtain Kd and Bmax. Competition curves were analyzed by ALLFIT (9) to obtain IC_{50}.

In vivo radioautography

The technique has been described in detail in previous studies (3,4). Briefly, Sprague-Dawley rats weighing 38-45 g received, under pentobarbital anesthesia, an intra-aortic injection of 10 pmol of ^{125}I-ANF (99-126) either alone (n=2) (total binding), or together with 10 nmol of ANF (99-126) (n-2) (non-specific binding), ACTH (n=2) or bradykinin (n=2)

(unrelated peptides). At 2 min after injection, the animals had their thorax opened and received through the left ventricle ~ 50 ml of ice cold phosphate buffer (1 min) followed by ~ 300 ml of 2% glutaraldehyde buffered with cacodylate HCl (0.1 M, pH 7.4) for 10 min. Pieces of the jejunum were processed for light and electron microscope radioautography as described in detail elsewhere (3,4).

FIGURE 1

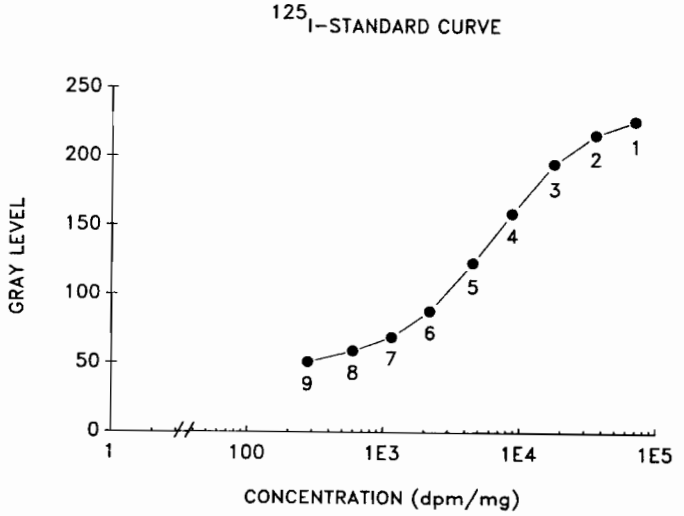

Fig. 1. Computerized microdensitometry of a X-ray film apposed for 48 hours to a commercially available ^{125}I-micro scale. The linear component of the sigmoid curve was located between standarts 3 and 6 which gave a correlation coefficient of 99.95% and was described by the equation: y = 118.64 X -309.04. Each 50 units of gray level (absorbed light) corresponded to 0.1 units of optical density.

RESULTS

In vitro radioautography

Depletion and degradation of ^{125}I-ANF

Depletion of the radioligand (measure of radioactivity in the incubation medium before and after exposure of sections) was always inferior to 15% even at low concentrations of ^{125}I-ANF (e.g. competition curves). The HPLC elution profiles before and after incubations were identical with less than 5% of degraded radioactivity eluting at the void volume (first 7 min) (data not shown).

^{125}I- Standards

The comparison of commercially available ^{125}I-standards and prepared ones from kidney homogenates for the same optical densities demonstrated a ratio of 1:20 from fmol/mg of standards (polymer) to that of fmol/mg of protein (kidney homogenates). Therefore, the binding data were expressed in mg of protein referring to kidney homogenates. A sigmoid curve of the X-ray film is shown in Fig.1.

Characteristics and localization of binding sites

Saturation curves demonstrated the presence of high affinity low capacity binding sites localized mainly at the tip of the jenunal villi (figs. 2-4). In 3 separate experiments in duplicate (one aninal per experiment), a Kd of 48 ± 9 pM and a Bmax of 63 ± 15 fmol/mg of protein (mean

FIGURES 2, 3 AND 4

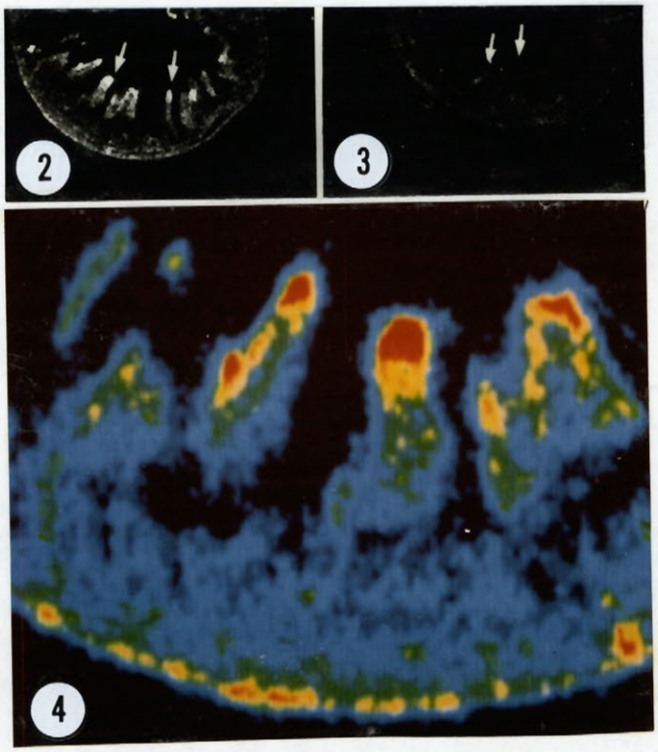

Fig. 2. Radioautograph taken directly from a X-ray film apposed for 48 hours to a transverse cryostat section (20 µM) of a rat jejunum labeled in vitro with 40 pM of ^{125}I-ANF (total binding). It shows the localization of silver grains (in white) mainly on the tip of the jejunal villi (arrows). (X ~ 9).

Fig. 3. Radioautograph taken directly from the same X-ray film in Fig. 1 (consecutive section) labeled with 40 pM of ^{125}I-ANF plus 10^{-7} ANF (non-specific binding). It shows that silver grains (in white) were greatly reduced on the jejunal villi (arrows) but still present in the remaining areas of the jejunal wall (X ~ 9).

Fig. 4. Color-coded computerized reconstruction of part of the section in Fig. 1. It shows the distribution of the radioautographic reaction in the jejunum. In (fmol/mg of protein): red (72); yellow (35); green (17) and blue (11). (X ~ 55).

± S.E.M.) were obtained (Fig. 5). Competition curves from 3 different animals in duplicate demonstrated a IC_{50} ANF (99-126) at low picomolar concentrations (55 ± 13 pM) while the IC_{50} for ANF (103-123) were situated in the nanomolar range (1560 ± 183 pM) (Fig. 6). The remaining of the jejunum had low levels of specific binding which includes the crypts, the submucosa and the muscular layers (Fig.4). Bradykinin and ACTH at 10^{-6} M did not compete with ^{125}I-ANF binding (data not shown).

In vivo radioautography

Light microscopy

Semi-thin sections of the jejunum of rats that received an injection of ^{125}I-ANF alone showed the distribution of silver grains (binding sites) at the base of the mature enterocytes of the upper part of the jejunal villi. Neither the crypt cells nor the submucosal and the muscular layers were labeled (Fig. 7). The radioautographic reaction was almost completely desplaced in the jejunum of rats that received an excess of unlabeled ANF (Fig.8) with no effect of either ACTH or bradykinin (data not shown).

Electron microscopy

Ultrastructural radioautographs showed that silver grains were mainly localized on fibroblast-like cells of the lamina propria. Silver grains were also observed at the base of mature enterocytes but none at the striated border. A

FIGURE 5

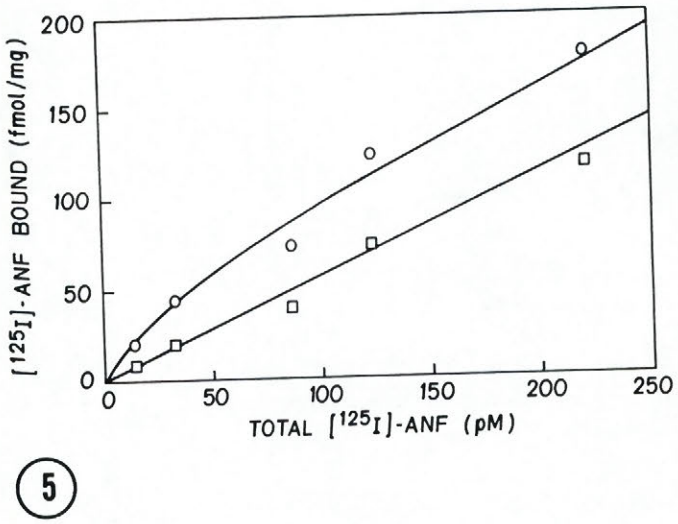

Fig. 5. Saturation curve of ^{125}I-ANF binding sites to the villi of the rat jejunum 20 µm cryostat sections. Open circles: total binding; open squares: non specific binding. Bound ^{125}I-ANF are means of 6-10 determinations from duplicate consecutive sections of a representative experiment. Kd: 52pM; Bmax: 60 fmol/mg of protein.

FIGURE 6

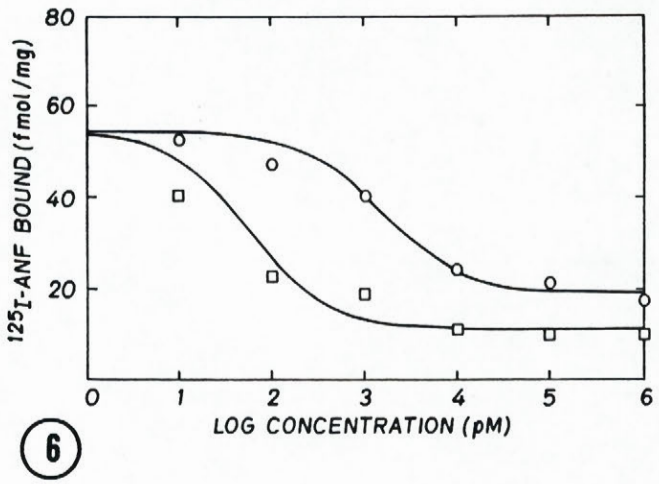

Fig, 6. Competition curves to the villi of rat jejunum (20 µm cryostat sections) incubated with 30 pM of ^{125}I-ANF (99-126) and various concentrations of either ANF (103-123) (open circles) or ANF (99-126) (open squares). Bound ^{125}I-ANF are means of 10-15 determinations from duplicate consecutive sections of a representative experiment. IC_{50}: ANF (103-123); 1350 pM; ANF (99-126) = 53 pM.

small number was observed in capillaries but none in the remaining layers of the small intestine (Table 1, Figs. 9-11).

DISCUSSION

The *in vitro* experiments demonstrated that in the rat jejunum, the majority of ANF binding sites were localized in a relatively narrow band at the tip of the jejunal villi. *In vivo* experiments revealed that binding sites were concentrated in fibroblast-like cells of the lamina propria and at the base of mature enterocytes. Thus, identical and complementary results were obtained with these techniques.

Saturation curves of ^{125}-IANF demonstrated that the radiolabeled ligand recognized ANF binding sites similarly to others already known rat targets for ANF (22). These binding sites had affinities close to circulating levels of immunoreactive ANF (12), were saturable and specific. Displacement curves demonstrated that ANF (103-123) was ~ 30 fold less potent than ANF (99-126) as it has been described for the adrenals, mesenteric arteries and aorta of rats (22). *In vitro* radioautographic localization of receptors for neurotensin (11), substance K (5), substance P (5,16) and cholecystokinin (26), peptides with already known effects on water and ion transport in the small intestine, are distinct from the distribution of ANF binding sites. Similar localization has been observed, however, with delta-opioid (20) and bradykinin (17) for which most of the receptors are localized at the tip of the jejunal villi. Previous *in vivo* light microscopic radioautographic studies

FIGURES 7 AND 8

Fig. 7. Light microscope radioautograph of the jejunum of a rat that received 10 pmol of ^{125}I-ANF alone. Silver grains (arrows) are localized on the lamina propria (LP) near the base of the mature enterocytes (ET). The remaining layers display a very weak radioautographic reaction. Crypts (CT); muscular layer (mm); submuscular layer (SM); capillaries (CP). (Semithin section, toluidine blue, X 400).

Fig. 8. Light microscope radioautograph of the jejunum of a rat that received 10 pmol of ^{125}I-ANF plus 9 nmol of ANF. Silver grains (arrows) are distributed sparsely on the jejunum. Lamina propria (LP); enterocytes (ET); crypts (CT); muscular layer (mm); submuscular layer (SM); capillaries (CP). (Semithin section, toluidine blue, X 400).

demonstrated the presence of ^{125}I-ANF (101-126) binding sites in the small intestine of rats but not in the stomach, large intestine and the rectum except for the muscular layers of the colon (3). Although <u>in vitro</u> radioautography confirmed the presence of binding sites in the muscular layers of the guinea pig colon (15), any appreciable ANF binding sites in both rat (29) and guinea pig (15) small intestine could not be demonstrated.

FIGURES 9, 10 AND 11

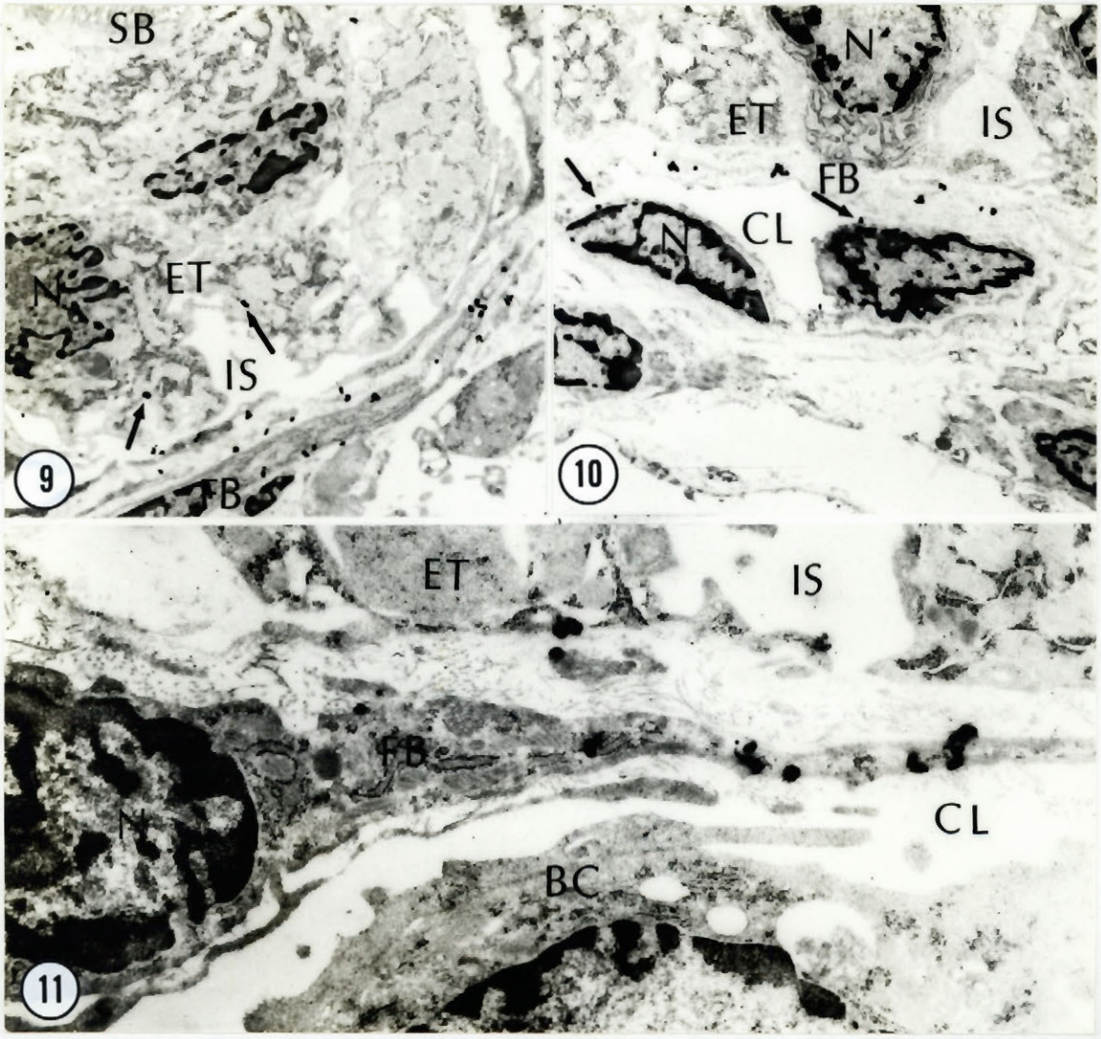

Figs. 9, 10 and 11 . Electron microscope radioautographs of part of the jejunal villi of a rat that received 10 pmol of ^{125}I-alone. Silver grains (black dots) are localized mainly on fibroblast-like cells (FB) of the lamina propria. Some silver grains (arrows) are localized at the base of mature enterocytes (ET). Nuclei (N); interstitial space (IS); striated border (SB); cappilary lumen (CL); blood cells (BC). (Uranyl acetate, lead citrate, Fig.9, X 4600; Fig. 10, X 4600; Fig. 11, X 14,260).

Such discrepancies remain to be explained but it does not seem to come from differences in the animal species used since ANF binding sites have also been demonstrated in solubilized membranes of the bovine small intestine (24), in the jejunal villi of rabbits and the muscular layer of the rat colon by in vitro radioautography (Bianchi et al., data not shown).

The similarities of the localization of ANF binding sites by both in vivo and in vitro approaches implies that many factors such as binding affinities and capacities, hormonal degradation, fixation and dehydration did not significantly influence the ultrastructural distribution of ANF binding sites in the jejunal villi. Likewise, the age of the rats used in the in vivo experiments did not play an important role since Kanai et al. (13) described similar radioautographic patterns in the small intestine of adult rats that received an intravascular injection of ^{125}I-ANF. In addition, the distribution of ANF binding sites in the jejunal villi, identical to those of the duodenum and ileum (3) are distinct from the distribution of ^{125}I-insulin (2) and ^{125}I-epidermal growth factor (7) using in vivo radioautographic techniques.

ANF possesses receptors coupled to guanylate cyclase in cultures of rat lung fibroblasts (14) suggesting that the

presence of ANF binding sites in the rat jejunum fibroblast-like cells are not exclusive to the small intestine. They seem, however, to be more abundant in this segment of the rat gastrointestinal tract. Their functions are unknown. The presence of ANF receptors in epithelial cells related to the transport of water and ions such as the renal inner medullary collecting duct cells (32), the choroid plexus of the brain (28) and the ciliary process of the eyes (19) may indicate that mature enterocytes could also be an important target cell.

Finally, the major contribution of the present study is the pharmacological characterization of ANF binding sites in the rat jejunum and their cellular distribution. The localization of ANF binding sites in fibroblast-like cells and enterocytes may be a valuable information for further studies addressing the possible role of ANF in the gastrointestinal tract. Whether ANF may have an indirect effect, through interactions with components of the lamina propria as described for bradykinin in the small intestine (31) and ANF in the shark rectal gland (25) or through a direct effect on mature enterocytes or both awaits further investigations.

Table 1. Distribution of silver grains on the jejunal villi of 40 g rats at 2 min after an intra-aortic injection of 10 pmol of ^{125}I- ANF (99-126).

Cell type	Number of silver grains	%
Fibroblast-like	425	80
Mature enterocyte	98	18
Endothelial	6	2
Total	529	100

Twenty five electron microscope radioautographs were taken over the jejunal villi wherever silver grains were located at a final magnification of X 6020. Silver grains overlaying the cells were directed scored and expressed as the percentage of the total number of silver grains analyzed.

REFERENCES

1. Ballermann, B.J., Brenner, B.M. Biologically active atrial peptide. J. Clin. Invest. 76:2041-2048, 1985.
2. Bergeron, J.J.M., Rachubinski, R., Searle, N., Borts, D., Silkstrom, R., Posner, B.I. Polypeptide hormone receptors in vivo. Demostration of insulin binding to adrenal gland and gastrointestinal epithelium by quantitative radioautography. J. Histochem. Cytochem. 28:824-835, 1980.
3. Bianchi, C., Gutkowska, J., Thibault, G., Genest. J., Cantin, M. Radioautographic localization of ^{125}I-atrial natriuretic factor (ANF) in rat tissues. Histochemistry 82:441-452, 1985.
4. Bianchi, C., Gutkowska, J., Thibault, G., Garcia, R., Genest, J., Cantin, M. Distinct localization of atrial natriuretic factor and angiotensin II binding sites in the glomerulus. Am. J. Physiol. 251:F594-602, 1986.
5. Burcher, F., Shults, C.W., Buck, S.H., Chase, T,N., O'Donohue, T.L. Autoradiographic distribution of substance K binding sites in rat gastrointestinal tract: a comparison with substance P. Eur. J. Pharmacol. 102:561-562, 1984.
6. Cantin, M., Genest, J. The heart and the atrial natriuretic factor. Endocr. Rev. 6:107-127, 1985.
7. Chabot, J.G., Walker, P., Pelletier, G. Demonstration of

epidermal growth factor binding sites in the adult rat small intestine by autoradiography. Can. J. Physiol. Pharmacol. 65:109-112, 1987.

8. De Léan, A., Hancock, A.A., Lefkowitz, R.J. Validation and statistical analysis of a computer modeling method for quantitative analysis of radioligand binding data for mixtures of pharmacological receptor subtypes. Mol. Pharmacol. 21:5-16, 1982.

9. De Léan, A., Munson, P.J., Rodbard, D. Simultaneous analysis of families of sigmoidal curves: application to bioassay, radioligand assay, and physiological dose-response curves. Am. J. Physiol. 235:E97-E102, 1978.

10. Genest, J., Cantin, M. The atrial natriuretic factor: its physiology and biochemistry. Rev. Physiol. Biochem. Pharmacol. 110:1-145, 1988.

11. Goedert, M., Hunter, J.C., Ninkovic, M. Evidence for neurotensin as a non-adrenergic non-cholinergic neurotransmitter in guinea pig ileum. Nature 311:59-61, 1984.

12. Gutkowska, J., Thibault, G., Januszewicz, P., Cantin, M., Genest, J. Direct radioimmunoassay of atrial natriuretic factor. Biochem. Biophys. Res. Commun. 122:593-601, 1985.

13. Kanai, Y., Ohmuna, N., Matsuo, H. Rat atrial natriuretic polypeptide increases net water, sodium and chloride absorption across rat small intestine in vivo. Japan J. Pharmacol. 45.7-13, 1987.

14. Leitman, D.C., Agnost, V.L., Tuan, J.J., Andresen J.W., Murad, F. Atrial natriuretic factor and sodium nitropusside increases cyclic GMP in cultured rat lung fibroblasts by activating different forms of guanylate cyclase. Biochem. J. 244:69-74, 1987.

15. Mantyh, C.R., Kruger, L., Brecha, N.C., Mantyh, P.W. Localization of specific binding sites for atrial natriuretic factor in peripheral tissues of the guinea pig, rat, and human. Hypertension 8:712-721, 1986.

16. Mantyh, P.W., Goedert, M., Hunt, S.P. Autoradiographic visualization of receptor binding sites for substance P in the gastrointestinal tract of the guinea pig. Eur. J. Pharmacol. 100:133-134, 1984.

17. Manning, D.C., Snyder, S.H., Kachur, J.F., Miller, R.J., Field, M. Bradykinin receptor-mediated chloride secretion in intestinal function. Nature 299:256-259, 1982.

18. Murthy, K.K., Thibault, G., Schinffrin, E.L., Garcia, R., Chartier, L., Gutkowska, J., Genest, J., Cantin, M. Disappearance of atrial natriuretic factor from circulation in the rat. Peptides 7:241-246, 1986.

19. Nathanson, J.A. Atriopeptin-activated guanylate cyclase in the anterior segment. Identification, localization and effects of atriopeptins on IOP. Inves. Ophthalm. Vis. Sci. 28:1357-1364, 1987.

20. Nishimura, E., Buchan, A.M.J., McIntosh, C.H.S. Autoradiographic localization of μ-and δ-type opioid

receptors in the gastrointestinal tract of the rat and guinea pig. Gastroenterology 91:1084-1094, 1986.

21. O'Grady, S.M., Field, M., Nash, N.T., Rao, M.C. Atrial natriuretic factor inhibits Na-K-Cl cotransport in teleost intestine. Am. J. Physiol. 249:C531-C534, 1985.

22. Schiffrin, E.L., Chartier, L., Thibault, G., St-Louis, J., Cantin, M., Genest, J. Vascular and adrenal receptors for atrial natriuretic factor in the rat. Circ. Res. 56:801-807, 1985.

23. Seeber, M.A., Vidal, N.A., Carchio, S.M., Karara, A.L. Inhibition of water-sodium intestinal absorption by an atrial extract. Can. J. Physiol. Pharmacol. 64:244-247,1986.

24. Sellitti, D.F. Solutilized ANF binding sites from bovine intestinal epithelium. 2nd BAAP Congress #B72, 1987.

25. Silva, P.J., Stroff, S., Solomon, R.J., Lear, S., Kniaz, D., Greger, R., Epstein, H. Atrial natriuretic peptide stimulates salt secretion by shark rectal gland by releasing VIP. Am. J. Physiol. 252:F99-F103, 1987.

26. Smith, G.T., Moran, T.H., Coyle, J.T., Kuhar, M.J., O'Donahue, T.L., McHugh, P.R. Anatomic localization of cholecystokinin receptors to the pyloric sphincter. Am. J. Physiol. 246:R127-R130, 1984.

27. Spector, T. Refinement of the Coomassie Blue method of protein quantitation. A simple and linear spectrophotometric assay for 0.5 to 50 µg of protein. Anal. Biochem.

86:142-146, 1978.

28. Steardo, L., Nathanson, J. Brain-barrier tissues: End organs for atriopeptins. Science 235:470-473, 1987.

29. Von Schroeder, H.P., Nishimura, E., McIntosh, C.H.S., Buchan, A.M.J., Wilson, N., Ledsome, J.R. Autoradiographic localization of binding sites for atrial natriuretic factor. Can. J. Physiol. Pharmacol. 63:1373-1377, 1985.

30. Waldman, S.A., Rapoport, R.M., Murad, F. Atrial natriuretic factor selectively activates particulate guanylate cyclase and elevates cGMP in rat tissues. J. Biol. Chem. 259:14332-14334, 1984.

31. Warhurst, G., Lees, M., Higgs, N.B., Turnberg, L.A. Site and mechanisms of action of kinins in the rat ileal mucosa. Am. J. Physiol. 252:G293-G300, 1987.

32. Zeidel, M.L., Silva, P., Brenner, B.M., Seifter, J.L. cGMP mediates effects of atrial peptides on medullary collecting duct cells. Am. J. Physiol. 252:F551-F559, 1987.

CHAPTER 6

The target cells for ANF have been described in the brain, kidney, eye and jejunum. The physiological implications of these results are briefly discussed.

GENERAL DISCUSSION AND CONCLUSIONS

BRAIN

Endothelium of capillaries, the choroid plexus and pia-arachnoid are brain structures responsible for the intracranial control of water and electrolytes, whereas circumventricular organs are implicated in salt appetite, water drinking and blood pressure. Because ANF is a key hormone in extracellular volume regulation, the presence of its binding sites in these regions (Chapter 2) suggests that they mediate ANF's functions. Indeed, intracerebroventricular injections of ANF decrease cerebrospinal fluid production by 35% (13), and increase cGMP in the choroid plexus, in intraparenchymal capillaries and, to a lesser extent in the pia-arachnoid of pigs and rabbits (13), and in the rat choroid plexus (15). Binding sites are also present in brain capillaries of cows (3). These results confirm our own observations and demonstrate that brain ANF binding sites localized by <u>in vivo</u> radioautography correspond to functional ANF receptors.

ANF binding sites have also been identified in some brain regions inside the blood- brain barrier (9, 10). Because the peptide does not seem to penetrate the brain, as first suggested by us (Chapter 2) and confirmed in rabbits (6), these target areas may be modulated by central sources

of ANF production. Saavedra (10) studied ANF receptors in the rat brain and consistently observed that they are only regulated in brain regions outside the blood-brain barrier, indicating an important role of circulating ANF in brain function.

KIDNEY

The mechanisms by which ANF induces diuresis and natriuresis are not fully understood, despite considerable interest in the kidney. ANF enhances the glomerular filtration rate (GFR) (2), reduces inner medullary hypertonicity (1) and produces a re-distribution of renal blood flow without,in this case, changes in the GFR (11). Recent studies have demonstrated that ANF increases hydraulic pressure in descending and ascending vasa recta with only small increments in the tubular segments of the rat renal papilla (4). Our radioautographic investigations suggest that all these mechanisms are involved because ANF binding sites are present in glomerular cells, in descending vasa recta and in collecting ducts (Chapter 3, Section A and B).

We have also shown that ANF binds to the glomerular tuft and that its radioautographic distribution is different from that of Angiotensin II. In addition, electron microscope radioautography has revealed that the podocytes of epithelial visceral cells are the major ANF target in glomeruli.

Recent *in vitro* electron microscope radioautographic studies confirmed that the major target in the glomerular tuft correspond to epithelial visceral cells (7).

We have also determined that ANF at picomolar concentrations inhibits the contractile effect of Angiotensin II in isolated glomeruli. From these results, two putative mechanisms of action were proposed: Increases in the ultrafiltration coefficient by changes in the surface area and in glomerular permeability. Using isolated dog glomeruli, Fried et al. (5) demonstrated that ANF elevates the ultrafiltration coefficient and a recent study has ascertained that the impaired glomerular function induced by Angiotensin II in rats can be reversed by ANF (12), confirming our hypothesis of ANF and Angiotensin II antagonism in the glomeruli.

EYE

The presence of ANF binding sites in the ciliary processes of the eye (Chapter 4) suggested that the peptide is involved in the control of intraocular pressure. This hypothesis has recently been confirmed. Intravitreal injections of ANF (8, 14) decrease intraocular pressure for several hours. In addition, isolated ciliary processes of rabbits can increase cGMP induced by ANF (8) indicating that both cGMP and cAMP (Chapter 4) may be second messengers for ANF's actions. It is not known, however, if changes in cir-

culating ANF levels modify intraocular pressure.

SMALL INTESTINE

Using *in vivo* and *in vitro* radioautographic techniques, we have demonstrated the exact localization of ANF binding sites and their pharmacological characteristics. Although the results on water transport and salt excretion are still controversial (Chapter 5) we do know that binding sites are present mainly in fibroblast-like cells and mature enterocytes.

In conclusion, we have described the precise localization of ^{125}I-ANF binding sites which can be reached by an intravascular injection. These binding sites in many tissues and cells, are generally related to water and salt homeostasis. We have not only defined the possible structural localization, in the kidney for example (Chapter 3) but have also identified new target organs (eyes and small intestine). Most of our results have been confirmed by other investigators. We have thus made a substantial contribution to the detection of new target organs and have helped delineate the possible mechanisms of ANF's actions.

REFERENCES

1. Borenstein, H.B., Cupples, W.A., Sonnenberg, H., Veress, A.T. The effect of a natriuretic atrial extract on renal haemodinamics and urinary excretion in anesthetized rats. J. Physiol. 334:133-140, 1983.
2. Camargo, M.J.F., Atlas, S.A., Maack, T. Role of increased glomerular filtration rate in atrial natriuretic factor induced natriuresis in the rat. Life Sci. 38:2397-2404, 1986.
3. Chabrier, P.E., Roubert, P., Braquet, P. Specific binding of natriuretic factor in brain microvessels. Proc. Natl. Acad. Sci. USA 84:2078-2081, 1987.
4. Dunn, B.R., Troy, J.L., Ichikawa, J.L., Brenner, B.M. Effect of atrial natriuretic peptide (ANP) on hydraulic pressures in the rat renal papilla: implications for ANP-induced natriuresis. Kidney Int. 29:382 (Abstract), 1986.
5. Fried, T.A., McCoy, R.N., Osgood, R.W., Stein, J.H. Effect of atriopeptin II on determinants of glomerular filtration rate in the in vitro perfused dog glomerulus. Am. J. Physiol. 250:F1119-F1122, 1986.
6. Levin, E.R., Frank, H.J.L., Weber, M.A., Ismail, M., Steven, M. Studies of the penetration of the blood brain barrier by atrial natriuretic factor. Biochem. Biophys.

Res. Commun. 147:1226-1231, 1987.

7. Mizukawa, K., Ogura, T., Yamamoto, I., Mitsui, T., Katayama, E., Ota, Z., Ogawa, N. Localization of receptors for atrial natriuretic polypeptide (ANP) in the glomerulus: in vitro electron microscopic autoradiographical investigation using ^{125}I- labeled ANP. Reg. Peptides 21:167-172, 1988.

8. Nathanson, J.A. Atriopeptin-activated guanylate cyclase in the anterior segment. Identification, localization, and effects of atriopeptins on IOP. Invest. Ophthalmol. Vis. Sci. 28:1357-1364, 1987.

9. Quirion, R., Dalpé, M., Dam, T.V. Characterization and distribution of receptors for the atrial natriuretic peptides in mammalian brain. Proc. Natl. Acad. Sci. USA 83:174-178, 1986.

10. Saavedra, J.M. Regulation of atrial natriuretic peptide receptors in the rat brain. Cell. Moll. Neurobiol. 7:151-175, 1987.

11. Salazar, F.J., Fiksen-Olsen, M.J., Apgenorth, T.J., Granger, J.P., Burnett, J.C.Jr., Romero, J.C. Renal effects of ANP without changes in glomerular filtration rate and blood pressure. Am. J. Physiol. 251:F532-F536, 1986.

12. Schafferhans, K., Heidbreder, E., Hummel, S., Heidland, A. Atrial natriuretic peptide counter-acts angiotensin

II-induced impairement of renal function. Z. Kardiol. 77:78-84, 1988.

13. Steardo, L., Nathanson, J.A. Brain barrier tissues: End organs for atriopeptins. 235:470-473, 1987.

14. Sugrue, M.F., Viader, M.P. Synthetic atrial natriuretic factor lowers rabbits intraocular pressure. Eur. J. Pharmacol. 130:349-350, 1986.

15. Tsutsumi, K., Niwa, M., Kawano, T., Ibaragi, M.A., Ozaki, M., Mori, K. Atrial natriuretic polypeptides elevate the level of cyclic GMP in the rat choroid plexus. Neurosci. Letters 79:174-178, 1987.

CLAIMS TO ORIGINALITY

(1) Chapter 2, is the first report on ANF binding sites in the brain of intact rats. Major new findings show that they are localized in circumventricular organs, and in the whole brain vasculature, including brain capillaries.

(2) Chapter 3, is the first description of ANF binding sites in the kidney of intact rats.

2a) ANF and Angiotensin II binding sites are distinctly distributed on glomerular cells.

2b) ANF antagonizes the contractile effect of Angiotensin II on isolated glomeruli.

2c) ANF binding sites in the outer medulla are localized mainly on descending vasa recta and in the inner medulla on collecting ducts.

(3) Chapter 4, is the first documentation of ANF binding sites in the eyes of intact animals by light and electron microscope radioautography.

3a) These sites are localized almost exclusively at the basilar infolding of "pigmented" cells of the ciliary process.

3b) They have the same pharmacological characteristics of ANF receptors already discribed in other target tissues.

3c) ANF binding sites are negatively coupled to adenylate cyclase.

(4) Chapter 5, is the first demonstration of ANF binding sites in the rat small intestine by light and electron microscope radioautography in vivo and by light microscopy in vitro.

4a) They are characterized pharmacologically.

4b) ANF binding sites are localized in fibroblast-like cells of the lamina propria and at the base of mature enterocytes.

APPENDIX I

Original Reports:

1. Bianchi C, Gutkowska J, Thibault G, Garcia R, Genest J, Cantin M. Radioautographic localization of 125-I Atrial Natriuretic Factor (ANF) in rat tissues. Histochemistry 1985; 82: 441-452.

2. Garay R, Hannaert P, Rodrigue F, Dunham B, Marche P, Genest J, Braquet P, Bianchi C, Cantin M, Meyer P. Atrial Natriuretic Factor inhibits Ca dependent, K-fluxes in cultured vascular smooth muscle cells. J.Hypert 1985; 3: S-297-S-298.

3. Bianchi C, Gutkowska J, De Léan A, Ballak M, Anand-Srivastava MB, Genest J, Cantin M. Fate of 125I-Angiotensin II in adrenal zona glomerulosa cells. Endocrinology 1986; 118: 2605-2607.

4. Bianchi C, Anand-Srivastava MB, De Léan A, Gutkowska J, Forthomme D, Genest J, Cantin M. Localization and characterization of specific receptors for Atrial Natriuretic Factor in the ciliary processes of the eyes. Curr. Eye Res. 1986; 5: 283-293.

5. Bianchi C, Gutkowska J, Ballak M, Thibault G, Garcia R, Genest J, Cantin M. Radioautographic localization of 125I-Atrial Natriuretic Factor Binding sites in the brain. Neuroendocrinology 1986; 44: 365-372.

6. Bianchi C, Gutkowska J, Thibault G, Garcia R, Genest J, Cantin M. Comparative localization of 125I-Atrial Natriuretic Factor and 125I-Angiotensin II binding sites in the glomerulus. Am. J. Physiol. 1986; 251: F594-F602.

7. Bianchi C, Gutkowska J, Charbonneau C, Ballak M, Anand-Srivastava MB, De Lean A, Genest J, Cantin M. Internalization and lysosomal association of 125I-Angiotensin II in norepinephrine-containing cells of the rat adrenal medulla. Endocrinology 1986; 119: 1873-1875.

8. Bianchi C, Gutkowska J, Ballak M, Thibault G, Garcia R, Genest J, Cantin M. Ultrastructural localization of 125I-ANF binding sites in the outer and inner medulla of the kidney. J. Histochem. Cytochem. 1987; 35: 149-153.

Abstracts

1. Cantin M, Gutkowska J, Anand-Srivastava MB, Leroux S, Bianchi C, Carriere P, Genest J. Binding and internalization of 125I-angiotensin II in the rat adrenal. An ultrastructural radioautographic study. J.Cell Biol.1982; 95, 411a.

2. Bianchi C, Gutkowska J, Cantin M, Genest J. Binding and internalization of angiotensin II in rat adrenal Fed.Proc.1983; vol.42, no.4, 1102.

3. Bianchi C, Gutkowska J, Anand-Srivastava MB, Cantin M, Genest J. Binding and internalization of angiotensin II in the rat adrenal. Canadian Federation of Biological Societies, 1983; vol.26, 87.

4. Bianchi C, Gutkowska J, De Léan A, Genest J, Cantin M. Internalization pathways of 125I-AII in the zona glomerulosa of the adrenal cortex. 1984; 7th International Congress of Endocrinology, no 18, 269.

5. Bianchi C, Gutkowska J, De Léan A, Genest J, Cantin M. Internalization and fate of [125 I]-labeled angiotensin II into zona glomerulosa. Fed.Proc. 1984; vol.43, no.4, 3035.

6. Bianchi C, Gutkowska J, Thibault G, Garcia R, Genest J, Cantin M. Localization of 125I-labeled atrial natriuretic factor in rat tissues. Fed. Proc. 1985; vol.44, no.3, 512.

7. Bianchi C, Gutkowska J, Thibault G, Garcia R, Genest J, Cantin M. 125 I-Atrial natriuretic factor receptors in rat tissues. An in vivo light microscopic radioautographic study. 1985; Interamerican Society of Hypertension,no.21.

8. Bianchi C, Gutkowska J, Genest J, Cantin M. Localisation radioautographique in vivo des sites de liason du facteur natriurétique des oreilletes -I125 (FNO-I125) chez le rat. Journée Scientique, Département de pathologie, 1985; Université de Montréal, resumé 12.

9. Bianchi C, Gutkowska J, Anand-Srivastava, De Léan A, Genest J, Cantin M. Localization and characterization of atrial natriuretic factor (ANF)

receptors in the ciliary processes of the eyes. 1985; The Endocrine Society Meeting, no.902, 226.

10. Cantin M, Bianchi C, Gutkowska J, Thibault G, Garcia R, Genest J. Comparative localization and effect of ANF and angiotensin II on the glomerulus An ultrastructural radioautographic and functional study. 1985; Hipertension, vol.7, no 5, 841.

11. Bianchi C, Gutkowska J, Genest J, Cantin M. Localisation rénale des sites de liasion du 125I-facteur natriurétique des oreillettes chez le rat. 1986; Troisième Journée Scientifique, Département de Pathologie, Université de Montréal, Résume 2.

12. Bianchi C, Gutkowska J, Thibault G, Garcia R, Genest J, Cantin M. Light and electron microscopic radioautographic localization of 125I-atrial natriuretic factor binding sites in the rat kidney 1986; The Endocrine Society Meeting, no.536,165.

13. Bianchi C, Gutkowska J, Garcia R, Thibault G, Genest J, Cantin M. Renal distribution of 125I-atrial natriuretic factor binding sites as visualized by ultrastructural radioautography. Hypertension (in press).

14. Bianchi C, Gutkowska J, Thibault G, Garcia R, Genest J, Cantin M. Comparative localization and effect of atrial natriuretic factor (ANF) and angiotensin II (AII) on the glomerulus. An ultrastructural radioautographic and functional study. 1986; Proceedings of the International Union of Physiological Sciences vol. 15, 424.

15. Bianchi C, Gutkowska J, Genest J, Cantin M. Ultrastructural localization of 125 I-atrial natriuretic factor binding sites in the kidney. 1986; J.Cardiovasc. Pharmacol. 8 (no.6):1327.

16. Garay RP, Hannaert P, Rodrigue F, Marche P, Dunham B, Bianchi C, Cantin M, Braquet P. Atrial natriuretic factor (ANF) inhibits Ca-dependent K-fluxes in cultured vascular smooth muscle cells. 1986; J. Cardiovasc. Pharmacol. 8 (no.6): 1290.

17. Grenier MC, deGuise J, Blanchard M, Bianchi C, Durand LG. Analyse d'images autoradiographiques

par ordinateur. VIieme Congres Annuel de l'Association des étudiants aux grades supériers. Faculté de Médecine. Université de Montréal (in press).

18. Bianchi C, Gutkowska J, Thibault G, Garcia R, Genest J, Cantin M. Localization of target cells for atrial natriuretic factor in the lung, liver and small intestine. Seventh Scientific Meeting of I.A.S.H. (in press).

19. Bianchi C, Gutkowska J, Thibault G, Garcia R, Genest J, Cantin M. Ultrastructural localization of atrial natriuretic factor binding sites in the lung, liver and small intestine. The Second World Congress on Biologically Active Atrial Peptides (in press).

20. Bianchi C. Atrial natriuretic factor (ANF). An overview. Atrial natriuretic factors and brain. 1987; Satellite Symposium of the First ISN/ASN Meeting, Venezuela.

21. Bianchi C, Grenier M-C, Durand LJ, Genest J, Cantin M. Atrial natriuretic factor binding sites in the rat small intestine. Third Annual World Congress on Biologically Active Atrial Peptides (in press).

22. Bianchi C, Grenier M-C, De Guise J, Genest J, Cantin M. Comparative study of atrial natriuretic factor (ANF) binding sites in rat and hamster. Third Annual World Congress on Biologically Active Atrial Peptides (in press).